Giant Synapses in Thalamic Relay Cells

Dissertation
submitted to the
Combined Faculties for the Natural Sciences and for Mathematics
of the Ruperto-Carola University of Heidelberg, Germany
for the degree of
Doctor of Natural Sciences

Submitted by
Francisco José Urra Quiroz
Santiago, Chile
2013

Dissertation
submitted to the
Combined Faculties for the Natural Sciences and for Mathematics
of the Ruperto-Carola University of Heidelberg, Germany
for the degree of
Doctor of Natural Sciences

presented by

Diplom in Biochemistry Francisco José Urra Quiroz
born in: Santiago, Chile
Oral-examination: February 27th, 2014

Giant Synapses in Thalamic Relay Cells

Referees: Prof. Dr. Thomas Kuner
Prof. Dr. Stephan Frings

Summary

The thalamus processes and relays sensory information from the periphery to the cortex and from the cortex to other areas of the cortex. A trisynaptic pathway connects the whiskers with the somatosensory cortex. The principal nucleus of the trigeminal nerve (Pr5) in the brainstem receives sensory information from the whiskers and sends them to the ventral posteromedial nucleus of the thalamus (VPM), which in turn projects to the somatosensory cortex. The synaptic transmission between Pr5 and relay cells of the VPM is mediated by giant synapses, however, this transmission is poorly characterized. In this study we labeled trigeminothalamic (Pr5-VPM) giant terminals by stereotaxic delivery of adeno-associated virus particles (AAV) encoding synaptophysin-EGFP into the Pr5 nucleus of rats. Pr5-VPM giant terminals were identified in the VPM and directly stimulated with a double-barrel electrode after establishing whole-cell patch-clamp recordings from the postsynaptic relay neuron. This allowed us to study synaptic transmission in identified Pr5-VPM giant synapses for the first time . We found that stimulation of single terminals generates large postsynaptic responses, with a low probability of release, short-term depression and a fast recovery after a train of stimuli. Moreover, a single synaptic input shows a synaptic transfer function capable of generating a voltage-dependent postsynaptic spike response.

Different currents modulate the spike response of relay cells. I_A correspond to fast outward potassium currents generated by Kv1, Kv3 and/or

Kv4 potassium channel subunits. We showed that I_A currents in VPM relay cells are in part generated by Kv4.3 channels. Blockade of Kv4.3 channels decreased the amplitude response of relay cells to stimulation of Pr5-VPM synapses.

In silico models can be used to explore the firing mechanisms of relay cells. We generated a model that considers the morphology of relay cells, the input location of large terminals and the electrophysiological information of Pr5-VPM synapses. The *in silico* model predicts stimulation of more than one terminal changes the spike response of the relay cell, increasing the number of spikes. The model also predicts the effects of decreasing I_A or I_T, the low threshold calcium current, in the relay cell response.

Layer 5B (L5B) pyramidal neurons of the somatosensory cortex connect via relay neurons from the posteromedial nucleus (POm) to neurons of higher order somatosensory cortex. The synaptic transmission between L5B pyramidal neurons and POm relay cells is mediated by L5B-POm synapses. To place the properties of this synapse in the context of behavioral abilities developing during the first two months of postnatal life, it is required to know the synaptic maturation changes. We used the same approach as for the Pr5-VPM synapses project but we injected the AVV particles in the L5B and we recorded the responses in POm relay cells from mice at different ages. The frequency of spontaneous activity decreased over time, however, L5B-POm synapses did not show differences in EPSC evoked responses. Nevertheless, stimulation of single large terminals could generate spike responses in animals older than 4 to 5 weeks old.

We described the properties of first order (Pr5-VPM) and higher order (L5B-POm) driver synapses involved in the whisker system of rodents. Stimulation of both synapses generated large amplitude responses and a strong depression. In addition, stimulation of single synapses in mature animals did generate spikes responses. Comparison of both giant synapses shows that both have remarkably similar properties, suggesting that both synaptic circuits, despite their different functions, employ similar information processing strategies.

Sensory information reaches the cortex by the thalamus. The thalamus

does not just work as the major relay center to the cortex, but it also processes the sensory information to be sent to the cortex depending on the level of attention of the organism. This work shows that the relay function of first order and higher order nuclei appears at the level of single synapses. In addition, the information processing function of the thalamus is also seen in a voltage-dependent transfer function of single synapses. The main task of the thalamus, to process and relay information, appears at the level of single relay cell synapses.

Zusammenfassung

Der Thalamus erhält zum einen sensorische Informationen aus der Peripherie und leitet diese zum Cortex weiter, zum anderen gibt es aber auch cortikale Projektionen, die im Thalamus pozessiert und dann zu anderen cortikalen Arealen weitergeleitet werden. Dabei sind die Schnurrhaare mit dem Somatosensorischen Cortex über eine trisynaptische Bahn verbunden. Der Nucleus principalis nervi trigemini (Pr5) im Hirnstamm erhält sensorische Informationen der Schnurrhaaren und leitet diese an den Nucleus ventralis posteromedialis des Thalamus (VPM) weiter, welcher sie wiederum an den somatosensorischen Cortex übermittelt. Die synaptische Übertragung zwischen dem Pr5 und den Relaiszellen des VPM wird von Riesensynapsen vermittelt, allerdings wurde diese Übertragung bisher kaum charakterisiert. In dieser Studie wurden die trigeminothalamischen Riesensynapsen (Pr5-VPM) markiert indem stereotakxisch synaptophysin-EGFP kodierende Adeno-assoziierte Viruspatikel (AAV) in den Pr5 nucleus von Ratten injiziert wurden. Dies erlaubte die Identifizierung der PR5-VPM Riesensynapse innerhalb des VPM, so dass eine whole-cell Patch-Clamb-Ableitung vom postsynaptischen Neuron etabliert und die Riesensynapsen mithilfe einer double-barrel Elektrode direkt stimuliert werden konnten. Dadurch war es zum ersten Mal möglich die synaptische übertragung in identifizierten Pr5-VPM Riesensynapsen zu untersuchen. Die Untersuchung ergab dass die Stimulation von einzelnen Nervenendigungen zu starken postsynaptischen Antworten mit geringer Freisetzungswahrschein-

lichkeit, Kurzzeitdepression und einer schnellen Erholung von dieser Kurzzeitdepression führt. Außerdem konnte gezeigt werden, dass die Aktivität eines einzelnen synaptischen Inputs ausreicht um in der postsynaptischen Zelle ein Aktionspotential auszulösen.

Die Reaktion der Relaiszellen auf Stimulierung wird durch verschiedene Ströme moduliert. I_A entspricht dabei einem schnellen, auswärtgerichteten Kaliumstrom, der von den Kaliumkanaluntereinheiten Kv1, Kv3 und/oder Kv4 generiert werden kann. Es konnte gezeigt werden, dass I_A-Ströme in den VPM-Relaiszellen teilweise von Kv4.3-Kanälen generiert werden. Eine Blockade von Kv4.3-Kanälen verringerte die Amplitude der Antwort der Relaiszellen bei einer Stimulation der Pr5-VPM-Synapse.

In silico Modelle können genutzt werden um die Feuereigenschaften der Relaiszellen zu simulieren und dadurch besser zu verstehen. Es wurde ein Modell generiert, das die Morphologie der Relaiszellen genauso berücksichtigt wie die Lokalisation und die elektrophysiologischen Eigenschaften der Pr5-VPM Synapsen. Das *in silico* Modell sagt vorraus, dass eine Stimulation von mehr als einer Nervenendigung das Verhlaten der Relaiszelle dahingehend verändert, dass sich die Anzahl der gefeuerten Aktionspotentiale erhöht. Das Modell sagt auch die Auswirkungen einer Verringerung von I_A und der bei niedrigen Potentialen aktivierbare Kalziumstrom I_T auf die Antwort der Relaiszelle vorraus.

Die Pyramidenzellen der Lamina 5B (L5B) des somatosensorischen Cortex sind über Relaisneurone des nucleus posteromedialis (POm) mit Neuronen höherer somatosensorischer Cortex-Areale verbunden. Um die Eigenschaften dieser L5B-POm Synapsen zur Verhaltensentwicklung der ersten zwei Lebensmonate in Beziehung zu setzen, ist es notwendig die Veränderungen der Synapse während der Entwicklung zu kennen. Hierzu wurde die selbe Herangehensweise benutzt wie bei der Untersuchung der PR5-VPM Synapse, mit dem Unterschied, dass die AVV-Partikel diesmal in die L5B Region injiziert wurden, und die Antwort von POm Relaisneuronen von Mäusen unterschiedlichen Alters abgeleitet wurde. Es zeigte sich, dass die Frequenz der spontanen Aktivität mit der Zeit abnahm, die L5B-POm Synapsen jedoch keine Unterschiede hinsichtlich der evozierten EPSC

Antworten zeigten. Nichtsdestotrotz konnte eine Simulation von einzelnen großen Nervenendigungen Aktionspotentiale nur in Tieren hervorrufen, die älter als vier bis fünf Wochen waren.

Es wurden die Eigenschaften von "driversynapsenërster Ordnung (Pr5-VPM) und höherer Ordnung (L5B-POm) untersucht, die Teil des somatosensorischen Schnurrhaarsystems von Nagern sind. Die Stimulation beider Synapsen erzeugte Antworten mit großer Amplitude und einer ausgeprägten Depression. Außerdem erzeugte eine Stimulation von einzelnen Synapsen in ausgewachsenen Tieren Aktionspotentiale in der postsynaptischen fulle. Der Vergleich dieser beiden Riesensynapsen zeigt, dass beide bemerkenswert ähnliche Eigenschaften besitzen.

Die sensorische Information erreicht den Cortex über den Thalamus. Der Thalamus fungiert dabei nicht nur als das Hauptrelaiszentrum zum Cortex, sondern verarbeitet auch die für den Cortex bestimmte sensorische Information in Abhängigkeit vom Aufmerksamkeitsgrad des Organismus. Diese Arbeit zeigt, dass sowohl die Relaisfunktion als auch die Verarbeitung von Information in Kernen erster und höherer Ordnung bereits auf der Ebene einzelner Synapsen erkennbar ist.

Contents

Abbreviations

4-AP	4-Aminopyridine
I_A	Transient and Depolarization-Activated K^+ Current
I_h	Hyperpolarization-Activated Cation Conductance
I_T	Low-threshold Ca^{2+} Current
ACSF	Artificial Cerebrospinal Fluid
AVV	Adeno-Associated Virus
CTC	Cortico-Thalamo-Cortical
EPSC	Excitatory Postsynaptic Current
EPSP	Excitatory Postsynaptic Potential
KYN	Kynurenic Acid
L4	Layer 4 of the Cortex
L5B	Layer 5B of the Cortex
LFVC	Low Frequency Voltage Clamp

LGN	Lateral Geniculate Nucleus
LTS	Low Threshold Calcium Spike
POm	Posteromedial Nucleus of the Thalamus
Pr5	Principal Trigeminal Nucleus
RL	Large Terminals with Round Vesicles
S1	Somatosensory Area 1
SP5	Spinal Trigeminal Nucleus
VPM	Ventral Posteromedial Nucleus of the Thalamus

CHAPTER 1

Introduction

1.1 Sensory Systems

The brain receives sensory information from the environment, processes it and generates the appropriate response, such as the movement of a hand, or uses the sensory information for higher order processing, like ideas or thought. The brain receives different inputs like visual stimuli or olfactory stimuli. In the first case, the retina receives visual stimulation, transduces it and sends it in form of action potentials to the visual cortex, where some cells fire according to different stimuli, like shape or movement. This information is afterwards sent to higher order areas where neurons process the information in a more semantic way. In this case the information is relayed to the thalamus, specifically to the lateral geniculate nucleus (LGN) . In the olfactory system olfactory receptor neurons in the olfactory epithelium transduce odorant information and project it to the olfactory bulb which in turn sends projections to different areas of the brain. However, the olfactory information is not relayed to the thalamus before reaching the cortex. In both cases, specific sensory cells translate the stimulus to a firing code

recognized by higher order centers in the brain (Paxinos, 2004).

The somatosensory system follows a similar pathway to the visual system. In this case mechanoreceptors in different areas of the body react to pressure and send firing patters to the brain (Paxinos, 2004). The function of the somatosensory system is to identify objects, shapes and textures (Diamond et al., 2008; Nicholls et al., 2012), allowing the organism, for instance, to direct the visual attention to a particular target, or to avoid those objects that generate pain (Nicholls et al., 2012). Sensory receptors of the somatosensory system are located on the entire body surface and not clustered, as in the retina of the visual or the olfactory epithelium of the olfactory systems (Nicholls et al., 2012). The sensory information travels through different pathways from tactile receptors in the periphery to the spinal cord or the brainstem and reaches the cortex by passing across multiple relay centers, such as the thalamus (Nicholls et al., 2012; Sherman and Guillery, 2009). The tactile and pressure information reaches the cortex by the dorsal column lemniscal pathway, while painful and thermal information reaches the cortex by the spinothalamic pathway (Purves, 2004). At each stage of the somatosensory pathway, neurons are arranged into topographic maps (Kandel et al., 2013; Nicholls et al., 2012; Paxinos, 2004; Purves, 2004). Some parts of the body are represented by a broader cortical surface, like the fingertips of primates, and this phenomena may be related to the density of tactile receptors (Nicholls et al., 2012). In some cases, like the somatosensory cortex of rodents, the cortical surface is much larger than primary visual or primary auditory cortex (Nicholls et al., 2012). Relay centers of the somatosensory system do not only send information to the cortex, but also receive descending cortical information that influences the information sent to the cortex (Beak et al., 2010; Groh et al., 2013; Hoogland et al., 1991; Liao et al., 2010; Nicholls et al., 2012).

1.2 Whisker System

The whisker system is part of the somatosensory system of rodents (Figure 1.1). Rats and mice are nocturnal animals that use whiskers to sense the environment (Diamond et al., 2008; Diamond and Arabzadeh, 2013; Watson et al., 2011). For example, whiskers allow rodents to discriminate textures (Safaai et al., 2013; Zuo et al., 2011), to calculate distances (Hutson and Masterton, 1986; Papaioannou et al., 2013), or possibly to sense the presence of predators (Diamond and Arabzadeh, 2013). Some of this information is related to contact or touch signals, whereas the other is associated to sensor motion or whisking (Yu et al., 2006).

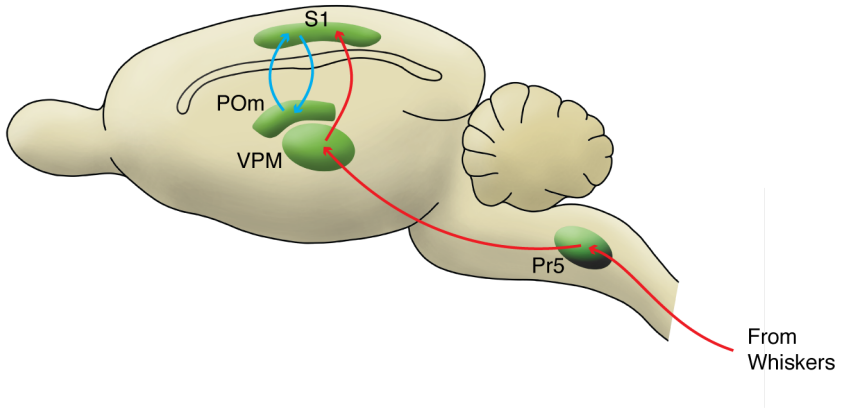

Figure 1.1: Whisker system
Simplified scheme of the rodent whisker system. Parts of the lemniscal pathway are shown in red, and in blue the corticothalamocortical loop between POm and S1.

Each whisker is anchored to the skin by a follicle, and each follicle is innervated by around 200 projections from neurons associated with a trigeminal ganglion (Diamond et al., 2008; Dörfl, 1985). These neurons, in turn, send the information to the cortex via three known pathways: lemniscal, paralemniscal and extralemniscal pathways (Yu et al., 2006). In the lemniscal pathway, projections from the trigeminal ganglia reach the trigeminal nucleus in the brainstem (Diamond et al., 2008; Dörfl, 1985). The principal trigeminal nucleus (Pr5) in the brainstem receives the projections coming

from the trigeminal ganglia. Pr5 projects to the ventral posteromedial nucleus of the thalamus (VPM) (Diamond et al., 2008; Hoogland et al., 1991; Spacek and Lieberman, 1974) , which works as a relay center, and neurons from VPM send projections to neurons in the layer 4 (L4) of the somatosensory cortex 1 (S1), also called barrel cortex (Fox, 2008; Petersen, 2007). VPM thalamocortical relay cells generate subthreshold potentials in cells from the barrel cortex (Brecht and Sakmann, 2003; Bruno and Sakmann, 2006; Feldmeyer, 2012). Finally, neurons from S1 send projections to other areas of the brain (Chen et al., 2013; Quairiaux et al., 2011) (Figure 1.2).

Cells in different nuclei along the pathway have different organization patterns. For instance, cells in the Pr5 nucleus are grouped in barrelettes (Paxinos, 2004), whereas VPM cells are grouped in barreloids (Van der Loos, 1976; Paxinos, 2004) and S1 cells are grouped in barrels (Wimmer et al., 2010; Woolsey and Van der Loos, 1970). Cells in each group respond strongly to the stimulation of one specific single whisker and more weakly to multiwhisker stimulation (Minnery and Simons, 2003; Veinante and Deschênes, 1999; Veinante et al., 2000). In addition, cells in each level receive connections from other areas of the brain, like basal ganglia, cerebellum or thalamic reticular nucleus, which modulate the signal sent to the cortex (Bosman et al., 2011; Paxinos, 2004).

Whisker information also reaches the cortex by the paralemniscal pathway. Hereby, the information from the whiskers relays in the interpolaris region of the spinal trigeminal nucleus (SP5) in the brainstem and in the rostral part of the posteromedial nucleus (POm) of the thalamus (Pierret et al., 2000; Yu et al., 2006) . POm sends projections to different areas, like L1 and L5A of S1 (Ahissar et al., 2000; Bourassa et al., 1995; Diamond et al., 1992; Koralek et al., 1988; Lu and Lin, 1993; Meyer et al., 2010; Ohno et al., 2012), L4 of S2 (Ohno et al., 2012; Viaene et al., 2011) , and L2/3 and L5A of M1 (Hooks et al., 2013) (Figure 1.2).

A third pathway, called extralemniscal pathway, includes the oral and the interpolaris region of the SP5 and Pr5 from the brainstem (Pierret et al., 2000). Projections from this nuclei reach the ventrolateral sector of VPM (Yu et al., 2006) and the information is relayed to L3, L4 and L6 of S1 and L4 and

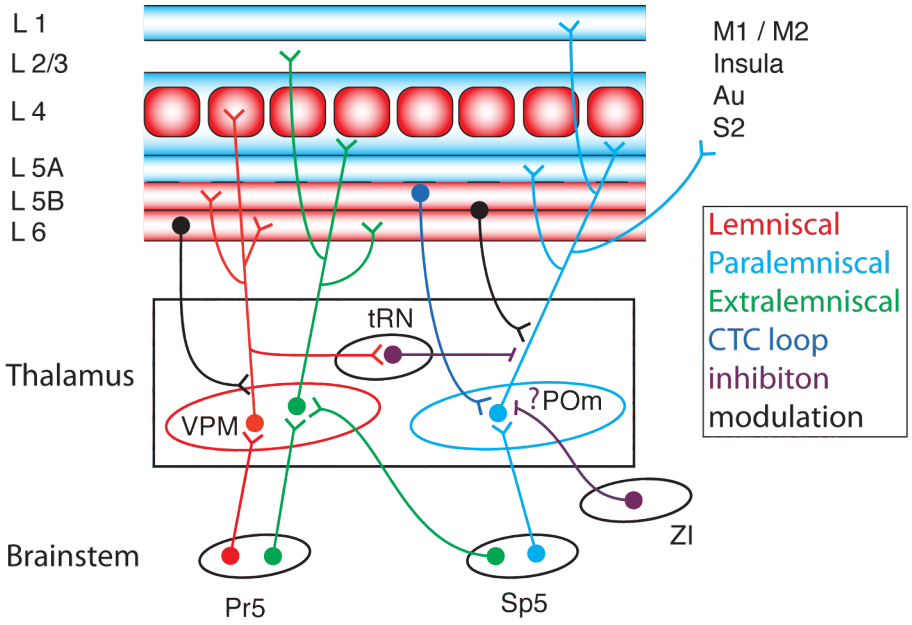

Figure 1.2: Input and output from VPM and POm
In "?" information still missing, like if inhibitory inputs from the zona incerta reach the same POm relay cells that receive paralemniscal and cortical driver inputst. The scheme is not complete. Scheme based in Ohno et al., 2011, and references in text

L6 of S2 (Bokor et al., 2008; Feldmeyer, 2012). The anatomical differences between these three pathways are related to functional differences: the lemniscal pathway carries both whisking and tactile signals; the paralemniscal pathway carries whisking signals; whereas the extralemniscal pathway carries only tactile signals (Yu et al., 2006).

Information from the whisker, such as whisker deflection or mechanical touch, is transduced and reaches the cortex in trains of action potentials. At the level of the trigeminal ganglia, neurons can follow firing patterns of hundreds of cycles per second. Pr5 neurons can follow trains of stimuli up to 300 Hz, but VPM neurons show depression already at the level of 10 or 50 Hz stimuli (Deschênes et al., 2003). The cortex receives this train of spikes. Whisker information reaches the VPM after 7 ms of whisker stimulation. In turn, stimulus information takes about 20 ms from the stimulation of the whisker until reach the barrel cortex (Ahissar et al., 2000). POm has a

delayed response, fire around 15 ms after whisker stimulation (Diamond et al., 1992).

1.3 Thalamus

The thalamus is located in the medial part of the brain and is subdivided in three areas: anterior, medial and lateral, which are separated by intralaminar white matter (Sherman and Guillery, 2009). In total, the thalamus has 20-30 nuclei.

The thalamus works as a relay center where specific nuclei receive information from different pathways (Sherman and Guillery, 2009). Some nuclei are involved in the direct control of the motor response.

The medial part of the thalamus is involved in higher order tasks like cognition and memory. Good examples are the mediodorsal nucleus, involved in cognitive tasks (Lee et al., 2012; Parnaudeau et al., 2013), and the ventral midline thalamus, involved in memory processing (Xu and Südhof, 2013; Cholvin et al., 2013). Also, a series of nuclei are involved in the relay of sensory information from the periphery to the cortex, like VPM, POm and LGN (Sherman and Guillery, 2009; Jones, 2007).

The whisker system is associated with the VPM and the POm (Diamond et al., 2008; Hoogland et al., 1991; Spacek and Lieberman, 1974) (Figure 1.1). VPM is considered a first order relay center, because it receives information from the periphery and sends it to the cortex. POm (Pierret et al., 2000; Yu et al., 2006) is located more dorsally. This nucleus participates in the paralemniscal pathway and also works as a higher order relay center that receives cortical information from the layer 5B of the cortex (L5B) (Groh et al., 2013; Hoogland et al., 1991; Liao et al., 2010). The L5B-POm synapse is called Rosebud synapse (Groh et al., 2008). POm relay cells send the cortical information to others areas of the cortex (Ohno et al., 2012; Theyel et al., 2010), forming a cortico-thalamo-cortical (CTC) loop (Bourassa et al., 1995; Deschênes et al., 1998; Diamond et al., 1992; Fox, 2008; Theyel et al., 2010).

Probably the same relay cell in POm receives paralemniscal and cortical driver inputs (Groh et al., 2013).

VPM and POm send projections to different areas and cells in the cortex (Figure 1.2). These nuclei are probably involved in different functions (Diamond, 2000). Both respond to whisker stimulation, and show depression if whiskers are stimulated at higher frequencies (Diamond, 2000; Sosnik et al., 2001). POm, but not VPM, increases the latency of the response to whisker stimulation (Diamond, 2000; Sosnik et al., 2001), probably as a mechanism to change the information from temporal to rate code (Ahissar et al., 2000). POm also receives strong inhibitory inputs from the zona incerta, which fires before POm following whisker stimulation (Lavallée et al., 2005). POm might be disinhibited in order to relay information to the cortex (Deschênes et al., 2005; Lavallée et al., 2005).

1.4 Relay Cells

Relay cells in the thalamus receive inputs and project to different areas of the cortex (Sherman and Guillery, 2009; Jones, 2007). Some nuclei, like LGN, have different types of relay cells, which can be differentiated by the shape and distribution of their dendritic branches (Sherman and Guillery, 2009; Jones, 2007; Varela and Sherman, 2009). VPM contains only one type of relay cell, which has proximal dendrites confined to an area called "barreloid" that represents a single whisker (Deschênes et al., 2005). Rat POm relay cells also have one type of relay cell (Ohara and Havton, 1994). Both nuclei have relay cells with somas in the order of 17 μm and 6 or 7 principal dendrites (Ohara and Havton, 1994). Relay cells do not only exhibit differences in morphology, but also in the driver input that they receive and the type and number of modulatory signals received (Sherman and Guillery, 2009).

Relay cells receive sensory or cortical information by large terminals located close to the soma or in the first branch of the dendrites (Çavdar et al., 2011; Peschanski et al., 1985; Spacek and Lieberman, 1974). These synapses are called driver synapses. In some cases, like the LGN of cats,

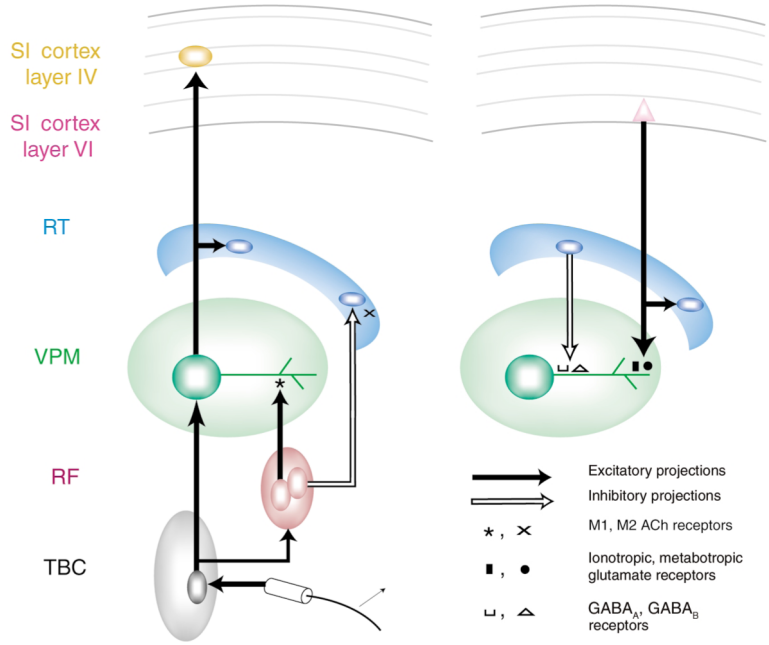

(a) Ascending projections **(b)** Descending projections

Figure 1.3: Input to VPM relay cells
Relay cells receive driver and modulatory inputs. VPM receive modulatory inputs from the trigeminal nucleus, and regulatory excitatory inputs from the reticular formation, and cortex. They receive inhibitory modulatory inputs from the thalamic reticular nucleus (From (Nicolelis and Fanselow, 2002))

driver synapses form structures called triads, composed by reticulothalamic terminals, inhibitory interneurons terminals and dendrites of the relay cell, all of them encapsulated in astrocytes (Lam et al., 2005; Sherman and Guillery, 2009). Rodent driver synapses of VPM and POm also present a complex connection between the presynaptic input and the postsynaptic relay cell, but those nuclei do not have interneurons, and do not form triads (Hoogland et al., 1991; Spacek and Lieberman, 1974). Each driver synapse in the VPM and POm is formed by several dendrite invaginations, with 10 or more active zones each. The synaptic vesicles are very close to the release site. Driver synapses are between 2 and 10 μm in diameter

(Spacek and Lieberman, 1974), and contain mitochondria and endoplasmic reticulum (Hoogland et al., 1991; Spacek and Lieberman, 1974). Driver synapses are glutamatergic and they have AMPA and NMDA components (Arsenault and Zhang, 2006; Groh et al., 2008; Sherman and Guillery, 2009; Wang and Zhang, 2008).

Relay cells receive also modulatory signals (Figure 1.3). Modulatory inputs can be inhibitory or excitatory and are usually formed by small synapses located in dendritic branches far away from the soma (Sherman and Guillery, 2009; Van Horn et al., 2000). One source of GABAergic inhibitory signal in nuclei like LGN are interneurons (Jones, 2007; McCormick, 1992), but POm and VPM from rodents do not have interneurons, and the main GABAergic inhibitory signal come from the reticular nucleus (Jones, 2007; Lee et al., 1994; McCormick, 1992; Nicolelis and Fanselow, 2002).

POm receives some inhibitory inputs that form large synapses, like those coming from the substantia nigra (Bodor et al., 2008), or the zona incerta (Barthó et al., 2002; Lavallée et al., 2005). Excitatory modulatory inputs come from the cortex and brainstem (Hallanger et al., 1987; Nicolelis and Fanselow, 2002) and they form adrenergic, cholinergic, serotoninergic or glutamatergic synapses (McCormick, 1992).

1.5 Cell Physiology of Relay Cells

The resting membrane potential of relay cells oscillates between -65 and -75 mV (Sherman and Guillery, 2009). The action potential response of relay cells is Na^+-dependent and K^+ dependent (Jones, 2007). Relay cells can fire in tonic or burst mode (Jones, 2007; Llinas and Jahnsen, 1982; Sherman and Guillery, 2009). Tonic mode is a steady firing (Sherman and Guillery, 2009), while in burst mode relay cells respond with 2-10 spikes at 300 - 500 Hz (Andersen et al., 1964; Llinas and Jahnsen, 1982; Nicolelis and Fanselow, 2002). The mode of firing depends on the resting membrane potential of the cell. A more hyperpolarized cell will fire in

burst mode, whereas a more depolarized cell will fire in tonic mode (Llinas and Jahnsen, 1982; Sherman and Guillery, 2009).

Burst firing depends on low threshold calcium spikes (LTS) that depolarize the relay cells and activate sodium-dependent voltage channels, generating sodium dependent spikes (Coulter et al., 1989; Deschênes et al., 1984). LTS is generated by a low-threshold Ca^{2+} current, I_T formed by T-type calcium channels (Tscherter et al., 2011). I_T is a voltage dependent fast inward calcium current. T-type channels have two activating gates that must be open in order to allow the flow of calcium ions. The activation gate opens at more depolarized potentials, whereas the inactivation gate opens at more hyperpolarized potentials. Curves of activation and inactivation describe the rate of current at different membrane potentials. At resting membrane potentials, the activation gate is open but the inactivation gate is closed, so there is no I_T. The threshold needed for activation is lower than those for voltage dependent sodium channels. Relay cells fire in burst mode only when they are hyperpolarized due to the deinactivating properties of I_T (Huguenard and Mccormick, 1992; Perez-Reyes, 2003; Sherman and Guillery, 2009; Tscherter et al., 2011).

LTS are also associated to the hyperpolarization-activated cation current, or I_h (Mccormick and Pape, 1990; Sherman and Guillery, 2009). This current is activated by hyperpolarization and tends to depolarize the relay cell (Sherman and Guillery, 2009).

Transient and depolarization-activated K^+ current, I_A is also involved in shaping the signal generated in relay cells of the thalamus (Huguenard and Mccormick, 1992; Sherman and Guillery, 2009). Activating and inactivating I_A curves are shifted to the right, compared to I_T curves. The threshold for activation of I_A is -60 mV (Huguenard and Mccormick, 1992). I_A is generated by the opening of Kv1, Kv3 and/or Kv4 potassium channels (Birnbaum et al., 2004; Jerng et al., 2004; Norris and Nerbonne, 2010). The flow of K^+ following the opening of these channels hyperpolarizes the membrane potential.

The function of I_A current in relay cells is still not clear. Elimination of I_A in an *in silico* model of a relay cell changes the spike response of

the relay cell to a depolarized current injection, increasing the spike firing frequency (Mccormick and Huguenard, 1992). I_A generates smaller and broader LTS during burst firing (Mccormick and Huguenard, 1992; Pape et al., 1994). One possible function of I_A is to increase the "input/output dynamic range", by avoiding the generation of spikes by low inputs, or decreasing the level of depolarization by a strong input that otherwise would saturate the relay cell (Connor and Stevens, 1971; Sherman and Guillery, 2009).

The location of the channels involved in I_T and I_A helps to elucidate their function (Destexhe et al., 1998). T-type calcium channels are distributed in the soma and proximal dendrites of relay cells, exhibiting a lower density in more distal dendrites (Errington et al., 2010; McKay et al., 2006; Williams and Stuart, 2000; Zhou et al., 1997).

The location of channels generating I_A in relay cells is not so clear. Hippocampal CA1 pyramidal cells have a high density of transient K^+ channels in distal dendrites (Hoffman et al., 1997), but in relay cells Kv4.3 subunits appear to be only present in dendrites close the soma of VPM relay cells (Giber et al., 2008). The distribution of Kv4.3 channels close to large terminals could allow I_A to affect the input response and excitability of the relay cell, as in other parts of the brain (Cai et al., 2004; Kim, 2005; Kim et al., 2007; Shibata et al., 2000; Yuan et al., 2005).

The resting membrane potential of relay cells is regulated by modulatory signals localized in distal dendrites (Jones, 2007; Sherman and Guillery, 2009). For example, corticothalamic synapses with group I mGluR subunits keep the cell at depolarized levels, producing a tonic response to a driver input (Godwin et al., 1996; Reichova and Sherman, 2004), while GABAergic synapses from the thalamic reticular nucleus keep the cell hyperpolarized (Huguenard and Prince, 1994), generating a response in burst mode by a driver input.

1.6 Thalamic Driver Synapses

Driver synapses are formed by large terminals with round vesicles (RL) of 2 to 10 μm in diameter (Hoogland et al., 1991; Sherman and Guillery, 2009; Spacek and Lieberman, 1974). RL are located in proximal large dendrites of relay neurons (Liu et al., 1995) and release glutamate as the principal neurotransmitter. The properties of giant synapses formed between layer 5B pyramidal neurons of the barrel cortex and relay neurons of the POm (L5B-POm synapses) were recently described (Groh et al., 2008). These synapses show more than 1 nA amplitude, strong frequency-dependent depression, and spike generation. First order relay cells of the VPM also receive giant synapses, albeit from subcortical nuclei (Pr5) of the trigeminal nerve (Spacek and Lieberman, 1974; Hoogland et al., 1991). Responses of VPM relay cells to medial lemniscus stimulation, which potentially activate all the driver synapses connected to one cell, show frequency-dependent depression. The response is abolished in the presence of the AMPA competitive antagonists CNQX or NBQX (Castro-Alamancos, 2002; Miyata and Imoto, 2006). The properties of identified individual peripheral Pr5-VPM driver synapses have not yet been elucidated with whole-cell patch-clamp recordings. It is not clear if the spike response of relay cells appears at the level of single terminals or whether it needs more inputs and computation processing in the relay cells. It is also not known what properties of relay cells, like frequency-dependent depression, are generated at the level of single driver synapses.

1.7 *In Silico* Relay cells

In silico models of cells and processes have been used to help answer specific questions, like what the ionic composition of the action potential is (Hodgkin and Huxley, 1952). Other models are used to explain dendritic behavior (Gold and Bear, 1994), cell response (London et al., 2008; Mccormick and Huguenard, 1992), thalamocortical (Traub et al., 2005) and cortical columns (Helmstaedter et al., 2007), circuits (Chersi et al., 2013), or

even the entire brain (Eliasmith et al., 2012; Markram, 2006).

The model used to describe ions involved in the action potential initiation and propagation (Hodgkin and Huxley, 1952) is called HH-type model. HH-type model uses a set of four differential equations to describe the currents involved in the generation of the passive and active properties of the cells (Sterratt et al., 2011). The HH-type model is useful if the goal is to determine the effects of a specific current in the active properties of the cell (Rhodes and Llinás, 2005), but it can also be used to model the interaction between cells described with HH-type models (Traub et al., 2005).

The HH-type model is not the only *in silico* approach to describe properties of a cell or circuit (Gerstner and Kistler, 2002; Sterratt et al., 2011). The integrate-and-fire model, or spiking neuron model, is a simplified HH-model in which the biophysical properties of the action potential are not included (Dayan and Abbott, 2005). This model simplifies the necessary calculations and is often used in models of circuits or networks (Chersi et al., 2013), but can also be used in single cell models (London et al., 2008). Another example is the two-dimensional neuron model, which describes the cell behavior with two differential equations instead of the four used in the HH-type model. The results of the simulations using the two-dimensional model are analyzed using phase plane analysis (Gerstner and Kistler, 2002). This model is useful to study oscillations and firing patterns (Drion et al., 2012; Lavrova et al., 2012).

Relay cells have tonic and burst firing modes (Sherman and Guillery, 2009). *In silico* cells models help to understand the mechanisms and currents involved in those firing modes (Meuth et al., 2005; Mccormick and Huguenard, 1992; Rhodes and Llinás, 2005). Specifically, the role of low threshold calcium currents in relay cells was modeled by different groups (Rhodes and Llinás, 2005; Tscherter et al., 2011; Wang et al., 1991; Williams et al., 1997), and they proved the role of this current in burst firing. Some models also can predict the distribution of T-type calcium channels in the dendritic tree (Antal et al., 1996; Destexhe and Sejnowski, 2003; Rhodes and Llinás, 2005), whereas others deal with the oscillation properties of relay cells (Tóth et al., 1998) or with thalamic networks (Destexhe

and Sejnowski, 1997; Traub et al., 2005).

Almost all the relay cell models use the HH-type model. Each current is described with a series of equations that relate the amplitude of the current with voltage dependent open and close gate probabilities (Sterratt et al., 2011). Some models use a single compartment, without any dendrite or axon (Mccormick and Huguenard, 1992). These models can reproduce the burst and tonic behavior of the relay cells. Others models include relay cell morphology (Destexhe and Sejnowski, 2003; Rhodes and Llinás, 2005; Traub et al., 2005), and they have been used to determine the current distribution along the dendritic tree. So far no relay cell model has considered the specific locations of synaptic inputs.

The problem of computation of inputs considering synaptic location is addressed in other cells. Models of pyramidal cells of the hippocampus include input origin. The model can be used to test how the localization of the inputs affect the cell response (Hao et al., 2009), and also to describe the specific properties of the inputs (Piskorowski and Chevaleyre, 2012). In this case the amplitude of unitary inputs is not enough, so cells need the integration of several synapses to generate a spike (Piskorowski and Chevaleyre, 2012). The computation rules generated by the model of a specific cell does not necessarily work for a model of another cell, as for example computational rules of CA1 versus CA2 pyramidal cells in the hippocampus (Piskorowski and Chevaleyre, 2012).

1.8 Development and Maturation

Structures involved in the whisker system are still changing during the first month after birth. Active whisker movement in mice starts around postnatal (P) P11-P12 days (Wang and Zhang, 2008). In rats, the whisker response in the thalamus and in the cortex changes after birth. In older animals, thalamocortical units increase the response to adjacent whisker stimulation, while cortical units increases the response to principal whisker stimulation (Shoykhet and Simons, 2008). Also the response latencies to

whisker stimulation decreases in the thalamus and in the cortex during maturation (Shoykhet and Simons, 2008).

The barrel cortex is still changing during the first weeks and needs sensory information for proper maturation. Trimming whiskers in rats at birth (Simons and Land, 1987), or even at P12, changes the response of the cortex (Shoykhet et al., 2005) and the ability to use the whisker system properly in surface discrimination tests between rough surfaces (Carvell and Simons, 1996).

The embryological origin of the thalamus is the diencephalon, which will be divided in a ventral part or hypothalamus, and a dorsal part or dorsal thalamus (Jones, 2007). The main nuclei of the thalamus can be recognized at embryonic (E) E20 in rats, but the differentiation of individual nuclei does not finish until the first week after birth (Jones, 2007). Almost all relay cells in the mouse thalamus are born between E10 and E16 (Jones, 2007). Projections from the thalamus reach the cortex at E13, whereas projections from the cortex reach the thalamus at E14.5-E15 (Auladell et al., 2000).

Relay cell maturation occurs during the first month. In the first two weeks, relay cells decrease the membrane time constant, the input resistance and the resting membrane potential (Warren and Jones, 1997). The morphology of relay cells also changes. In the ventral posterior nucleus of mice, relay cells increase the number of primary dendritic branches during the first 3 weeks (Warren and Jones, 1997). Relay cells undergo sensory dependent synaptic pruning and changes in the synaptic response (Wang and Zhang, 2008). Axons of relay cells are myelinated during maturation. The process finishes around week 4. The myelination changes the latency of the response in the cortex (Shoykhet and Simons, 2008).

In mice, VPM driver synaptic maturation occurs during the first month (Arsenault and Zhang, 2006). VPM relay cells receive less lemniscal fibers after the second postnatal week (Arsenault and Zhang, 2006; Wang et al., 2011). Stimulation of the leminiscal pathway in acute brain slices of VPM relay cells at different age showed EPSC amplitude decreases during the second postnatal week, but the strength of depression does not change

(Arsenault and Zhang, 2006). The AMPA/NMDA ratio changes during the first 3 weeks (Arsenault and Zhang, 2006; Wang et al., 2011). The NMDA decay constant decreases and the relay cell response become less sensitive to ifenprodil, a NR2B/NR1 receptor blocker (Arsenault and Zhang, 2006; Liu et al., 2004; Williams, 1993). The decrease of NR2B subunits is a characteristic of maturation in others areas of the brain (Robert W Gereau and Swanson, 2008), and is related to sensory stimulation, like visual stimuli to the cortex (Erisir and Harris, 2003; Quinlan et al., 1999). So far, there is no information about maturation at the level of single synapses in first order or higher order nuclei of the thalamus.

1.9 Aims of the Study

The aims of this study are to describe the synaptic properties of Pr5-VPM synapses, to generate an *in silico* model of relay cells that includes the location of driver synapses, and to describe the maturation of L5B-POm synapses.

A previous study described the synaptic properties of the L5B-POm synapse (Groh et al., 2008), but this synapse conveys cortical information. However, there is no information about the response of relay cells to stimulation of a single synapse transfering sensory inputs. Relay cells in VPM, via Pr5-VPM synapses, receive sensory information related to the whisker system, a known system to study sensory processing (Diamond and Arabzadeh, 2013). The thalamus receives sensory information and changes the properties of the information to be sent to the cortex (Deschênes et al., 2003; Fanselow and Nicolelis, 1999; Golomb et al., 2006; Sosnik et al., 2001) probably in the relay cells, although it is not clear whether these changes are the response to the computation process of relay cells, or whether they appear already at the level of single synapses. The first part of this thesis describes the properties of Pr5-VPM synapses and whether this first order synapse shows large amplitude, depression and spike generation, as in higher order synapses.

Several currents are involved in spike generation (Huguenard and Mccormick, 1992; Sherman and Guillery, 2009). I_A is a fast potassium outward current (Huguenard and Mccormick, 1992). I_A affects the depolarization by stimulation (Huguenard and Mccormick, 1992; Sherman and Guillery, 2009), but it is not clear how this current alters the response to a sensory stimulus. I_A is generated by the opening of Kv1, Kv3 or Kv4 voltage-gated potassium channels (Norris and Nerbonne, 2010). In VPM, Kv4.3 subunits are localized in the postsynaptic site of large synapses localized in the first branches of dendrites (Giber et al., 2008), probably the same Pr5-VPM synapses that carries the sensory information. This project aims to determine the subunit composition of I_A and the role of the I_A in the excitatory postsynaptic potential (EPSP) generated in the relay cell following stimulation of a single large terminal.

Single relay cells of VPM and POm receive more than one large terminal (Liu et al., 1995; Spacek and Lieberman, 1974; Veinante and Deschênes, 1999; Williams et al., 1994). The goal of this work is to describe the response of relay cells to stimulation of single terminals, but we decided to use *in silico* models to explore the relay cell response to stimulation of more than one terminal, and how the information is transformed at the level of relay cells.

Finally, a previous study showed that L5B-POm synapses in rats have large amplitude, short-term depression and generate a spike response (Groh et al., 2008). It is not known whether mice L5B-POm synapses have the same response. If we want to describe this synapse in more detail we need some tools to alter its normal function. Even though it is possible to genetically manipulate rats (Geurts et al., 2009; Homberg et al., 2007; Sun et al., 2013), mice offer more options and tools, like a larger library of genetically modified mice (Feng et al., 2000; Gavériaux-Ruff and Kieffer, 2007; Li et al., 2013; Liao et al., 2010; Zembrzycki et al., 2013). The last part of the thesis describes the properties of L5B-POm synapses in mice. It also describes the properties of L5B-POm synapses during maturation, in order to determine whether the L5B-POm synaptic properties appear already at birth or later, considering that the whisker system also has maturation changes (Mosconi et al., 2010).

CHAPTER 2

Materials and Methods

2.1 Drugs Used

In acute brain slices recordings we used the sodium channel blocker TTX (AbcamBiochemicals, 1 μM) (Lee and Ruben, 2008), general potassium channel blockers TEA (Sigma, 20 mM) (Khodakhah et al., 1997), general I_A current blocker 4-Aminopyridine or 4-AP (Ascent Scientific, 5 mM) (Thompson, 1982), Kv4.3 blocker phrixotoxin-2 (Sigma, around 1 μM) (Diochot et al., 1999), Na^+ channel blocker QX-314 (Tocris Bioscience, 5 mM) (Schwarz and Puil, 2002; Strichartz, 1973), and AMPA desensitization blocker kynurenic acid (Tocris Bioscience, KYN, 1 mM) (Diamond and Jahr, 1997; Taschenberger et al., 2002). AMPA receptor blocker CNQX (Tocris Bioscience, 20 μM) (Groh et al., 2008; Honoré et al., 1988). NMDA receptor blocker APV (Tocris Bioscience, 50 μm) (Groh et al., 2008; Morris, 1989).

2.2 Virus Generation And Production

cDNA of synaptophysin-EGFP (Wimmer et al., 2004) was subcloned into a pAM plasmid that had an adeno-associated virus 2 (AAV2) inverted terminal repeats and a cassette with a 1.1 kb cytomegalovirus enhancer/chicken β-actin promoter (Garg et al., 2004), the woodchuck post-transcriptional regulatory element (Zufferey et al., 1999) and the bovine growth hormone polyA (Groh et al., 2008; Wimmer et al., 2004).

Virus particles were produced transfecting $4 * 10^6$ HEK293 cells (Cell Biolabs, San Diego, CA) in DMEM (Gibco) on 14 cm cell culture dishes, The cells were transfected with a mixture of 125 mM $CaCl_2$, HBS (140 mM NaCl, 25 mM HEPES, 0.7 mM Na_2HPO_4, pH 7.05) and 37.5 µg DNA from pAM, pDP1rs and pDP2rs. Each dish received one drop of the mix. The medium was changed 24 hours later to stop transfection. Virus particles were harvested 3 days later. Cells were removed from the dish, pelleted (200 g, 10 min), resuspended in a lysis buffer (150 mM NaCl, 50 mM Tris-HCl, pH 8.5) and lysed via a three freeze/thaw cycle. Genomic DNA was removed by digestion with 500 units of benzonase endonuclease (Sigma) for 2 hours at 37°C. Pipetting dissolved the cell debris and the supernatant was passed by a 0.45 µm pore diameter filter. AAV particles were purified using a heparin-agarose column (Biorad, cat. no: 7321010). The column was washed with 10 ml equilibrium buffer (1 mM $MgCl_2$, 2.5 mM KCl in PBS, pH 7.2) and filled with 5 ml heparin-agarose (Sigma, cat. no.: H6508) and 10 ml of equilibrium buffer. The lysate was added to the column and incubated for 2 hours at 4°C on a shaker. Later the column was washed with 20 ml equilibration buffer, and the virus particles were eluted with 15 ml elution buffer (500 mM NaCl, 50 mM Tris-HCl, pH 7.2) into a filter tube (Amicon Ultra Filter, Milliore, Cat. no.: UFC9 100 24). The eluate was concentrated by centrifugation twice with 15 ml PBS. The virus particle solution was filtered (0.22 µm pore diameter), aliquoted and stored at +4°C (Körber, 2011).

2.3 Stereotaxic Injection

Stereotaxic setup: Model 1900 stereotaxic alignment system (David Kopf Instruments, California, USA) and an eLeVeLeR electronic leveling device (Wimmer et al., 2004). The coordinates were corrected by brain size from those obtained from the books "The Mouse Brain in Stereotaxic Coordinates" (Paxinos and Franklin, 1997) and from "The Rat Brain in Stereotaxic Coordinates, 2nd edition" (Paxinos and Watson, 1986).

2.3.1 Injection of Pr5 in Rats

12 day-old rats were used for virus particle injection. They were anesthetized with 5% mix isoflurane (Baxter, Deerfield, IL) / oxygen (Vaporizer Isotec4, Surgivet, Dublin, OH) for 2 minutes. Local anesthesia, 1% lidocain, was added to the surface of each ear and in the surface of the skull. 100 μl of subcutaneous lidocain 1% was injected to the head. The rodent was tested for reflexes before executing the incision. The local anesthetic mix isoflurane/oxygen was decreased to 2%. The skin was open, bregma and lambda marked, and the position of the head was corrected using the eLeVeLeR. 1.5 μl of virus was loaded to a capillary glass. The skull was drilled in the desired coordinate. The capillary glass with the virus was connected to a 50 mL syringe and fixed to and adapter in the same position of the stereotaxic ocular. The virus was injected evenly in 3 coordinates in the brain (Table 2.1). Sometimes the rat bled, and the blood was removed with small cotton triangles. The virus was added by positive pressure. The virus was added slowly and after waiting for 2 minutes the capillary glass was moved out and placed to the other coordinates. The total time of the procedure was around 30 minutes for each animal. The rats where injected in Pr5 and it was possible to see the expression of EGFP in VPM after one or two weeks (Figure 2.1).

X	Y	Z
-1.9	- 6.8	- 8.1
- 1.6	-6.5	-7.8
- 1.6	-7.2	-7.8

Table 2.1: Rat Stereotaxic Coordinates

X	Y	Z
- 3	0	- 0.6
- 3	- 0.4	- 0.6
- 3	- 0.8	- 0.6
- 3	0.4	- 0.6
- 3.3	- 0.4	- 0.6
- 3.3	- 0.8	- 0.6

Table 2.2: Mouse Stereotaxic Coordinates

2.3.2 Injection of Deep Cortical Layers in Mice

The mouse procedure required some small changes. Mice younger than 2 weeks were anesthetized with a 5% isoflurane mix as with rats, while mice older than 2 weeks were placed first in a chamber with an enrichment isoflurane environment until the mouse stoped moving. For P12 or older animals, before the animal was put in the stereotaxic setup, the hair of the top of the head was removed with an electric trimmer. For P10 or younger animals, a blunt ear bar was used, and held by pressure of the head, not the ear. P12 mice were injected in the L5B with the coordinates in Table 2.2. The coordinates used for younger animals were based on Table 2.2 but corrected for bregma-lambda distance, z-distance from bregma to the injection site, and for overall size of the head. It was possible to see the expression of EGFP in POm after one or two weeks (Figure 2.2a).

2.4 Preparation of Acute Brain Slices

Rats or mice previously injected with adeno-associated virus particles (AAV) were decapitated. Brains were removed in ice-cold slicing solution (ACSF slicing solution, Table 2.4). Coronal sections of a 150 μm thickness, at the level of the thalamus were prepared on a Leica VT1200S vibratome. The slices where done with a speed of 0.08 mm/s. The slices were stored in artificial cerebrospinal fluid (ACSF) bath solution (Table 2.4). The slices were kept in a bubble solution all the time with an O_2/CO_2 mix. They were stored for 30 minutes at 37°C and 30 minutes at room temperature before use.

2.5 Electrophysiology

2.5.1 Recordings from VPM Relay Cells

Patch-clamp recordings were established in VPM relay cells from acute brain slices from P24-P32 rats (EPC-10 amplifier and PatchMaster software, HEKA Electronics). The brain slice was perfused continuously at 2.2 ml / min with the recording solution (Table 2.4). Spontaneous activity data were filtered at 2.9 Khz, whereas all the other data were filtered at 10 Khz (Bessel filter, HEKA amplifier). The data were digitalized at 20 Khz (current injection experiments), 40 Khz (spontaneous activity experiments) or 100 Khz. The slice was bathed with the specific ACSF solution at room temperature (Table 2.4). The solution was bubbled with a O_2/CO_2 mix. The VPM was recognized in transmitted light as an area ventral to the hippocampus and medial to the reticular nucleus of the thalamus (Figure 2.1a). The expression of synaptophysin-EGFP was visible in fluorescent light and in confocal images (SP5 Leica infrared scanning gradient contrast (IR-SGC) and confocal system, Leica Mikrosysteme Vertrieb GmbH, Germany). Cells close to synaptophysin-EGFP labeled terminals were patched with a pipette with high K^+ internal solution or Cs^+ internal solution containing 0.03 mM alexa 594 (Molecular Probes, Table 2.5, Figure 2.1b). The relay cell potential

was held at -60 mV in the whole-cell voltage clamp mode, or at different potentials in current clamp mode using LFVC (low frequency voltage clamp, in patchmaster) (Peters et al., 2000) . We used only relay cells that had large labeled terminals close to the soma and or the first dendritic branches. In general, for all the experiments where we used specific blockers, we made the specific experiment in ACSF, changed the solution by ACSF plus the specific drug and we waited for at least 10 minutes before repeating the experiment in presence of the drug.

2.5.1.1 Isolation of Potassium Currents of VPM Relay Cells

We used acute brain slices in a bathing ACSF normal solution (Table 2.4). We recorded the response of relay cells to voltage steps. We added 1 μM TTX and 20 mM TEA to the external solution to block the fast sodium current and the slow inward potassium current. After 10 minutes we recorded the response of relay cells to the same voltage steps. We added 5 mM 4-AP to the external solution to block I_A and we let it run for 10 minutes. We compared the response of the relay cells to voltage steps protocols with and without the fast outward potassium current blocker 4-AP. The current difference was considered as the I_A. We also used around 1 μM 2-phrixotoxin instead of 4-AP to obtain the Kv4.3 dependent I_A fast outward potassium current. The liquid junction potential was 13.8 mV, but the recordings were not corrected.

2.5.1.2 Recording of VPM Relay Cells Response to Stimuli

Labeled terminals were stimulated with a double-barrel stimulation pipette (10 to 90 μs, 20 to 70 V) filled with normal ACSF (Table 2.4) and 0.03 mM alexa 594. We only used those responses in which we saw a clear time difference between the stimulus artifact and the EPSC. We increased the stimulus duration and amplitude until we saw a response. Increasing the amplitude of the stimulus did not change the response amplitude. The stimulus pipette was closer than 1 μm from the labeled terminal (Figure 2.1b). Slight movement of the pipette generated a loss of the stimulus response.

In some experiments we used 10 μM CNQX to block AMPA receptors (Groh et al., 2008; Honoré et al., 1988) or 50 μM APV to block NMDA receptors (Groh et al., 2008; Morris, 1989). We added the drug in the bath solution and waited for 10 minutes before doing the recordings.

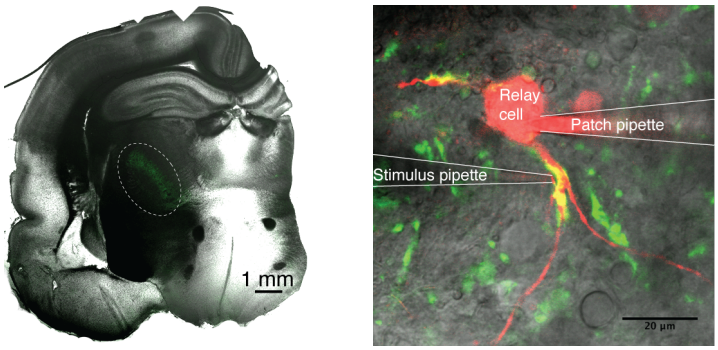

(a) Acute brain slice

(b) Relay cell and labeled terminals

Figure 2.1: EGFP expression in Pr5-VPM synapses
(a) Visualization of expression of EGFP in thalamus, after two weeks of incubation. VPM nucleus outlined by a circle. (b) Multichannel confocal image of relay cell and labeled terminals. Relay cell from the VPM labeled using a patch pipette with alexa 594 (red) and labeled terminals expressing synaptophysin-EGFP (green). Patch pipette and stimulus pipette labeled with alexa 594 (red). Slice morphology was visualized with infrared scanning gradient contrast (IR-SGC).

2.5.2 Recordings from POm Relay Cells

We followed the same procedure as with VPM relay cells from rat, but we used acute brain slices from P8-P56 mice. The POm was recognized by the expression of synaptophysin-EGFP in fluorescent light and confocal images (SP5 Leica infrared scanning gradient contrast (IR-SGC) and confocal system, Leica Mikrosysteme Vertrieb GmbH, Germany). Cells close to synaptophysin-EGFP labeled terminals were patched with a pipette with high K^+ internal solution or Cs^+ base internal solution (Table 2.5). Both internal solutions contained 0.03 mM alexa 594. The relay cell potential was fixed at the specific potential in the whole-cell voltage clamp mode,

or using LFVC (Peters et al., 2000) in current clamp mode. We used only relay cells that had large labeled terminals close to the soma and or the first dendritic branches. Labeled terminals were stimulated with a double-barrel stimulation pipette (10 to 90 μs, 20 to 70 V) filled with normal ACSF (Table 2.4) and 0.03 mM alexa 594 (Figure 2.2b).

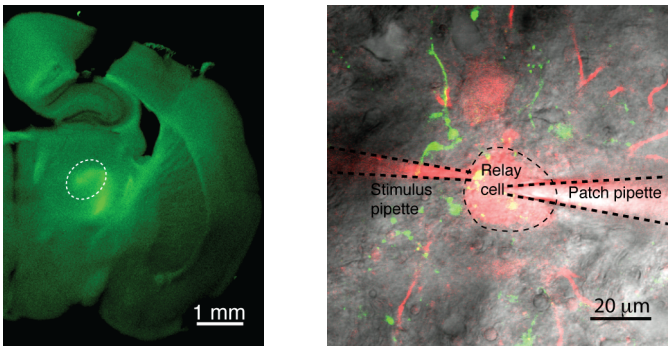

(a) Acute brain slice **(b)** Relay cell and labeled terminals

Figure 2.2: EGFP expression in rosebud synapses
(a) Visualization of the expression of GFP in thalamus, after two weeks of incubation. POm nucleus is outlined by a circle. (b) Multi-channel confocal image of relay cell and labeled terminals. Relay cell from the POm labeled using a patch pipette with alexa 594 (red) and labeled terminals expressing synaptophysin-EGFP (green). Patch pipette and Stimulus pipette labeled with alexa 594 (red). Slice morphology was visualized with infrared scanning gradient contrast (IR-SGC).

2.5.3 Data Analysis

For the L5B-POm synapse maturation project passive properties data (Figure 3.22) and spontaneous responses (Figure 3.24) show a clear difference between the data from the 2 first postnatal weeks and older animals. We separate the data in 2 week bins.

All the data was measured with custom made routines using Igor Pro (Wavemetrics Inc., Lake Oswego, OR). The data was analyzed using Prism software (GraphPad software Inc., California) with 1-way ANOVA and Bonferroni post test, or student t-test.

2.6 VPM Relay Cell *In Silico* Model

2.6.1 Current Curves

We used the activation and inactivation kinetics of fast Na^+ currents, delayed K^+ currents, I_T, I_A and I_h from previous works (Antal et al., 1996; Mccormick and Huguenard, 1992; Rhodes and Llinás, 2005), using a HH-type model (Sterratt et al., 2011). The code was written in nmodl (Hines and Carnevale, 2000), to be used in the Neuron simulation environment (Carnevale and Hines, 2006; Hines and Carnevale, 1997; Hines and Carnevale, 2001), or as functions in Igor Pro (Table 2.3).

2.6.2 Single Cell Model

We created a single compartment model in Igor Pro. The model was used to test the basic properties of relay cells, like burst and tonic firing (Sherman and Guillery, 2009).

2.6.3 Dendritic Branches Model

We created a multiple compartment model in the Neuron simulation environment. The model had soma and 4 branches with 2 apical dendrites each. We added a fast Na^+ current, a delayed K^+ current, I_T, I_A and I_h (Table 2.3). We modeled synaptic inputs using alpha-synapses (Carnevale and Hines, 2006; Sterratt et al., 2011) to model response of the relay cell to a different number of inputs.

2.6.4 Relay Cell Model

2.6.4.1 Neuronal Morphology

We obtained a stack of confocal images with synaptophysin-EGFP labeled terminals and alexa 594 labeled relay cells from a patch clamp experiment. We used a Leica SP5 microscope to obtain the images. The images were processed in FIJI (Schindelin et al., 2012) using the Bio-Formats plugin

(Linkert et al., 2010). We traced the 3D morphology of the relay cells using the 3D filter plugin (Ollion et al., 2013) and the simple neurite tracer plugin (Longair et al., 2011). We used the Segmentation editor plugin to trace the soma shape. We combined the soma and dendrites to create a template and we isolated the relay cell from the background. We saved the filtered relay cell in a multi-image TIFF file. We segmented the isolated relay cell using the 3D segmentation plugin (Ollion et al., 2013) in FIJI.

We used the Neuron simulation environment (Carnevale and Hines, 2006) to model neuron morphology and the distance of terminals to the soma. First we reconstructed the isolated relay cell from the multi-image TIFF file using NeuronStudio software (Wearne et al., 2005) and we exported the tree information as a hoc file, ready to be used in the Neuron simulation environment. We separated each branch or section of the neuron in different internal nodes (Carnevale and Hines, 2006) using a home made hoc procedure that considers the δ-lambda rule (Carnevale and Hines, 2006; Hines and Carnevale, 2001). We considered only odd numbers of internal nodes to facilitate the calculation (Appendix A.1).

2.6.4.2 Passive Parameters of Relay Cell

The axial or cytoplasmic resistivity was set to 35.4 Ωcm. The membrane capacitance is conventionally assumed to be 1 μm F/cm^2, but recent experiments suggest a value of 0.9 μm F/cm^2 in neuronal cells (de Schutter, 2010; Gentet et al., 2000). We used 1 μm F/cm^2 as membrane capacitance in the model. We added a passive leak conductance of 0.0002 S / cm^2 with
- 60 mV leakage equilibrium potential.

2.6.4.3 Voltage-Dependent Currents Distribution in the Relay Cell Model

We combined the hoc file describing the morphology of the relay cell (Appendix A.1) with nmodl (Hines and Carnevale, 2000) files describing the activation and inactivation kinetics of fast Na^+ currents, delayed K^+ currents, I_T, I_A and I_h (Table 2.3) (Antal et al., 1996; Mccormick and Huguenard, 1992; Rhodes and Llinás, 2005). We divided the relay cell in soma, basal and

apical dendrites. We determined the conductance of each current in the compartments by trial-and-error until we could mimic the burst and tonic response of relay cells to a voltage-step protocol.

2.6.4.4 Labeled Terminal Location

We used the 3D filter plugin (Ollion et al., 2013) and the 3D segmentation plugin (Ollion et al., 2013) in FIJI to isolate labeled terminals from the background. We used segmented relay cells and segmented labeled terminals and the 3D segmentation plugin (Ollion et al., 2013) with home made scripts to isolate terminals close (0 μm) to the relay cell.

We combined the isolated relay cell and isolated terminals close to the relay cell in a single stack using FIJI and we determined the position of the terminals by visual inspection using the Fiji 3D viewer plugin or the Vaa3D software (Peng et al., 2010). Home made hoc procedures calculated the distance from the synaptic input to the soma (Appendix A.3).

2.6.4.5 Labeled Terminal Stimulation

We added the synapses location to the relay cell model (Appendix A.3). We modeled the synapses with alpha functions (Carnevale and Hines, 2006; Sterratt et al., 2011), where g_{syn} was the synaptic conductance over time, $\bar{g}_{syn}$ was the maximum conductance calculated from the EPSC response at - 60 mV (0.016 μS), τ was 1.5 ms and t is time.

$$g_{syn}(t) = \bar{g}_{syn} \times \frac{t}{\tau} \times \exp(1 - \frac{t}{\tau}) \tag{2.1}$$

We recorded the voltage response in the soma of the model cell to the stimulation of one, two or three of the terminals at different resting membrane conditions (Appendix A.4).

Current	Property
Na^{2+} current	$\alpha_m = 0.32 \times \frac{13.1-(v+40)}{\exp(\frac{(13.1-(v+40))}{4.0})-1}$ $\beta_m = 0.280 \times \frac{(v+40)-40.1}{\exp(\frac{(v+40)-40.1}{5.0}-1)}$ $m_\infty = \frac{\alpha_m}{\alpha_m+\beta_m}$ $\tau_m = \frac{1}{\alpha_m+\beta_m}$ $\alpha_h = 0.128 \times \exp(\frac{17-v}{18})$ $\beta_h = \frac{4}{1.0+\exp(\frac{40-v}{5.0})}$ $h_\infty = \frac{\alpha_h}{\alpha_h+\beta_h}$ $\tau_h = \frac{1}{\alpha_h+\beta_h}$ $g_{Na} = g_{max,Na} \times m^2 \times h$
K^+ current	$\alpha_n = 0.16 \times \frac{35.1-(v+20)}{\exp(\frac{35.1-(v+20)}{5.0})-1}$ $\beta_n = 0.250 \times \exp(\frac{20-v)}{40.0})$ $n_\infty = \frac{\alpha_n}{\alpha_n+\beta_n}$ $\tau_n = \frac{1}{\alpha_n+\beta_n}$ $g_K = g_{max,K} \times m$
I_T	$m_\infty = \frac{1.0}{1.0+\exp(-\frac{v+50)}{5})}$ $\tau_m = 2.44 + 0.02505 \times \exp(-0.0984 \times v)$ $h_\infty = \frac{1.0}{1.0+\exp(\frac{v+83.5)}{4.0})}$ $\tau_h = 7.66 + 0.02866 \times \exp(-0.1054 \times v)$ $g_{I_T} = g_{max,I_T} \times m^3 \times h$

I_A	$m_\infty = \frac{1.0}{1.0+\exp(-\frac{v-(-60)}{8.5})}$
	$\tau_m = 0.67$
	$h_\infty = \frac{1.0}{1.0+\exp(\frac{v-(-78)}{6})}$
	if (v $\geq$ - 63), $\tau_h = 7.0$
	if (v $<$ - 63), $\tau_h = \frac{0.33}{\exp(\frac{v-(-46)}{5})} + \exp(-\frac{v-(-238)}{37.5})$
	$g_{I_A} = g_{max,I_A} \times m \times h$

I_h	$m_\infty = \frac{1.0}{1.0+\exp(\frac{v+75)}{7.5})}$ if (v $>$ - 77.5), $\tau_m = \frac{120820}{\exp(0.061 \times v)}$ else, $\tau_m = \frac{29.54}{\exp(-0.046 \times v)}$ $g_{I_h} = g_{max,I_h} \times m^3$

Table 2.3: Ion channel kinetics

Solution	Compounds, in mM
Slicing	85 NaCl, 2.5 KCl, 25 Glucose, 25 $NaHCO_3$, 1.25 NaH_2PO_4, 75 Sucrose, 0.5 $CaCl_2$, 7 $MgCl_2$
ACSF bath	109 NaCl, 5 KCl, 10 Glucose, 25 $NaHCO_3$, 1.25 NaH_2PO_4, 1.5 $CaCl_2$, 1.3 $MgCl_2$, 20 HEPES
Normal ACSF	125 NaCl, 2.5 KCl, 25 glucose, 25 $NaHCO_3$, 1.25 NaH_2PO_4, 2 $CaCl_2$, 1 $MgCl_2$

Table 2.4: External solutions

Solution	Compounds, in mM
High K^+	130 K^+ gluconate, 20 KCl , 5 Na_2 phosphocreatine, 10 HEPES, 5 EGTA , 4 Mg-ATP, 0.5 GTP, 0.03 Alexa 594.
Cs^+ base	120 Cs^+ gluconate, 10 HEPES, 10 Na_2 phosphocreatine, 10 Na^+ gluconate, 4 ATP-Mg, 4 NaCl, 0.3 GTP, 0.1 EGTA, 0.1 spermine, 2.5 QX- 314

Table 2.5: Internal solutions

CHAPTER 3

Results

3.1 Pr5-VPM Synapses

3.1.1 Minimal Synaptic Transmission in Pr5-VPM Synapses

Relay cells receive driver and modulatory inputs. We decided to measure the response of VPM relay cells to the spontaneous release from the synapses (Figure 3.1a). Spontaneous events had an amplitude of 22.31 $\pm$ 0.75 pA and a frequency of 4.616 $\pm$ 1.3 events/s (average of 22 cells). Cells also showed multi spontaneous events (Figure 3.1b), where the amplitude of the events is two or more times larger than the smaller events. It is possible these events are due to different glutamatergic inputs contacting the same relay cell.

We calculated the quantal size of the Pr5-VPM synapse. Spontaneous events are considered unitary events equivalent to the quantal size of the synapse. Relay cells receive driver but also modulatory synapses, and the spontaneous response could be due to the spontaneous release from modulatory synapses. We measured the minimal stimulation response of relay cells to stimulation of labeled terminals in a low calcium medium

(Figure 3.1c and Figure 3.1d), where almost 20% of the stimulation gave no response. The evoked response, or quantal size, had an amplitude of 32 pA, almost twice that of the spontaneous release.

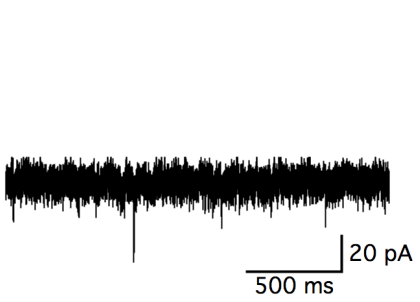

(a) Spontaneous activity

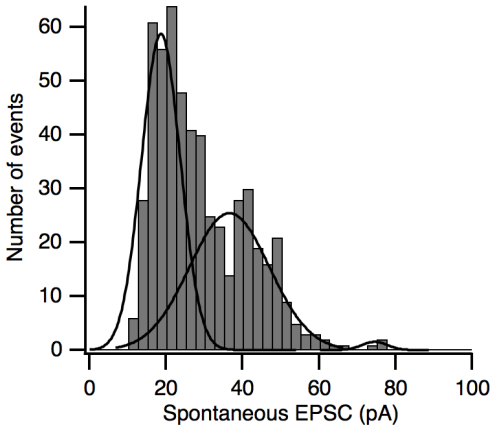

(b) Histogram spontaneous activity

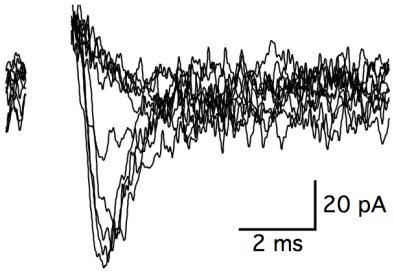

(c) Ekoved response in low calcium solution

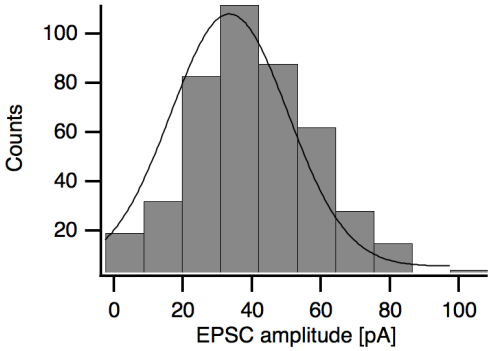

(d) Histogram evoked response

Figure 3.1: Minimal synaptic transmission in Pr5-VPM synapses
(a) Spontaneous activity of a relay cell. External solution was normal ACSF. (b) Histogram of spontaneous activity in a relay cell. Gaussian curve showing 2 peaks. (c) Evoked response in presence of low calcium in the external solution. (d) Distribution of amplitude of EPSC in a low calcium medium. All the experiments were done in whole-cell voltage clamp with a - 60 mV holding membrane potential. Patch pipette filled with high potassium base internal solution.

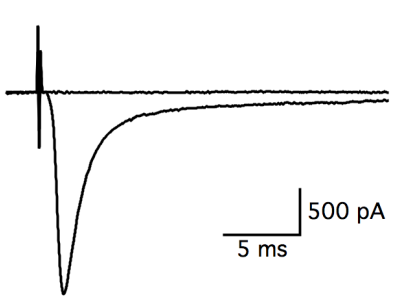

(a) EPSC

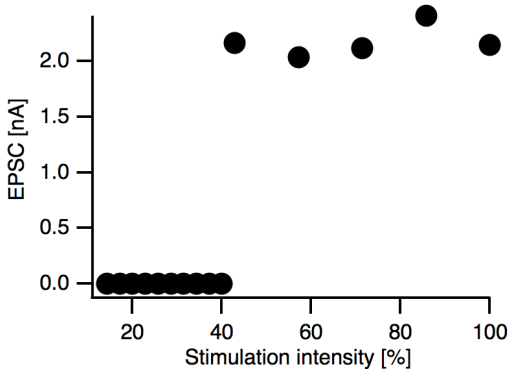

(b) All-or-none response

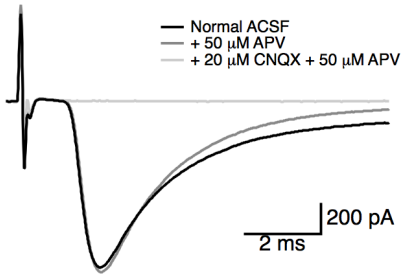

(c) EPSC with CNQX or APV

Figure 3.2: Synaptic transmission of Pr5-VPM synapses
(a) EPSC response of relay cell to different stimuli amplitudes in labeled terminals. (b) Plot of the EPSC response versus amplitude response of a relay cell to different stimuli amplitudes in labeled terminals. (c) Evoked EPSC response of a relay cell in presence of 20 mm CNQX and 50 μM APV (light gray), 50 μM APV (grey) or normal ACSF (black) in the bath solution. All experiments done in whole-cell voltage clamp with -60 mV holding membrane potential. High potassium base internal solution.

3.1.2 Synaptic Transmission of Pr5-VPM Synapses

The response of relay cells to stimulation of labeled terminal was recorded using the patch-clamp technique. Whole-cell recordings showed an all-or-none response to variation in stimulus amplitude (Figure 3.2a and Figure 3.2b). Responses of relay cells to 0.5 Hz stimulation of labeled terminals

generated an average excitatory postsynaptic current (EPSC) of 0.99 $\pm$ 0.24 nA, rise time of 0.41 $\pm$ 0.03 ms and average decay time of 1.92 $\pm$ 0.24 ms (average of 15 cells, Figure 3.2c). The quantum content per stimulus was 31, and was considered as the amplitude of EPSC (0.99 nA, Figure 3.2c) divided by the amplitude of the minimal stimulation response (32 pA, Figure 3.1d). The values of the response of the relay cell to the stimulus of a single terminal was consistent with a large terminal forming a giant synapse.

The Pr5-VPM synapse has a large AMPA receptor component. In the presence of 20 μM of the AMPA - kainate blocker CNQX (Groh et al., 2008; Honoré et al., 1988) the EPSC was almost abolished. On the contrary, 50 μM of the NMDA channel blocker APV (Groh et al., 2008; Morris, 1989) failed to diminish the amplitude of the EPSC at a holding potential of - 60 mV, but it decreased the slower component (Figure 3.2c), suggesting that NMDAR are present in the Pr5-VPM synapse.

3.1.3 Short-term Plasticity of Pr5-VPM Synapses

Large Pr5-VPM synapses showed depression during trains of high frequency stimulation. Train of stimuli of 10 Hz or more generated an EPSC depression in the relay cells response (Figure 3.3a and Figure 3.3b). The effect of the depression was stronger at higher stimulation frequencies (Figure 3.3b, from 10 Hz to 100 Hz stimulation). The response of the relay cell was composed of a fast and a slow component (Figure 3.3c).

We measured how much time the relay cells needed to recover from depression. We used a paired pulse protocol to determine the interval between 2 stimuli in which the first one does not affect the amplitude of the second one (Figure 3.3d). We increased the inter-stimulus interval until 500 ms. Pr5-VPM synapses recovered 80% of its EPSC amplitude with intervals of 400 ms between stimuli. The time response was close to those in other relay cells of the thalamus (Groh et al., 2008).

Short-term depression can be generated by pre or post synaptic mechanisms (Fioravante and Regehr, 2011; Von Gersdorff and Borst, 2002). A

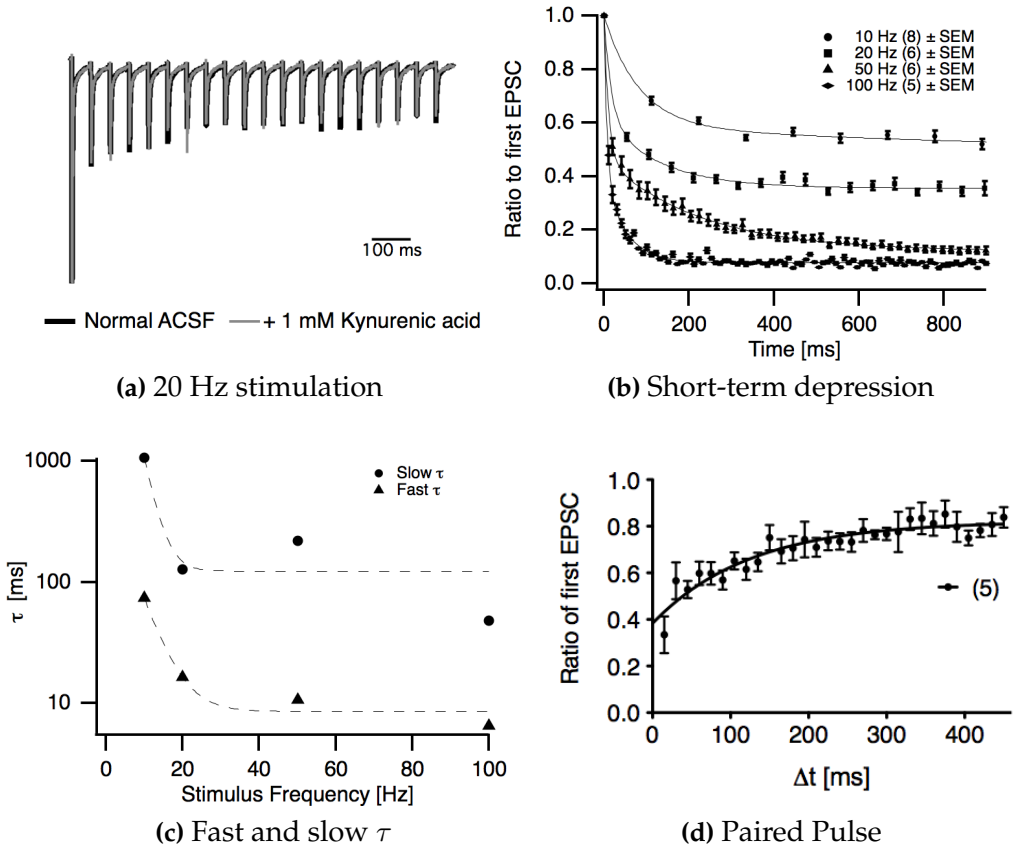

(a) 20 Hz stimulation

(b) Short-term depression

(c) Fast and slow τ

(d) Paired Pulse

Figure 3.3: Synaptic plasticity in Pr5-VPM synapses
Response of relay cell to high frequency stimulation of labeled terminals. (a) Example of response of a relay cell to 20 Hz stimulation in labeled terminals. In gray, response in the presence of 1 mM kynurenic acid; in black, response in normal ACSF conditions. (b) Graph showing the normalized evoked response of relay cells to different frequency of stimulation. Normalization of the first stimulus compared to the others. Average and SEM. In parentheses number of cells analyzed. (c) Fast and slow exponential τ constants. (d) Graph showing Paired-pulse ratios. Average of 5 cells and SEM. All the experiments done in whole-cell voltage clamp at - 60 mV holding membrane potential. External solution was normal ACSF, and high potassium base internal solution.

postsynaptic mechanism is the desensitization of AMPA receptors. We used 1 mM KYN, a known inhibitor of saturation and desensitization of AMPA receptors (Diamond and Jahr, 1997; Taschenberger et al., 2002;

Sun and Wu, 2001) to rule out possible postsynaptic mechanisms. Relay cells showed the same amount of depression with or without KYN (Figure 3.3a).

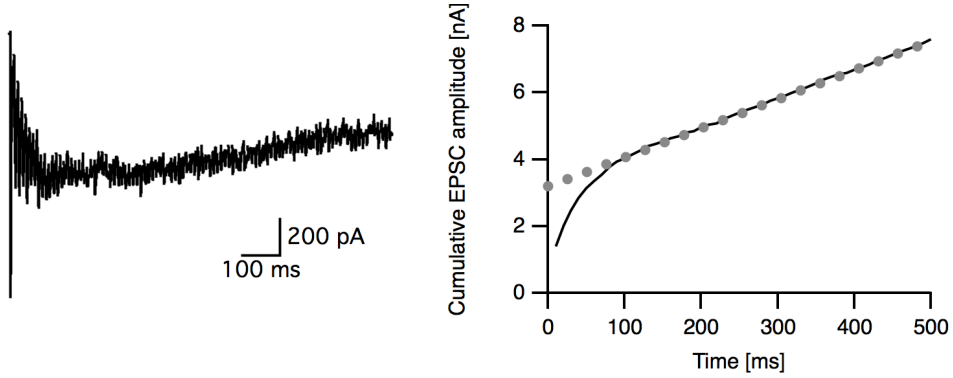

(a) 100 Hz stimulation **(b)** Cummulative EPSC response

Figure 3.4: Vesicle release pool in Pr5-VPM synapses
Estimation of vesicle pool size. (a) Example of responses of relay cells to 100 Hz stimulation in labelled terminals. (b) Cumulative EPSC response of (a), and linear function of points between 200 and 800 ms. Back-extrapolation of linear function to 0 ms to estimate the total pool current (gray dots).

3.1.4 Size of the Readily Releasable Pool in Pr5-VPM Synapses

One explanation for the large amplitude of the evoked response of the Pr5-VPM synapse is the release of more than one vesicle as a response of a single terminal (Groh et al., 2008). We decided to calculate the vesicle pool size using values of quantal size (Figure 3.1d) and back extrapolation of a cumulative EPSC response of relay cells to 100 Hz stimulation (Figure 3.4). The vesicle pool size was 5.1 ± 1.3 nA (5 cells), corresponding to around 160 vesicles. With the vesicle pool size and the quantum content per stimulus we calculated a probability of release of 0.2 per single synaptic stimulus. The data shows a Pr5-VPM synapse with a low probability of release, as those found in calyx of Held (Branco and Staras, 2009; Meyer et al., 2001;

Sakaba et al., 2002; Schneggenburger et al., 1999).

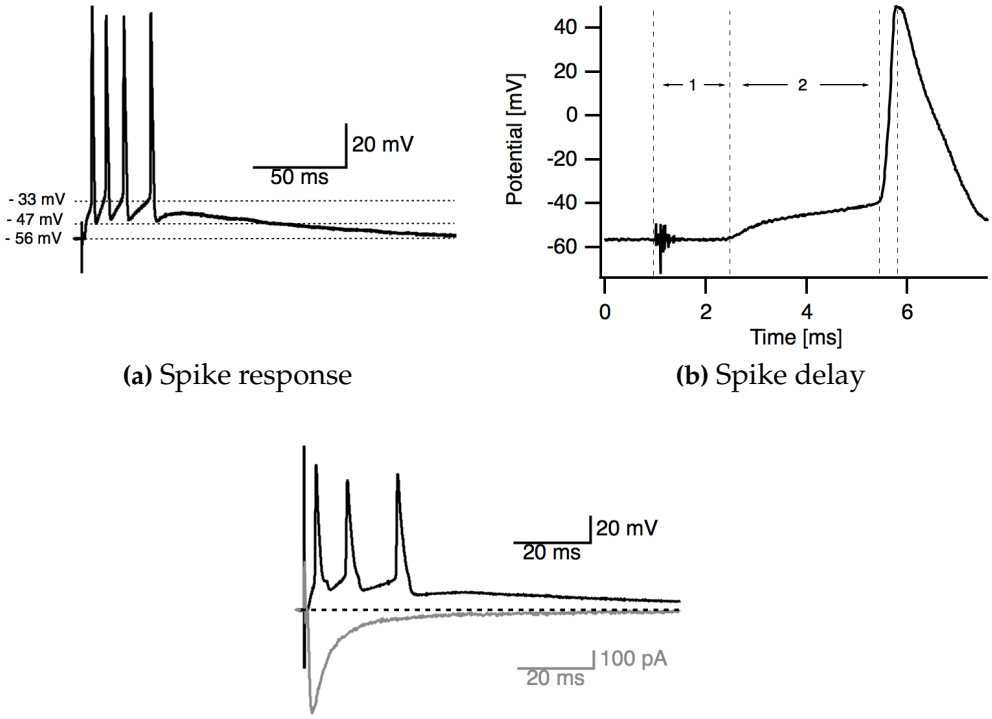

(a) Spike response

(b) Spike delay

(c) Spike and EPSC

Figure 3.5: Spike generation of Pr5-VPM synapses
Single stimulation of a labeled terminal generate spikes in the relay cell. (a) Spike response. (b) Increase magnification of (a). (c) Spike and EPSC response of the same cell.

3.1.5 Spike Response of VPM Relay Cells

The role of relay cells is to convey sensory and cortical information to the cortex (Sherman and Guillery, 2009). We tested if the large amplitude response of Pr5-VPM synapses was enough to generate spikes in the relay cell. A single stimulation of Pr5-VPM synapse could generate multiple spikes in the relay cells (Figure 3.5a). The spike delay had 2 components, 1) delay between time of stimulation and response of the relay cell and,

2) increase of membrane potential until reaching the threshold for spike generation (Figure 3.5b). The delay of the EPSC and of the first part of the spike delay was the same, but the EPSC length was shorter than the spike response (Figure 3.5c).

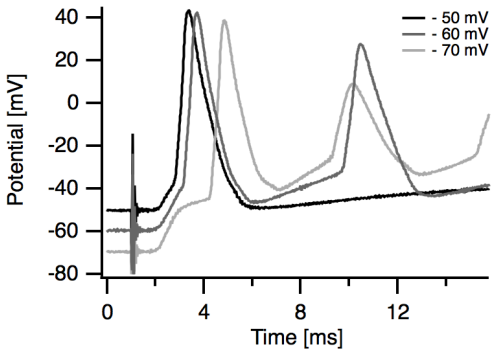

(a) Spike response at different membrane potentials

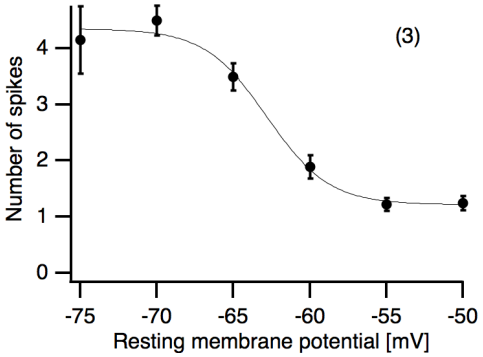

(b) Number of spike versus membrane potential

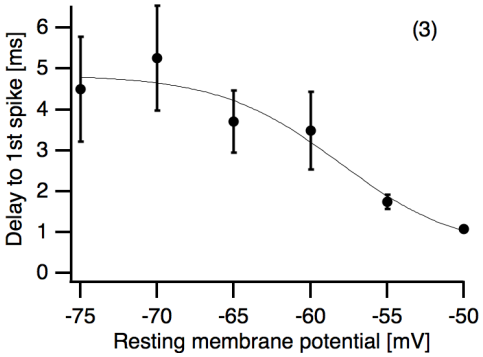

(c) Delay before spike versus membrane potential

Figure 3.6: Voltage-dependent spike response
(a) Response of a relay cell to a single synaptic stimulation at different membrane potentials. (b) Average number of spikes generated by a single synaptic stimulation at different membrane potentials. (c) Average response delay. In parentheses the number of cells analyzed.

3.1.6 Voltage Dependent Spike Response of VPM Relay Cells

Relay cells fire in tonic or burst mode depending on the resting membrane potential (Sherman and Guillery, 2009). We recorded the response of relay cells to stimulation of Pr5-VPM synapses at hyperpolarizing and depolarizing potentials (Figure 3.6a). The multiplication function of relay cells was membrane potential dependent. More hyperpolarized cells fired more spikes in response to a single stimulation (Figure 3.6b). The second part of the spike delay was also membrane potential-dependent. More depolarized relay cells showed a decrease in the time delay (Figure 3.6c). These results suggest that some properties related to the tonic or burst fire response of relay cells appears already at the level of single synaptic stimulation, and probably that I_T are involved in the increase of postsynaptic spike number at more hyperpolarized potentials.

3.1.7 Spike Plasticity of VPM Relay Cells

The number of spikes generated postsynaptically in response to stimulation of Pr5-VPM terminals was affected by the stimulation frequency (Figure 3.7). At 20 Hz, the number of spikes decreased by 20% after the four stimulus (Figure 3.7a and Figure 3.7d), while there was no spikes after the third stimulus at 100 Hz (Figure 3.7c). The ability to fire spikes was diminished at higher frequency of stimulation. Small EPSCs (20% of amplitude) could generate a postsynaptic spike response at 50 Hz (3rd and 4th response in Figure 3.7b), but not at 100 Hz (Figure 3.7c). Pr5-VPM had a frequency-dependent transfer function. A single EPSC could generate more than one postsynaptic spike (Figure 3.5). 20 Hz stimulation generated a 70 Hz response (four stimuli to a Pr5-VPM terminal in 200 ms generate fourteen postsynaptic spikes, Figure 3.7a), while a 50 Hz stimulus generated a 100 Hz response (four stimuli to a Pr5-VPM terminal in 80 ms generate eight postsynaptic spikes, Figure 3.7b). At 100 Hz there was no transfer function, and even no spike generation after the third stimulus (Figure 3.7c). This

suggest that the information received from Pr5 as a train of stimuli is transformed at the level of single synapses. It also suggests that at least for higher frequency of stimuli the depression seen in *in vivo* recordings of the VPM nucleus by whisker stimulation appears at the level of single synapses.

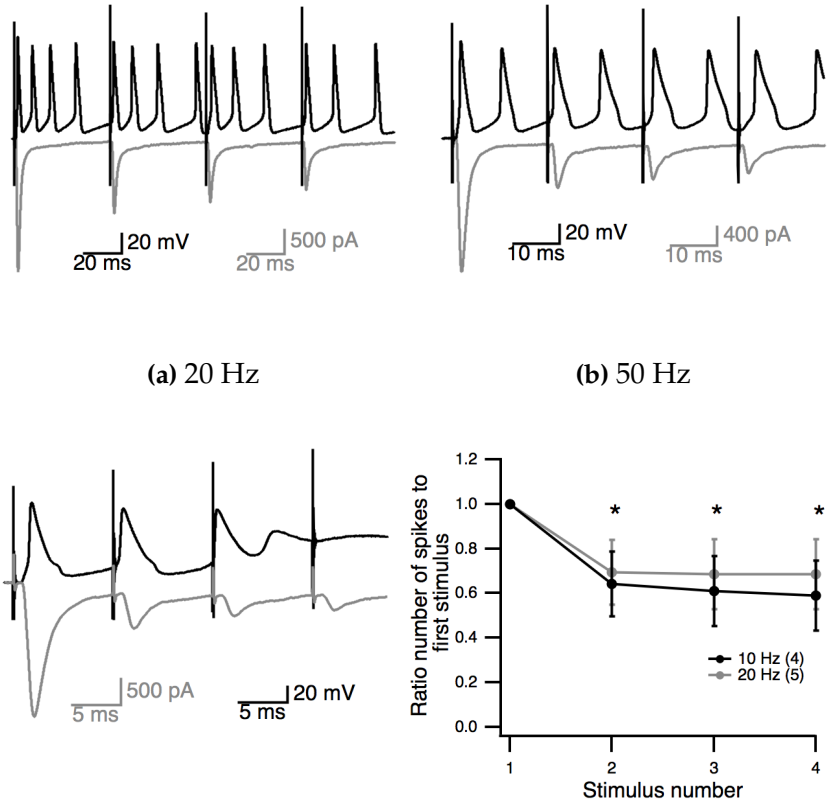

(a) 20 Hz

(b) 50 Hz

(c) 100 Hz

(d) Number of spikes versus stimulus number

Figure 3.7: Spike plasticity
Relay cell response to 20 Hz (a), 50 Hz (b) or 100 Hz (c) Pr5-VPM stimulation. On the top postsynaptic spike response, on the bottom EPSC response. (d) Change in the number of spikes generated per stimulus at 10 Hz (black) or 20 Hz (gray) Pr5-VPM stimulation. The number of spikes were normalized to the number of spikes generated by the first stimulus. In parentheses the number of cells analyzed. * significative difference ($p < 0.05$) compared to the first stimulus. T-student test.

3.2 I_A in VPM Relay Cells

Relay cells in VPM transmit information from subcortical areas to the cortex. Relay cells have several inward and outward currents activated during changes in voltage (Mccormick and Huguenard, 1992). I_A is a fast K^+ outward current (Wang and Schreurs, 2006; Shibata et al., 2000; Huguenard et al., 1991) postulated to regulate the shape of the EPSP generated (Sherman and Guillery, 2009).

3.2.1 Activating and Inactivating Curves of I_A in VPM Relay Cells

I_A has two gates, an opening and a closing gate (Wang and Schreurs, 2006; Shibata et al., 2000; Huguenard et al., 1991). In order to determine the activation and inactivation kinetics of I_A we used voltage steps protocols (Figure 3.8) and compared the response with or without I_A blockers. The activation protocol consisted of two voltage steps, the first after an hyperpolarizing period and the second without a pre-hyperpolarizing period. The inactivating protocol consisted of a voltage step starting with hyperpolarizing values and a test voltage after that.

VPM relay cells had an I_A (Figure 3.9a and Figure 3.9b) that peaks at 20 mV and has a half-width of -20 mV. The activation starts at -50 mV.

3.2.2 I_A Has Kv4.3 Subunits

I_A can be generated by the expression of different subunits of potassium channels. Kv4.3 subunits are localized close to large terminals in rat VPM (Giber et al., 2008). We tested the I_A curves in presence of the Kv4.2 and K4.3 blocker phrixotoxin-2 (Diochot et al., 1999). Phrixotoxin-2 decreased the amount of I_A generated (Figure 3.9e and Figure 3.9f).

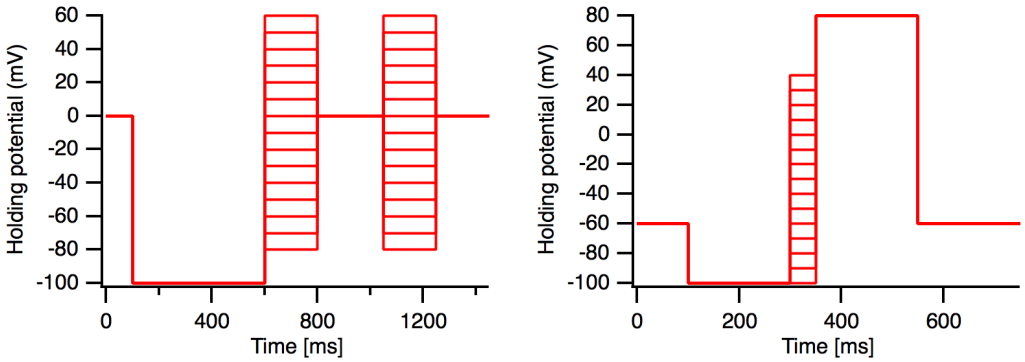

(a) Ia activation **(b)** Ia inactivation

Figure 3.8: Protocols used to obtain Ia currents
I_A has an activation and an inactivation gate. The inactivation gate is open during hyperpolarization. (a) The difference between the voltage steps after hyperpolarization and after resting membrane potential will give the value of the I_A activation curve. (b) The inactivation curve is obtained by opening the inactivation gate by an hyperpolarizing potential, followed by a voltage step and a depolarizing activating potential. The difference of the current response at the activating potential is due to the closing of the inactivation gate during the voltage step.

3.2.3 Effects of the Blockade of Kv4.3 Subunits in the Spike Response of VPM Relay Cells

We wanted to compare the VPM relay cell response with or without I_A. 4-AP was the first choice (Thompson, 1982). It blocks I_A, but also potentiates synaptic transmission (Wu et al., 2009) and altered the firing properties (Figure 3.10).

We decided to use phrixotoxin-2 (Diochot et al., 1999) to determine the effects of Kv4.3 subunits in the response of VPM relay cells to stimuli. The use of phrixotoxin-2 decreased the delay of the relay cell to spike by current injection. The time of rebound burst spike also depends of Kv4.3 subunits (Figure 3.11).

The postulated role of I_A is to decrease the action potential delay. The goal was to determine the response of relay cells to stimulation of single large terminal in presence of I_A blockers. The response of relay cells to

terminal stimulation generated a spike that hinders the role of the I_A in the EPSP. To characterize the role of I_A, QX-314, a Na^+ channel blocker (Schwarz and Puil, 2002; Strichartz, 1973), was added to the internal solution. The Na^+ current could not be blocked completely at resting membrane potentials (Figure 3.12), so it was necessary to record EPSP at hyperpolarizing values.

We recorded the response of relay cells to stimulation of a single labeled terminal in presence of the Kv4.3 blocker 2-phrixotoxin. The blockade of Kv4.3 subunits generated a decay in the amplitude of the EPSP (Figure 3.13b), but not a strong change in the EPSC response (Figure 3.13a).

In conclusion, VPM relay cells possess I_A. Part of the current depends of Kv4.3. I_A alters the amplitude of the EPSP.

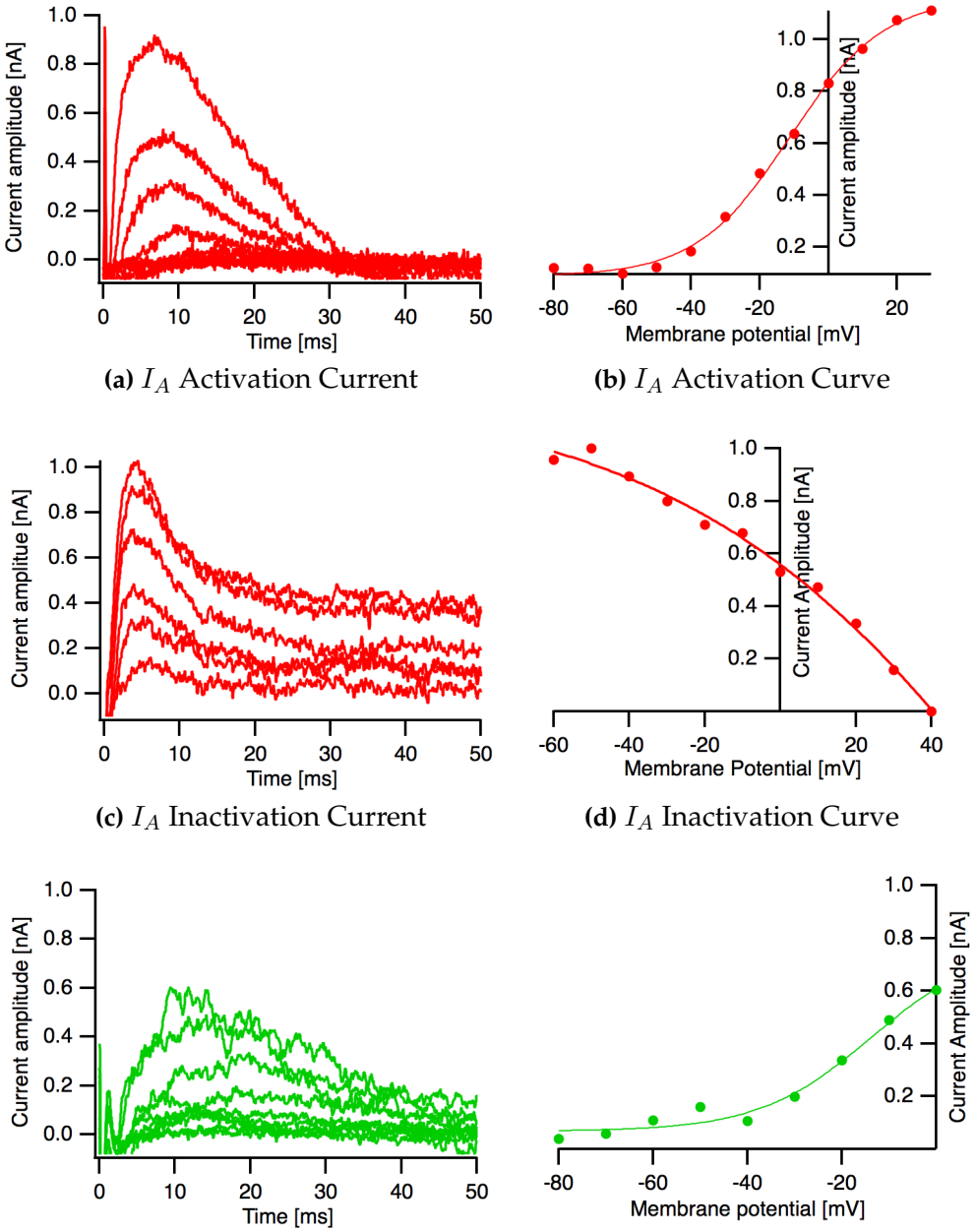

(a) I_A Activation Current

(b) I_A Activation Curve

(c) I_A Inactivation Current

(d) I_A Inactivation Curve

(e) I_A Activation current in presence of phrixotoxin-2

(f) Amplitude of I_A in presence of phrixotoxin-2

Figure 3.9: I_A **current in VPM relay cells**

(a) I_A currents as the difference between activation protocols with and without 4-AP. (b) IV curve of current from (a). (c) I_A currents as the difference between inactivation protocols with and without 4-AP. (d) IV curve of current from (c). (e) I_A currents as the difference between activation protocols with and without 2-phrixotoxin. (f) IV curve of current from (e). In (a), (c) and (e) some traces were removed for clarity. In (b), (d) and (f) the data was fit with a sigmoid function.

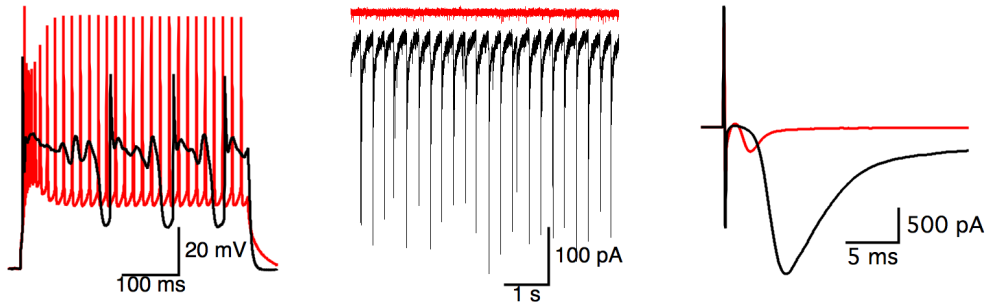

(a) Current Injection **(b)** Spontaneous response **(c)** EPSC response

Figure 3.10: Effects of 4-AP in the Relay Response
(a) Response of relay cells to 500 pA injected current. (b) Spontaneous response of a relay cell. (c) Response of VPM relay cell to single Pr5-VPM synaptic stimulation. Responses with (black) or without (red) 5 mM of I_A blocker 4-AP in the bath solution. In (a) relay cell with high K^+ internal solution and in (b) and (c), relay cells with Cs^+ base internal solution

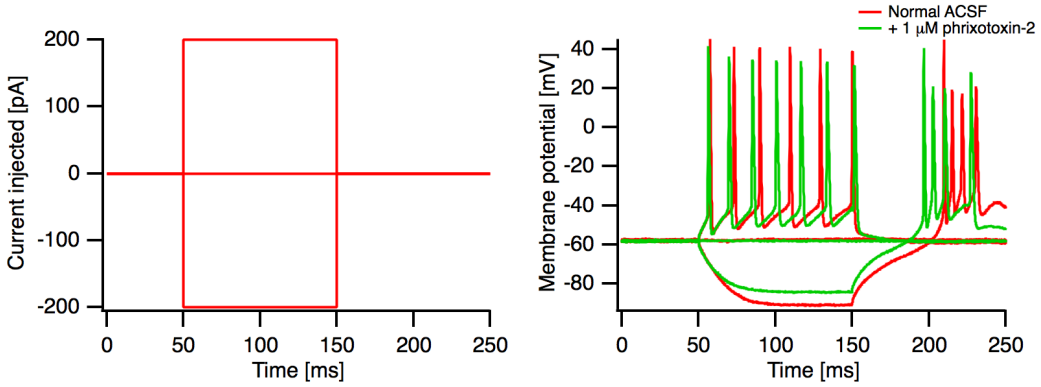

(a) Current step protocol **(b)** Relay cell response

Figure 3.11: Effect of I_A in firing properties of relay cells
(a) Step current injection protocol. (b) Relay cell response in ACSF normal solution and in presence of 1 μM Kv4.3 blocker phrixotoxin-2. The cell resting membrane potential was - 58 mV.

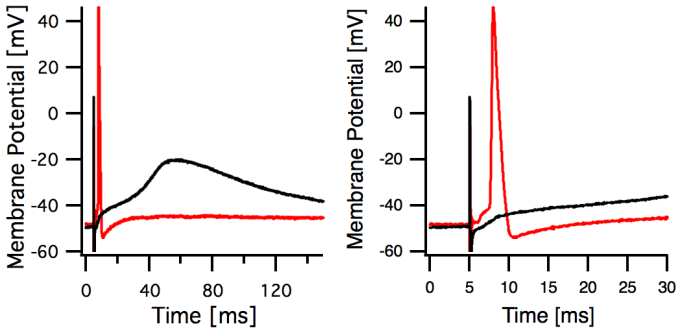

(a) Relay cell spike response **(b)** Zoom of response

Figure 3.12: Spike Generation with Sodium Channels Blocker
(a) VPM spike generation in response to Pr5-VPM stimulation in normal conditions or in presence of the sodium channel blocker QX-314. In both conditions the resting membrane potential was around - 50 mV. (b) Zoom of the spike response. Stimulus artifact due to Pr5-VPM synapse stimulation at 5 ms. In red VPM relay cell with normal ACSF external solution. In black, same cell with 5 mM QX-314 in the external solution.

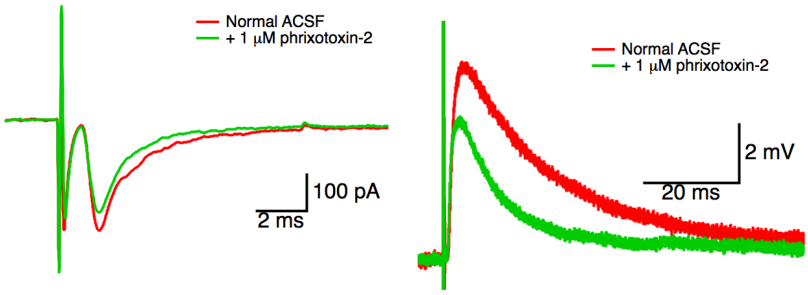

(a) EPSC **(b)** EPSP

Figure 3.13: Effect of Ia current in relay response
(a) EPSC response of relay cell to stimulation of a single labeled terminal, in normal ACSF external solution, or with 1 μM phrixotoxin-2 in the external solution. The cell was held at - 60 mV. (b) EPSP response of a relay cell at the same conditions as (a), but the membrane potential was - 80 mV.

3.3 *In Silico* VPM Relay Cell

Relay cells receive 20 to 60 terminals (Spacek and Lieberman, 1974; Veinante and Deschênes, 1999; Williams et al., 1994). In single confocal frames we found more than one large terminal close to a relay cell (Figure 3.14b). 3D reconstructions of confocal images showed more than one terminal per cell (Figure 3.14a). Stimulation of different single terminals in the same relay cell showed that they generate a similar response (Figure 3.14c). Because of the difficulty and low yield of dual or triple synapse stimulation experiments, we decided to use a relay cell *in silico* model to predict the relay cell response due to the stimulation of more than one terminal.

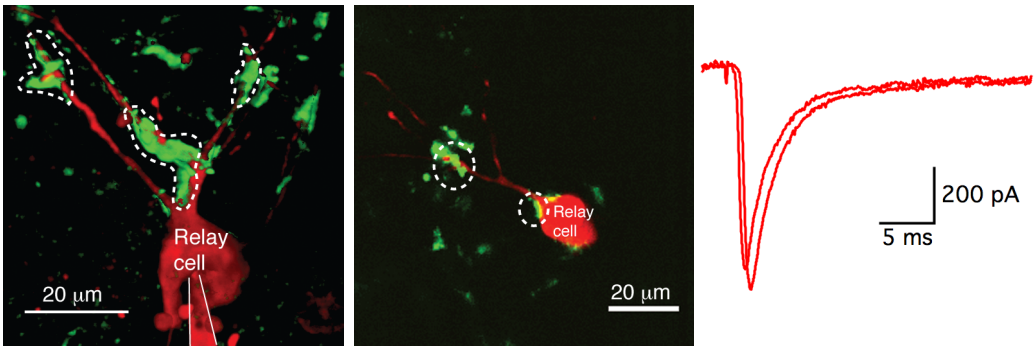

(a) 3D reconstruction **(b)** Relay cell **(c)** EPSC response

Figure 3.14: Labeled terminals close to relay cell
(a) 3D reconstruction of relay cell and labeled terminals. (b) Confocal image of labeled relay cell and labeled terminals. In (a) and (b), labeled terminals in green encircled by a discontinuous trace; relay cell in red. In (b), the patch pipette is marked by continuous line. (c) EPSC response of the relay cell in (b) to stimulation of each one of the two labeled terminals encircled in (b).

3.3.1 Single Cell Model

The action potential generation and the burst and tonic response of relay cells depend of voltage-dependent currents. We used a single compartment model (Figure 3.15c) with fast Na^+ currents, delayed K^+ currents, I_T, I_A and I_h (Table 2.3) to try to mimic the burst and tonic response of a relay cell

to current injections. These currents were enough to mimic those relay cells firing properties (compare Figure 3.15b with Figure 3.15d).

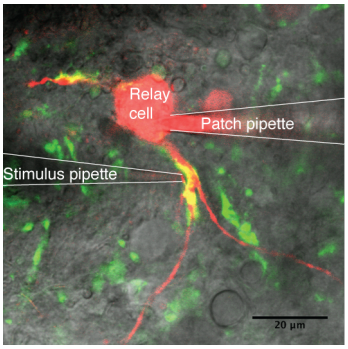

(a) Relay cell

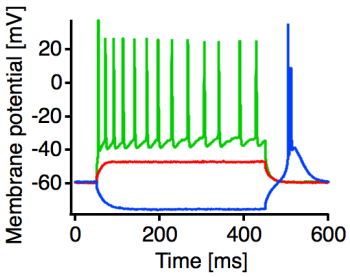

(b) Firing properties

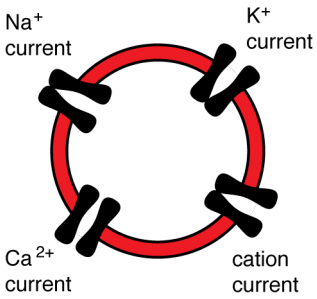

(c) Single compartment model

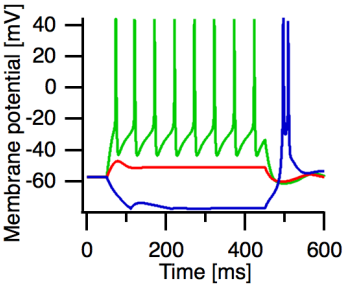

(d) Firing properties

Figure 3.15: Firing properties of single compartment
(a) Single image frame of a labeled relay cell and a labeled terminals. (b) Example of relay cell response to hyperpolarizing (blue) or depolarizing (red and green) current injections. (c) Scheme of single compartment model. (d) Response of single compartment model to hyperpolarizing (blue) or depolarizing (red and green) injection current.

3.3.2 4-Synapses Model

We decided to test the response of a model relay cell to synaptic inputs. The input was modeled using an alpha function (Equation 2.1). We used a simplified model with soma, four principal dendrites and two daughter dendrites each (Figure 3.16a). We assumed 100 µm length of each principal

dendrite and at the end of each one we put a single synapse . Stimulation of more than one terminal at the same time generated a faster response and an increase in the number of spikes generated (Figure 3.16b).

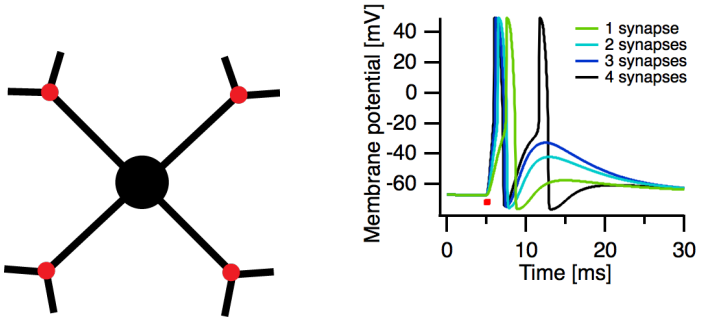

(a) 4-synapses relay cell model

(b) Response to synaptic stimulation

Figure 3.16: 4 synapses model
(a) Model of a relay cell with 4 principal branches, 2 daughter branch each, and 1 synapse (red) in each principal branch. (b) Response of relay cell model to stimulation of 1, 2, 3 or 4 synapses at the same time. In red the stimulation time used.

3.3.3 Relay Cell Model Including Morphology And Current Distribution

We wanted to add the morphology of relay cells to the *in silico* model. We used one VPM relay cell labeled with alexa 594 and we isolated the relay cell and terminals. We reconstructed the relay cell morphology and added the information to the model (Figure 3.17 and Appendix A.1).

We included fast Na^+ currents, delayed K^+ currents, I_T I_A and I_h in the relay cell model (Table 2.3). Specific currents are not distributed evenly along the relay cells (Rhodes and Llinás, 2005). We added the currents with specific conductances per cm^2 along the model cell (Table 3.1).

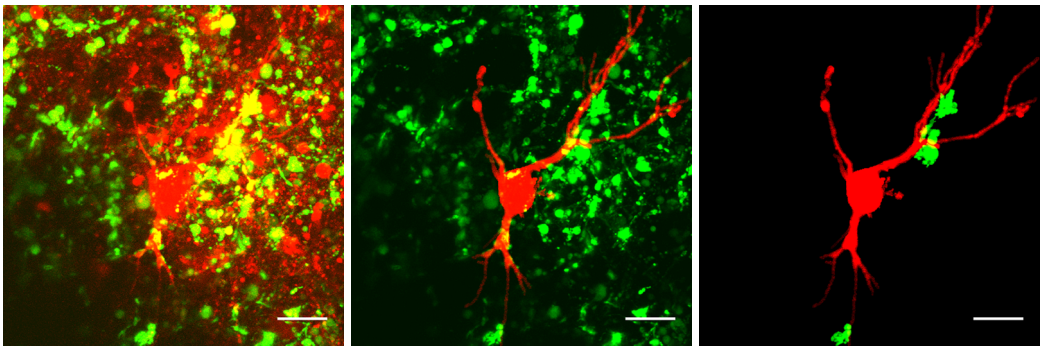

(a) Z-projection from confocal images

(b) Relay cell and labeled terminals

(c) Relay cell and connected labeled terminals

(d) 3D neuron

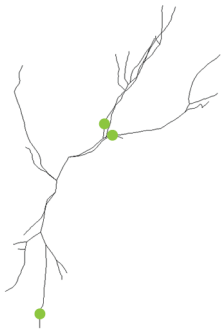

(e) 3D neuron in hoc format

Figure 3.17: VPM relay cell
Relay cell reconstruction and use in Neuron environment. (a) Z-projection of a stack of confocal images of a VPM relay cell (red) and labeled terminals (green) from an acute brain slice of rat. (b) Isolation of relay cell. (c) Isolation of relay cell and labeled terminals close to the relay cell. (d) 3D reconstruction of relay cell morphology. (e) Compartment model of relay cell in Neuron environment.

3.3.4 Firing Properties of Relay Cell Model

VPM relay cells fire in tonic or burst mode (Sherman and Guillery, 2009). We tested if the model can generate tonic and burst firing with the same protocol used in the real cell. We added currents with maximum conductance specific to each compartment (Table 3.1) and we injected current in the soma, while we recorded the voltage response in the soma. The model

Current	soma	basal dendrites	apical dendrites
Na^{2+}	1	0.01	0
K^{+}	1.3925	0.36	0
I_T	15	0.005	0
I_A	2	0.01	0
I_h	0.01	0.01	0

Table 3.1: Current conductances in model relay cell
Maximum conductance in siemens/cm^2 of the specific current in each compartment of the *in silico* model of the relay cell

could fire in tonic mode by depolarizing currents, and also could generate a burst rebound spike after hyperpolarizing currents (Figure 3.18b).

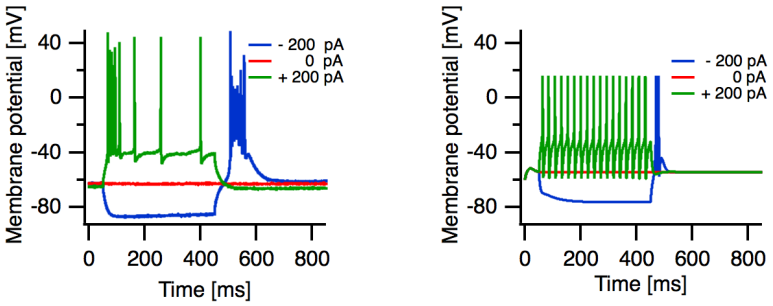

(a) Relay cell response **(b)** Model response

Figure 3.18: Firing properties of in silico relay cell
(a) Example of relay cell response to hyperpolarizing (blue) or depolarizing (green) current injections. (b) Response of relay cell model to hyperpolarizing (blue) or depolarizing (green) injection current. Response measured in the soma.

The current injected (Figure 3.18a) or the decrease in I_T or I_A (Sherman and Guillery, 2009) can change the firing properties of relay cells (Sherman and Guillery, 2009). We tested how the *in silico* model would respond to changes in the current injected or the amount of I_T or I_A. The *in silico* model predicted more positive currents will generate a faster response (Figure 3.19a), as the decreases in overall I_T (Figure 3.19b). The *in silico* model also predicted that a decrease in overall I_A will decrease the spike delay and also will decrease the resting membrane potential (Figure 3.19c).

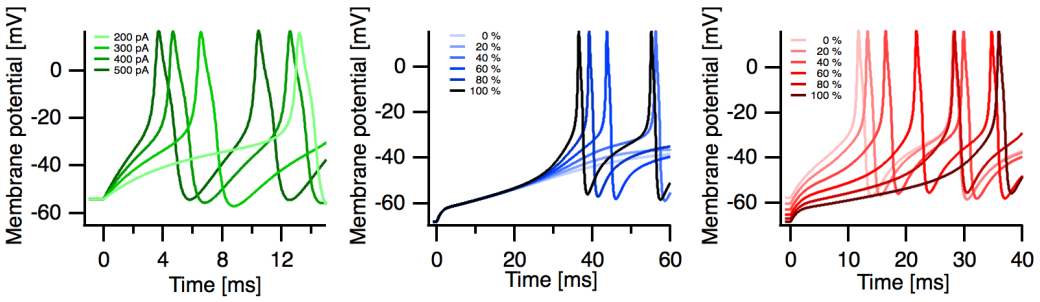

(a) Delay **(b)** I_T **(c)** I_A

Figure 3.19: Firing properties of in *in silico* relay cell
(a) Delay of spike generation to a current input. (b) Response of relay cell to 200 pA injected current at different percentages of I_T. (c) Response of relay cell to 200 pA injected current at different percentages of I_A.

3.3.5 Response of Relay Cell Model to Synaptic Stimulation

We aimed at creating a model that can mimic the response of VPM relay cells to stimulation of single Pr5-VPM terminals (such as Figure 3.5, 3.6 or 3.7). We used morphological information from 3D reconstructions of relay cells (Figure 3.17) to determine the location of the terminals close to the dendritic tree (Figure 3.17c and Figure 3.17e). We chose one of those terminals, and we modeled the synaptic input as alpha functions (Equation 2.1). The *in silico* model could generate responses similar to those of real cells. A single synaptic input could generate a voltage-dependent postsynaptic spike response (Figure 3.6 for a real cell, and Figure 3.20 for the *in silico* model).

Relay cells receive more than one terminal (Figure 3.14). We wanted to predict how the relay cell response changes between stimuli from a single terminal to that from all the labeled terminals connected to the relay cell. We modeled all the labeled terminals as synapses with alpha functions (Equation 2.1) and we tested the *in silico* model to a single stimulation from one, two or the three synapses. The model predicts that more inputs will

generate a faster response (Figure 3.20b).

In conclusion, we generated an *in silico* relay cell model that included the morphology of a relay cell and the location of large synaptic inputs (Figure 3.17e). The *in silico* model could mimic the burst and tonic firing pattern of the real relay cell (Figure 3.18b) and the postsynaptic voltage-dependent spike generation due to a single synaptic stimulus (Figure 3.20a). The model can be used to predict the effect of specific currents in the firing pattern of relay cells (Figure 3.19b and Figure 3.19c), and the postsynaptic spike response to stimulation of more than one synaptic input (Figure 3.20b).

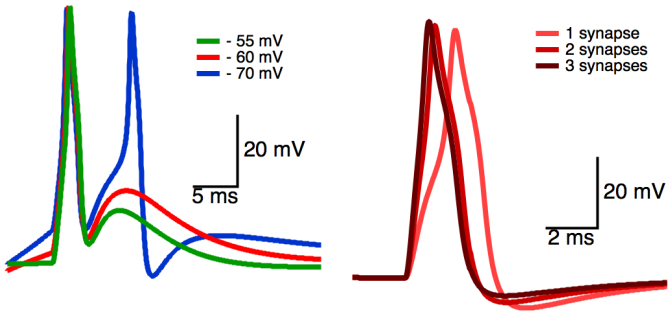

(a) Voltage-dependent response **(b)** Synaptic integration

Figure 3.20: Response of *in silico* model cell to synaptic stimulation
(a) Response of *in silico* model to a single synaptic stimulation. The model started at different membrane potentials. The synaptic stimulus was generated after 50 ms of initializing the model. (b) Response of *in silico* model to one, two or three single synaptic stimuli at the same time. The synaptic stimuli were generated after 50 ms of initializing the model. The plot started from 2 ms before the begin of the synaptic input.

3.4 Maturation of Mouse L5B-POm Synapses

3.4.1 Morphology of POm Relay Cells

Relay cells from VPM and POm have a characteristic morphology composed of 7 or 6 principal dendrites (Ohara and Havton, 1994; Sherman and Guillery, 2009). In other thalamic nuclei relay cells show morphological changes during maturation (Warren and Jones, 1997). We wanted to address the question of possible morphological changes in mice POm relay cells during maturation. We used the same cells used for electrophysiology and labeled with Alexa 594 to determine possible differences in the number of dendritic branches during maturation. We used sholl analysis (Longair et al., 2011) to determine the number of dendritic branches in POm relay cells at concentric distances from the soma at different maturation stages. We found a decrease in the number of branches in older animals (Figure 3.21).

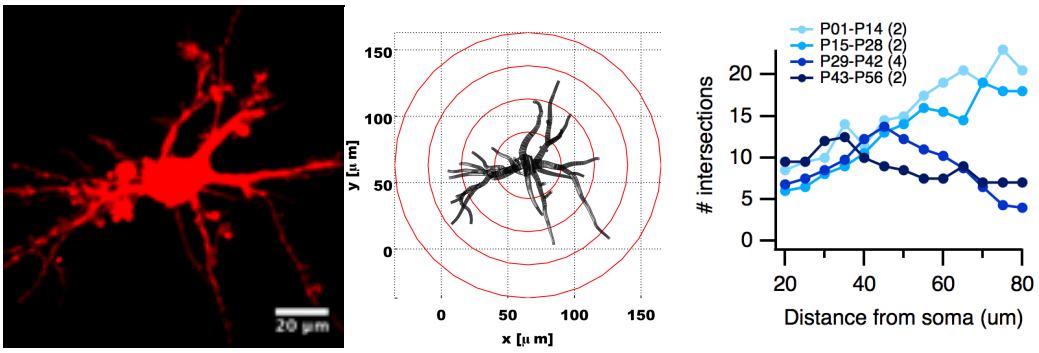

(a) POm relay cell **(b)** Sholl graph **(c)** Number of branches

Figure 3.21: Change in number of branches in POm relay cells during maturation
(a) Morphology of a P12 POm relay cell. (b) Sholl graph. Relay cell over circles at 25 μm distance. (c) Plot of number of branches versus distance from soma for POm relay cells at 4 age groups. In parentheses the number of cells analyzed.

3.4.2 Passive Properties of POm Relay Cells

The aim of the project was to characterize L5B-POm synapses in mice using whole-cell voltage clamp and double-barrel stimulation. We recorded the response of relay cells from P8 mice to P56 mice. Properties like the resting membrane potential did not change during maturation, but the access resistance decreased after the third week (Figure 3.22).

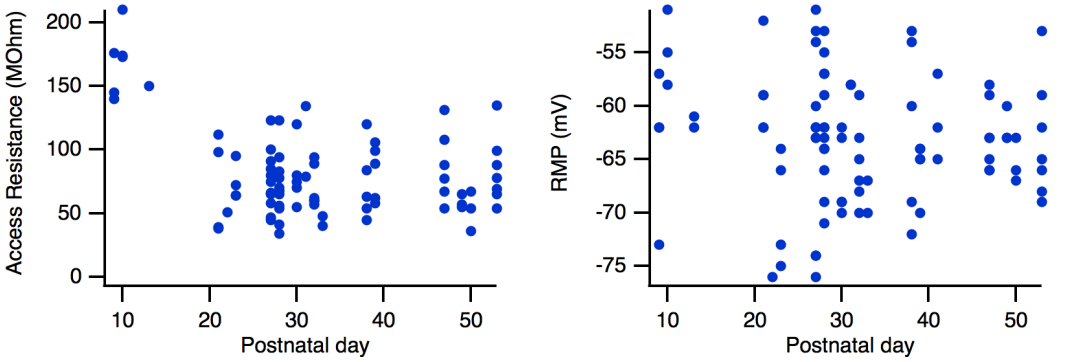

(a) Access resistance **(b)** Resting membrane potential (RMP)

Figure 3.22: Passive properties of POm relay cells
(a) Resting membrane potential (RMP) of relay cells at different ages. (b) Access resistance of relay cells at different ages. All the recordings done at room temperature. RMP recorded just after breaking the seal, in current mode, with no current injection. Cs^+ base internal solution (Table 2.5).

POm relay cells fire in tonic or burst mode in mature animals (Groh et al., 2008). We tested the response of POm relay cells of different ages to hyperpolarizing and depolarizing current injections. Sufficient depolarizing currents generated a tonic response in mice for P13 and also for P45 mice. P13 and P45 mice also showed rebound spikes after hyperpolarizing current injections (Figure 3.23).

3.4.3 Spontaneous Responses of POm Relay Cells

Synaptic elimination is a common process during development and maturation (Arsenault and Zhang, 2006; Low and Cheng, 2006). We wanted to

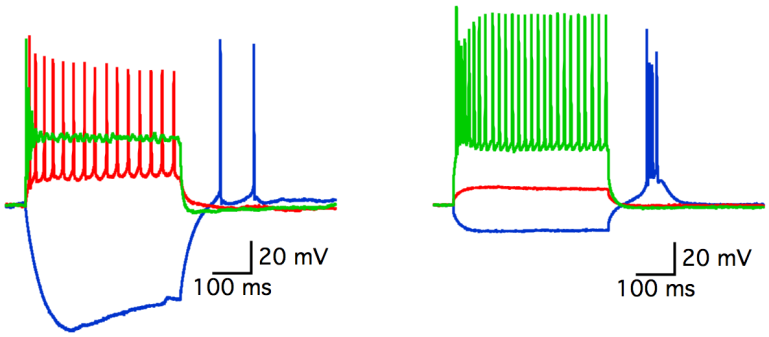

(a) P13 **(b)** P45

Figure 3.23: Firing properties of POm relay cells
Examples of relay cell responses to - 150 pA (blue), 100 pA (red) or 500 pA (green) current injection. (a) P13. (b) P45.

determine if this can be reflected in the spontaneous inputs to POm relay cells during maturation. We recorded the spontaneous activity of relay cells of POm from P8 to P56 to determine if there were changes in the amplitude or frequency of spontaneous activity. Younger animals showed a significant ($p < 0.05$) increase in the frequency of spontaneous events (Figure 3.24).

3.4.4 Evoked Response of L5B-POm Synapses

In rat L5B-POm synapses, P28 - P31 animals present a strong response, with a large amplitude, in line with a large synapse (Groh et al., 2008). Mouse L5B-POm synapses are large, with more than one active zone (Hoogland et al., 1991). We decided to investigate the amplitude response in mice at different maturation stages. We recorded the response of relay cells to stimulation of labeled terminals (Figure 3.25). There was no difference in the amplitude of the response, but the amplitude was around 200 pA , 20% of the amplitude reported for rat L5B-POm synapses (Groh et al., 2008).

3.4.5 Change in Glutamate Receptors of L5B-POm Synapses

The L5B-POm synapse is glutamatergic (Groh et al., 2008) and rat L5B-POm synapse shows a fast and slow component depending on the membrane

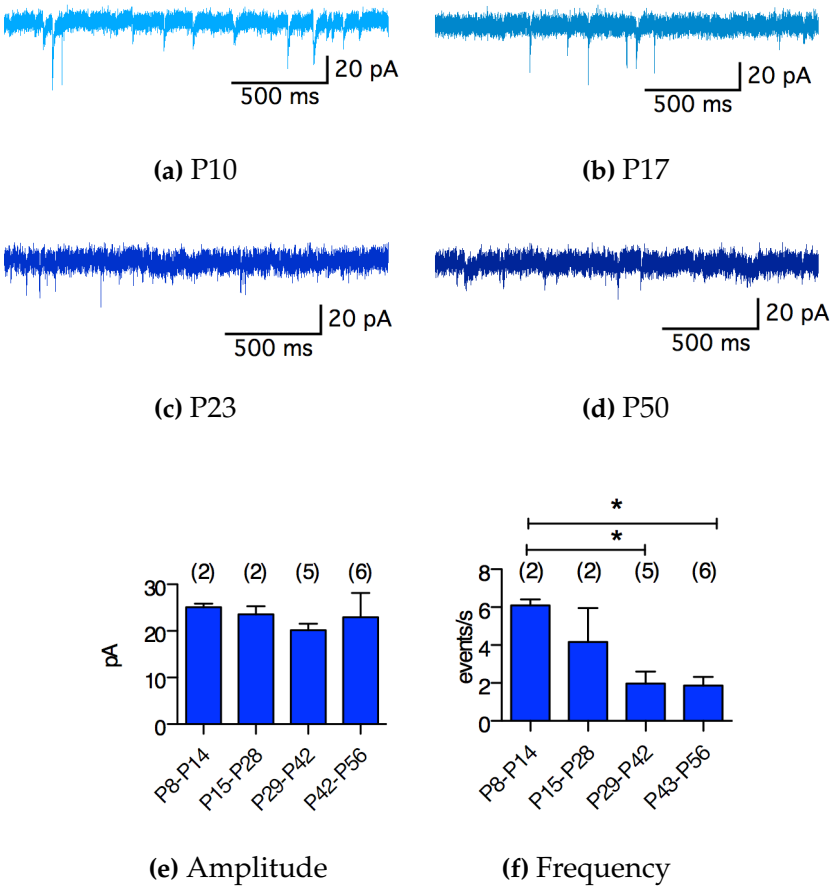

(a) P10 **(b)** P17

(c) P23 **(d)** P50

(e) Amplitude **(f)** Frequency

Figure 3.24: Spontaneous activity of POm relay cells
(a) to (d), POm relay cells from mouse P10, P17, P23 and P50. (e) Average amplitude response. (f) Average frequency of spontaneous events. In parentheses the number of cells recorded. Data divided in groups of 2 weeks. All the values are averages with their SEM. * significative difference ($p < 0.05$) between the groups. 1-way ANOVA and Bonferroni correction.

potential at which they are stimulated, possibly due to AMPA and NMDA component. During maturation, synapses in other areas of the thalamus (Arsenault and Zhang, 2006) change the AMPA/NMDA ratio. We recorded the response of mice POm relay cells to single terminal stimulation at - 60 mV and at + 40 mV in order to determine the presence of this fast and slow component (Figure 3.26). The fast AMPA component was calculated

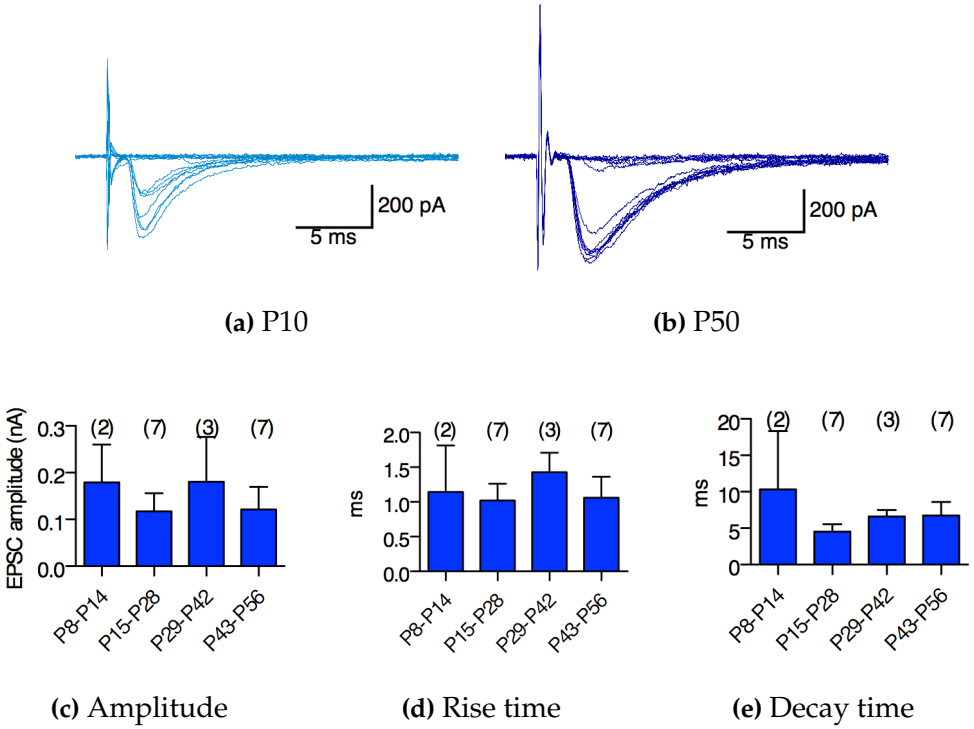

(a) P10 **(b)** P50

(c) Amplitude **(d)** Rise time **(e)** Decay time

Figure 3.25: Evoked current in POm relay cells
Responses of relay cells to stimulation of a labeled terminal. (a) P10, (b) P50. (c) EPSC amplitude, (d) EPSC rise time, (e) EPSC decay time. In parentheses the number of cells analyzed. No significative difference ($p < 0.05$) between any of the groups. 1-way ANOVA and Bonferroni correction.

as the peak amplitude at - 60 mV, and the slow NMDA component was calculated as the current value after 10 ms of stimulation in recordings at + 40 mV. Mice L5B-POm synapses did not show any difference in the AMPA/NMDA ratio from week 3 (Figure 3.26) .

3.4.6 Short-term Plasticity of L5B-POm Synapses

Driver synapses, but not modulatory synapses, show depression (Arsenault and Zhang, 2006; Groh et al., 2008; Reichova and Sherman, 2004). We recorded the response of POm relay cells to 20 Hz stimulation of single labeled terminal. Relay cells from even one week-old mice showed depres-

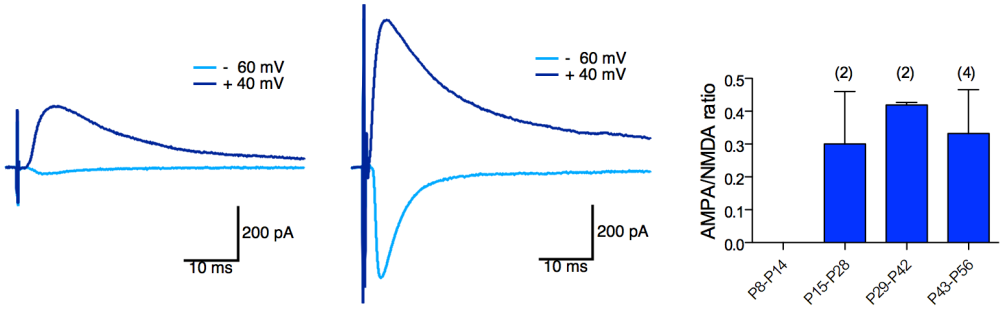

(a) P23 **(b)** P50 **(c)** AMPA/NMDA ratio

Figure 3.26: Rosebud synapse response at different membrane potentials
(a) EPSC response of P23 POm relay cell. (b) EPSC response of P50 POm relay cell. (c) Plot of average rates at the different age groups. In parentheses the number of cells analyzed. No significative difference. 1-way ANOVA and Bonferroni correction.

sion (Figure 3.27). The amount of depression was stronger in older animals (Figure 3.27).

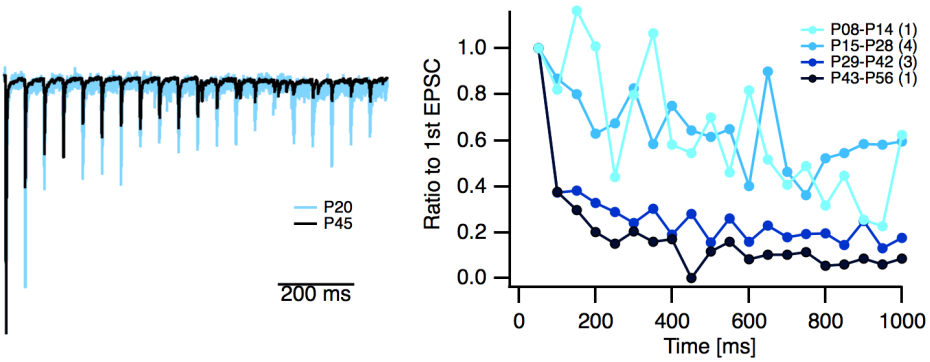

(a) Short-term plasticity **(b)** Ratio quantification

Figure 3.27: Short-term plasticity in rosebud terminals
Response of relay cells to 20 Hz stimulation of a labeled terminal. (a) Example of relay cell response. The stimulus artifact was deleted and the recordings were normalized to the amplitude of the first EPSC. (b) Response normalized to the first EPSC for relay cells at different ages. Number of relay cells analyzed in parentheses. SEM not included. No statistic analysis because only one sample in 2 groups.

3.4.7 Spike Response of POm Relay Cells

Stimulation of L5B-POm synapses in rats generates postsynaptic spike responses (Groh et al., 2008). We recorded the response of mice POm relay cells to stimulation of L5B-POm synapses in current clamp mode (Figure 3.28). Only relay cells from older mice showed a spike response, while cells from younger animals showed EPSPs with amplitude of only a few mV (Figure 3.28). The spike response was voltage-dependent (Figure 3.28b).

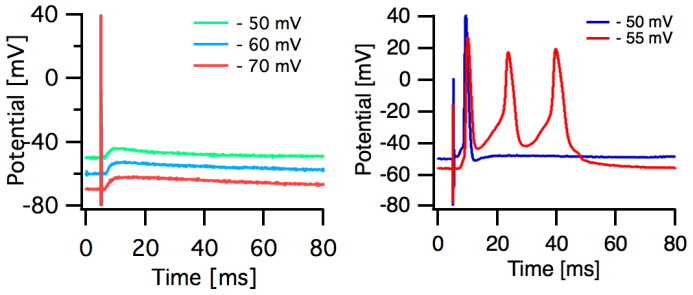

(a) P20 **(b)** P33

Figure 3.28: Spike response
(a) Response of a P20 relay cell to stimulation of a labeled terminal, recorded in current clamp mode. Cell resting potential at - 50 (green), - 60 (blue) or - 70 mV (red). (b) Response of a P33 relay cell to stimulation of a labeled terminal, recorded in current clamp mode. Cell resting potential at - 50 (blue) or - 55 mV (red). Patch pipette with K^+ base internal solution. Before week fourth, stimulation of a single terminal does not generate spikes in the relay cell.

L5B-POm synapses showed changes in maturation even after 4 or 5 weeks of age. The EPSC response did not change during maturation, but the response to high frequency stimulation decreased over time. Stimulation of single terminals generated spike response only in older animals. Hence, mice have a mature POm only after the first month.

CHAPTER 4

Discussion

In this thesis, we showed synaptic transmission between VPM relay cells and identified individual terminals of neurons projecting from Pr5 to VPM relay neurons for the first time (Figure 3.2). The response generated by Pr5-VPM synapse stimulation was modulated by I_A mediated by Kv4.3 K^+ channel subunits (Figure 3.13). Relay cells have more than one driver synapse (Figure 3.14) and we postulate a possible input computation mechanism in relay cells (Figure 3.16 and Figure 3.20). Finally, a higher order driver synapse, L5B-POm synapse, undergoes a process of maturation during the first postnatal weeks (Figure 3.28).

4.1 Single Synapse Stimulation

We labeled giant terminals from Pr5 or L5B neurons, stimulated them and recorded the response of the relay cell. The localization of the stimulating pipette (Figure 2.1 and 2.2) and the response of the relay cell, all-or-none (Figure 3.2b), allowed us to conclude that a presynaptic action potential was triggered as a response of a single large terminal stimulation. The

delay between the stimulus artifact and the generation of the response ruled out direct stimulation (around 2 ms, Figure 3.2c and 3.25), which could influence the EPSC. The stimulus artifact did not generate any effect over the ESPC or spike shape (Figure 3.2c and 3.25). The delay of the response was similar for all the EPSCs generated by stimulating the same terminal. The rise time of Pr5-VPM EPSC (Figure 3.2c) was consistent with a single synchronous release. The rise time of L5B-POm synapses was also consistent with a single synchronous release at a single terminal after the second week (Figure 3.25). We had only a 16% success ratio of patched relay cells with close-labeled terminals that could be reached by the stimulus pipette and that could generate a response. Optogenetic techniques could be used to increase the success ratio (Cruikshank et al., 2010; Poulet et al., 2012), because we could stimulate the terminal without the need of a stimulation pipette (Petreanu et al., 2007), however the resolution is not sufficient to stimulate small areas restricted in axial dimensions (due to the axial composition of the illuminated volume). Optogenetic approaches can reach 5-10 μm (Petreanu et al., 2007) and can stimulate more than one cell (Avermann et al., 2012; Mateo et al., 2011), or activate multiple terminals localized in different planes of the slice.

4.2 Pr5-VPM Synapse

4.2.1 VPM Relay Cell Current Response to Stimulation of Single Large Terminals

The EPSC amplitude observed in the Pr5-VPM (Figure 3.2c) synapses was similar to that observed in L5B-POm synapses from rats (Groh et al., 2008), but was larger than those observed in mice (Figure 3.25). The relay cell response was similar to the response of VPM relay cells to medial lemniscus stimulations in mice (Arsenault and Zhang, 2006). Driver synapses in different nuclei of the same animal have similar amplitude response.

The fast kinetics of the response, and the sensitivity to the AMPA-kainate blocker CNQX (Groh et al., 2008; Honoré et al., 1988) showed that

this synapse is AMPA receptor-dependent (Figure 3.2c), an observation in agreement with the relay cell response to medial lemniscus stimulation (Castro-Alamancos, 2002; Hsu et al., 2010). Interestingly, the NMDA blocker APV (Groh et al., 2008; Morris, 1989) showed almost no effect at - 60 mV holding potentials, but a giant synapse localized in POm (Groh et al., 2008) exhibits a NMDA component. We need recordings at more depolarized potentials to determine the role of NMDA in the Pr5-VPM synapse.

The morphological information correlates to the physiological information. Large terminals from VPM have around 45 active zones (Spacek and Lieberman, 1974), and this synapse releases 31 quantals per evoked response (Figure 3.1 and 3.2c). External solutions with a higher calcium concentration can probably generate a larger response. We also estimated around 160 vesicles in the readily releasable pool and a probability of release of 0.2 (Figure 3.4). The calyx of Held or the mossy fiber in the cerebellum are examples of large synapses in the brain. A release probability of about 0.2 is similar to those from the calyx of Held, between 0.2 and 0.4 (Branco and Staras, 2009; Meyer et al., 2001; Sakaba et al., 2002; Schneggenburger et al., 1999). Other giant synapses, like those from the cerebellar mossy fibers or rat L5B-Pom, have larger probability of release (Delvendahl et al., 2013; Groh et al., 2008; Hallermann et al., 2010). The size of the readily releasable pool of vesicles from Pr5-VPM synapses is smaller than from the calyx of Held, 160 vesicles versus thousands (Rizzoli and Betz, 2005), and could explain in part the stronger Pr5-VPM depression at higher frequency of stimulation, but not at lower frequencies.

Large terminals, like calyx of Held and mossy fibers in the cerebellum show depression due to the spillover of glutamate and desensitization of AMPA receptor (Sätzler et al., 2002; Trussell et al., 1993; Xu-Friedman and Regehr, 2003). Pr5-VPM synapses also show strong depression but almost no AMPA desensitization (Figure 3.2c). We used the AMPA desensitization and saturation inhibitor kynurenic acid (Diamond and Jahr, 1997; Taschenberger et al., 2002; Sun and Wu, 2001). Another compound used as desensitization inhibitor is cyclothiazide, or CTZ, (Trussell et al., 1993; Yamada and Tang, 1993) but we did not use it because it can also induce

presynaptic effects (Bellingham and Walmsley, 1999; Diamond and Jahr, 1995; Scheuss et al., 2002).

The structure of the synapse could explain the lack of AMPA desensitization. Pr5-VPM synapses are composed of a presynaptic terminal engulfing a series of dendrite invaginations, each one with 1 to 10 contact zones (Spacek and Lieberman, 1974), probably separating the contact zones and avoiding glutamate spillover. Pr5-VPM synapses showed low probability of release (Figure 3.1 and 3.2c), decreasing the chances of two neighboring active zones releasing at the same time. We did not explore any other possible mechanism of depression, such as inactivation of release sites or decrease in the presynaptic calcium influx (Fioravante and Regehr, 2011; Hosoi et al., 2009; Neher and Sakaba, 2008).

Pr5-VPM synapses showed a fast recovery after depression (Figure 3.3), in line with other synapses within the thalamus (Groh et al., 2008) and cortex (Varela et al., 1997) , but much faster than large terminals in other areas of the CNS, like the calyx of Held (Wimmer et al., 2004), which needs 20 s to reach around 80% recovery. Maybe the low probability of release helps to avoid the depletion of all the available vesicles at moderate stimulus frequencies, allowing a postsynaptic response to the next sensory input.

Each VPM relay cell receives around 25-60 large terminals (Spacek and Lieberman, 1974; Williams et al., 1994) and 1 to 3 Pr5 axons (Arsenault and Zhang, 2006; Deschênes et al., 2003) coming from the medial lemniscus (Haidarliu et al., 2008; Sugitani et al., 1990). The response of relay cells of VPM to stimulation in the medial lemniscus shows an all-or-none response and depression (Castro-Alamancos, 2002). The present work showed that stimulation of single terminals also generated all-or-none responses and depression (Figure 3.2b and 3.3). Some of the computation of the relay cell occurs already at the level of single synapses.

4.2.2 VPM Relay Cell Spike Response to Stimulation of Single Large Terminals

Stimulation of a single labeled Pr5-VPM synapse generated spike firing in the postsynaptic relay cell (Figure 3.5). The EPSC amplitude of Pr5-VPM synapses showed depression even at 10 Hz (Figure 3.3b), however, each of four stimuli at 50 Hz could still generate a spike response (Figure 3.7b). Therefore, a smaller EPSC could be enough to generate a spike response. Probably this mechanism ensures a spike response each time a new sensory input arrives.

A single EPSC response can generate changes in the membrane potential lasting for 50 ms or more (Figure 3.5c). The response depends on the membrane potential (Figure 3.6), which could activate or inactivate voltage-dependent channels . T-type calcium channels are potential candidates, as well as fast outward potassium channels. Future work will help to elucidate the role of T-type calcium channels at the level of a single synapse.

The firing properties of relay cells change with the membrane potential of the cell. More hyperpolarized cells will fire a burst of spikes, and more depolarized cells will fire a tonic train of spikes (Castro-Alamancos, 2002). At the level of the single terminal, the response of the relay cell was also voltage-dependent (Figure 3.6). The number and delay of the spikes increased with increased hyperpolarization of the membrane. Pr5-VPM synapses showed a non-linear response that amplified the input signal if the cell is at more hyperpolarized potentials.

The amplification properties of the Pr5-VPM synapse may be related to the separation between a sensory signal and the noise of the system, allowing the rat to "optimize the detection of stimuli that are novel or difficult to sense" (Nicolelis and Fanselow, 2002). A more hyperpolarized cell will be tuned to detect fast changes in the input signal, while a more depolarized cell will be tuned to reproduce a more detailed stimulus representation (Fanselow et al., 2001; Sherman, 2001; Sherman and Guillery, 2009). This tuning could be generated at the level of single synapses. A more hyperpolarized cell could amplify the novelty signal by means of a

multispike response, while a more depolarized cell could transmit a more faithfull representation of the stimulus by means of unitary spike responses (Figure 3.6a and Figure 3.6b).

The generation of spikes also depended on the previous activity of the synapse (Figure 3.7). Trains of 10 or 20 Hz generated a decrease in the number of spikes generated. *In vivo* recordings also show firing depression in VPM by an increase in the frequency of whisker stimulation (Sosnik et al., 2001) or *in vitro* stimulation of medial lemniscus (Castro-Alamancos, 2002). At the level of a single synapse, relay cells also exhibited depression in terms of number of spikes fired (Figure 3.7).

The function of voltage-dependent relay center is already present at the level of single synapses. *In vivo* recordings proved that cells from the trigeminal nucleus and cells from the Pr5 in the brainstem can follow whisker stimulation of high frequency. VPM shows depression even from 50 Hz whisker stimulation (Deschênes et al., 2003; Castro-Alamancos, 2002). At the level of single synapses, relay cells of VPM already show EPSC depression at 10 Hz. Pr5-VPM synapses showed more than one postsynapic spike per stimulus at lower frequencies, but a strong spike depression at 100 Hz. The number of postsynaptic spikes generated by stimulus was also frequency-dependent and showed depression already at 10 Hz of Pr5-VPM synaptic stimulation (Figure 3.3 and 3.7).

The cortex computes information considering latency and spike count (Sosnik et al., 2001), and both parameters can be altered at the level of a single synapse (Figure 3.6 and 3.7). Information relayed to the cortex by the thalamus can be modulated at the level of single synapses.

4.3 Input Modulation by I_A Current

We confirmed the presence of I_A in VPM relay cells. I_A in the VPM is formed partially by Kv4.3 subunits (Figure 3.9). Blockade of Kv4.3 subunits decreased the EPSC and EPSP amplitude (Figure 3.13). I_A also regulates the intrinsic excitability of VPM relay cells (Figure 3.11).

I_A are formed by homo or heterotetramers of α subunits, with β subunits as control subunits. Kv1.4, Kv3.3, Kv3.4, Kv4.1, Kv4.2 and Kv4.3 form I_A (Birnbaum et al., 2004; Jerng et al., 2004; Norris and Nerbonne, 2010) and different Kv subunits have different properties. Kv4.3 needs a slower time to reach the peak as compared to Kv4.2. The half-width of steady-state inactivation is more hyperpolarized for Kv4.3 (-68 mV versus -57 mV) (Jerng et al., 2004). I_A subunits are localized in different regions of the brain. Kv4.3 is found in substantia nigra, superior colliculus, and dorsal thalamus, while Kv4.2 and Kv4.3 are found in the medial nuclei of the thalamus. Kv4.2 and Kv4.3 subunits are found in the hippocampus, but Kv4.3 is located in CA2 and CA3 pyramidal cells, while Kv4.2 is located in CA1 cells (Hoffman et al., 1997; Serôdio and Rudy, 1998).

4-AP is a blocker of I_A (Thompson, 1982), and we used it to determine the presence of I_A in VPM relay cells. Phrixotoxin-2 is a Kv4.2 and Kv4.3 specific blocker (Diochot et al., 1999), and we used it to test the involvement of Kv4.3 subunits in I_A currents from VPM relay cells. We could not reach levels of concentration enough to rule out the presence of other subunits in the I_A formation. We could not use 4-AP to block I_A during EPSC or EPSP recordings (Figure 3.10) because 4-AP potentiates synaptic transmission (Wu et al., 2009).

Kv4.3 subunits are localized close to large terminals in VPM relay cells (Giber et al., 2008). I_A subunits are localized in the brain in different parts of the cell (Luján, 2010). For example, channels containing Kv1.4 subunits are localized in axons and probably terminals, while Kv4.2 and Kv4.3 are found in soma and dendrites of neurons from the hippocampus (Burkhalter et al., 2006; Sheng et al., 1992), in GABAergic, but not glutamatergic synapses (Jinno et al., 2005). Kv4.2 subunits are localized in increased density from the soma to distal dendrites in CA1 hippocampal neurons (Hoffman et al., 1997)), whereas it is localized in clusters in visual cortical neurons of mice (Burkhalter et al., 2006), in connections between mitral cells of the olfactory bulb (Kollo et al., 2006), or in connections between climbing fibers and stellate or basket cells of the cerebellum (Kollo et al., 2006). Channels generating I_A are localized in different subcompartments of cells in different

parts of the brain. Localization of channels producing I_A give hints about their functions. Kv4.3 channels are localized in close proximity to large terminals in VPM relay cells (Giber et al., 2008), I_A probably regulates the driver input (Figure 3.11 and 3.13).

The function of I_A in other cells can help to elucidate their role in the Pr5-VPM synapse. I_A hyperpolarizes the cell and blocks the generation of action potentials in hippocampal CA1 dendrites (Hoffman et al., 1997). They have a compartment function that limits the back-propagation and prevents dendritic depolarization (Hoffman et al., 1997). In VPM relay cells they regulate the delay of the EPSP and probably the firing frequency, but I_A did not block spike generation (Figure 3.11 and 3.19c). We could only test the effects of Kv4.3 subunits in the VPM relay response to Pr5-VPM synaptic inputs at hyperpolarized potentials because Pr5-VPM synapses generated spike responses that hide the effects of I_A (Figure 3.6). We could not completely block the spike response using QX-314 (Figure 3.12). We could only partially block I_A using 2-phrixotoxin since the amount of drug available was not enough to reach a higher concentration in the external solution, or to have more trails to test the effects of Kv4.3 subunits in the spike response of VPM relay cells at different membrane potentials.

4.4 Input Computation in Relay Cells

4.4.1 Modeling of Relay Cells

The aims of the model were to: 1) mimic the burst and tonic behavior of the relay cell to current injection, 2) mimic the relay response to a driver synapse stimulation, 3) predict the relay cell response to stimulation of more than one terminal. The parameters used to generate the model are not necessarily the same obtained in *in vitro* or *in vivo* conditions. *In vivo* and *in vitro* recordings show differences (Sherman and Guillery, 2009), probably due to destruction of branches in brain slices, and the increase of activity in *in vivo* recordings. For example, the destruction of branches decreases the membrane conductance in cells recorded in *in vitro* conditions

(Holmes and Woody, 1989). The *in silico* model presented here also doesn't have a specific compartment equivalent to an axon and an axon initial segment. We increased the sodium and potassium conductances in the soma to compensate for it.

Single mature driver synapses from POm and VPM generated spikes (Figure 3.5 and 3.28). Synaptic integration in relay cells could regulate the number and delay of spikes (Figure 3.16 and Figure 3.20b), but not the generation of spikes. In immature synapses, relay cells probably integrate different inputs as in pyramidal cells of the hippocampus (Spruston, 2008), so more than one L5B-POm synaptic input could be needed to generate a spike response in the immature POm relay cell.

4.4.2 Input Distance

Driver synapses are located close to the soma, in the dendritic principal branch (Liu et al., 1995). The distance to the soma and characteristics of the relay cells allow a stronger response. In CA1 pyramidal neurons EPSP have a 50% of attenuation at 250 μm from the soma, and 80% of attenuation at 100 μm from the soma (Golding et al., 2005). In thalamic relay cells the attenuation might be lower because relay cells have thicker dendrites (Jones, 2007; Ohara et al., 1995) that will allow more axial current to flow. Driver synapses are close to the soma. The distance is not far enough to generate a difference or decrease due to cable properties of the cell (Rall, 1967).

4.5 L5B-POm Synapse Maturation

Relay cells from the thalamus present morphological and electrophysiological changes during the first 3 weeks (Arsenault and Zhang, 2006; Wang and Zhang, 2008; Warren and Jones, 1997). Relay cells from mouse POm also presented changes in cell morphology (Figure 3.21), passive properties (Figure 3.22), firing properties (Figure 3.23), spontaneous response

(Figure 3.24), short-term plasticity (Figure 3.27) and spike generation (Figure 3.28) during the first weeks.

4.5.1 POm Relay Cell Morphology

POm relay cells from mice decreased the number of dendritic branches during maturation (Figure 3.21). In other nuclei of the thalamus cells increase the number of primary branches (Warren and Jones, 1997) during the first three weeks.

We decided to use the same cells recorded to analyze the morphology. This approach did not allow us to follow all the relay cell branches. One constrain was that we could only patch cells in the surface of the slice, probably losing most of the branches in top of the relay cells when slicing of the brain. We used 150 μm slices, but we could only access the first 60 or 80 μm of the labeled relay cells using confocal microscopy. One solution is the use of *in vivo* patch clamp with dyes in the pipette (Ohara and Havton, 1994), or injection of AAV with fluorescent proteins and subsequent post-fixation and slicing of the brains.

We also didn't calculate the total number and location of large terminals at different ages. This point is out of the scope of this thesis, which deals with the maturation of single terminals. The same constrains to get the morphology of relay cells apply to the number and location of the terminals.

4.5.2 POm Relay Cell Current Response to Stimulation of Single Large Terminals

L5B-POm synapses in the rat show a large AMPA/NMDA response (Groh et al., 2008). We also showed a large response in L5B-POm synapses of mice (Figure 3.25). The EPSC amplitude of mice was around 200 pA and in rats is around 3 nA (Groh et al., 2008). Relay cells from rats were recorded at - 70 mV at 33 - 35°C, whereas relay cells from mice were recorded at - 60 mV at room temperature. Relay cells with more hyperpolarized holding potentials will have larger EPSC amplitudes (Groh et al., 2008), but neither

factor can fully explain the difference between L5B-POms of rat and mouse. L5B-POm synapses or POm relay cells from rats and mice probably have different ultrastructural properties, like the vesicle pool size or release probability, that may explain the differences.

The EPSC amplitude response is stable in mice from 2 to 8 weeks (Figure 3.25). In some areas of the brain the subunit composition of NMDA receptors change from NR2B to NR2A during maturation (Liu et al., 2004; Quinlan et al., 1999; Robert W Gereau and Swanson, 2008). Different NMDA subunits have different decay constants, with NR1/NR2B subunits having a longer deactivation constant than NR1/NR2A subunits (Robert W Gereau and Swanson, 2008). In the visual cortex the change in subunit composition depends on sensory stimulation (Quinlan et al., 1999). One possible mechanism of subunit change is the mobilization of NR2B subunits to extrasynaptic compartments (Robert W Gereau and Swanson, 2008), but relay cells from the ventral posterior nucleus of mice do not accumulate extrasynaptic NR2B subunits (Liu et al., 2004). The change in NMDA composition could change the amount of calcium entering the cell, changing the type of response (Quinlan et al., 1999). We did not find a change in the AMPA/NMDA ratio during maturation with recordings at - 60 mV and + 40 mV holding potentials (Figure 3.26c). Probably we need to record the relay cell response at different holding potentials to generate a IV curve, or use specific drugs to block NMDA channels in order to determine the presence of this channels in the synapse and their change during maturation stages.

We could not get a large number of samples of mice younger than 2 weeks old. AAV virus in our hands express strongly only 2 weeks after injection, similar to expression of AAV in hippocampal cell culture (Howard et al., 2008). We injected pups from P0 to P7, but the survival rate was very low because cannibalism by their own mother. We tried to confuse the mother and increase the survival rate of the pups by mixing the injected pups with the bedding or putting some food and water in the bedding, but this strategy was not successful. Virus like Semlike Forest virus (Ehrengruber et al., 2001; Wimmer et al., 2004) has a shorter

time of expression, but we did not have time to try them. Other option could be the use of transgenic mice expressing GFP in L5 cortical neurons, as the *thy*1 transgenic mice (Feng et al., 2000; Liao et al., 2010; Stritt and Knöll, 2010), that express GFP in L5 neurons at least from the second week (Stritt and Knöll, 2010). The lab does not have this mice in house, and establishing this mouse line was not possible within the time line of this work.

L5B-POm synapses showed an increase in the strength of depression during maturation (Figure 3.27). This is the first study of maturation at the level of single driver synapses in the thalamus. Other study in which they activated all the driver synapses from the lemniscal pathway showed no differences in depression strength during maturation in VPM relay cells from rats (Arsenault and Zhang, 2006). It is possible that two nuclei have different properties because they have different functions. Probably a functional VPM is needed earlier than POm because whisker inputs are needed for barrel cortex maturation (Carvell and Simons, 1996; Shoykhet et al., 2005; Simons and Land, 1987), and the maturation of corticothalamic connections to higher order relay cells needs a mature sensory pathway to the cortex (Sherman and Guillery, 2013). One point in favor of this idea is that cortical areas receiving inputs from first order nuclei of the thalamus mature earlier than those sending projections to higher order relay centers in the thalamus (Guillery, 2005; Sherman and Guillery, 2009; Sherman and Guillery, 2013).

4.5.3 POm Relay Cell Firing Response to Stimulation of Single Large Terminals

Possible targets of POm relay cells, like supragranular layers of the somatosensory cortex, reach adult form during the first 2 weeks (Erzurumlu and Gaspar, 2012; Stern et al., 2001). Some properties of the relay cells were also in a maturation process during the first 2 weeks (Figure 3.22 or Figure 3.24). Other parameters, like the EEG patterns, reach adult form after 30 days (Jouvet-Mounier et al., 1970). The EEG patterns need functional T-type

currents and sodium/potassium spikes (Bal et al., 1995b; Bal et al., 1995a; von Krosigk et al., 1993).

The maturation of spike response of POm relay cells take longer than POm relay cell targets. Responses to a single stimulation of L5B-POm synapses did not generate a spike response in mice younger than 4 or 5 weeks (Figure 3.28). We can rule out changes in input resistance because it did not change after the second week (Figure 3.22). A possible explanation is the change in the composition or distribution of sodium channels (Boiko et al., 2001; Kaplan et al., 2001; Lupa et al., 1993; Rios et al., 2003), that will allow the spike generation at different starting conditions (Rush et al., 2005). Another possibility is a change in receptor composition (Arsenault and Zhang, 2006; Henson et al., 2012; Joshi and Wang, 2002) that could generate a smaller EPSP response.

Relay cells receive more than a single driver input (Liu et al., 1995) (Figure 2.2). POm relay cells showed a larger frequency of spontaneous events at early age (Figure 3.24), that could be correlated to relay cells receiving more inputs than older mice (Arsenault and Zhang, 2006; Wang and Zhang, 2008; Wang et al., 2011). L5B-POm synapses can probably generate spikes in younger mice if more than one synapse stimulates the relay cell at the same time and the combined response reaches a threshold for spike firing, as in other cells (Katz et al., 2009; Stuart et al., 2008).

The ability of L5B-POm synapses to generate spikes in relay cells is already present at the end of the third week in POm from rats (Groh et al., 2008) but was not present even after the third week in POm of mice (Figure 3.28). Pr5-VPM inputs can generate spikes in 3 week-old rats (Figure 3.5). It is still not known whether mice Pr5-VPM synapses also show a maturation delay compared to rats.

In conclusion, mice L5B-POm synapses are still changing their synaptic strength and spike generation in relay cells during the critical period of whisker mapping in the cortex.

4.6 Comparison of Two Thalamic Driver Synapses

Rats VPM and rats POm synapses present differences in the EPSC response, the size of the vesicle pool, 160 in VPM-Pr5 versus 64 in L5B-POm synapses, differences in the release probability, and in the NMDA composition (Groh et al, 2008 and Figure 3.1, Figure 3.2c and Figure 3.4). The decay time of EPSC is slower in VPM from rats versus POm from rats (1.9 $\pm$ 0.24 ms, versus 1.23 $\pm$ 0.27 ms) (Groh et al., 2008). Probably a longer EPSC in VPM ensures the generation of postsynaptic spikes in a wide range of conditions, while a shorter ESPC in POm will not. In that regard, the presence of I_T or I_A will regulate the number or delay of postsynaptic spikes in VPM, but they will not be needed for the spike generation. In POm, these currents could be necessary to generate the spike response. The EPSC kinetics difference probably offers clues about another regulatory mechanism present in higher order relay cells but not in first order relay cells.

VPM and POm both participate in the whisker system. Pr5-VPM synapses carry sensory inputs, while L5B-POm synapses carry cortical inputs. Both synapses can generate multiple spikes as a response to a single presynaptic input (Figure 3.5a, Figure 3.28b and Groh et al, 2008). This amplifier function in relay cells from first order and from higher order relay nuclei supports the idea that the thalamus is not just a relay center, but it processes the information to be sent to the cortex (Sherman and Guillery, 2013). The data also showed that this processing function appears already at the level of single synapses.

VPM and POm relay cells could fire in tonic mode or generate rebound burst spikes (Figure 3.15b for VPM, and Figure 3.23b for POm). The firing mode was voltage-dependent because a depolarizing current generated a tonic firing pattern, whereas a hyperpolarizing current injection generated a rebound burst spike. The transfer function of rats Pr5-VPM synapses (Figure 3.6) and mice (Figure 3.28b) and rats L5B-Pom (Groh, 2007) was also voltage-dependent. A relay cell at enough depolarized membrane potential fired one spike per stimulus. However, a more hyperpolarized relay

cell fired three or more spikes per stimulus (Figure 3.6b and Figure 3.28b). Maybe this voltage-dependent transfer function helps to generate the burst fire at more hyperpolarized potentials, and to transmit more faithfull information at more depolarized potentials.

VPM (Figure 3.6c) and POm (Groh, 2007) relay cells from rats show a voltage-dependent delay in the response to single terminal stimulation. However, VPM relay cells showed a faster response at any membrane potential. Differences in the delay response between nuclei could be related to differences in EPSC kinetics, such as larger decay times in Pr5-VPM EPSCs, and suggest voltage-dependent currents are directly involved in the spike generation in POm relay cells, but only modulate the spike response in VPM relay cells.

Both rat VPM (Figure 3.5b) and rat POm (Groh, 2007) relay cells showed a slower spike response at more hyperpolarized potentials. Probably an increased delay at more hyperpolarized potentials shows a longer time to reach a threshold to activate voltage-dependent Na^+ channels or the possible effect of other voltage dependent currents. Previous work (Connor and Stevens, 1971; Mccormick and Huguenard, 1992; Pape et al., 1994; Sherman and Guillery, 2009) and the relay cell response to injecting current in presence of 2-phrixotoxin (Figure 3.11b) or the *in silico* model response to injecting current with diminished I_T and I_A (Figure 3.19b and Figure 3.19c) suggest I_T and I_A could mediate the response delay. However, it is necessary to record the response of relay cells to single synaptic stimulations in presence of specific blockers against I_T or I_A to determine their effect.

Differences in synaptic properties could be related to the different function of both nuclei. VPM relay cells receive somatosensory information and send mainly to L4 of S1; POm relay cells receive also subthalamic sensory information, but also information from cortical area S1 and have a more spread area, connecting L5A of S1, S2, M1/M2, striatum, and others (Bourassa et al., 1995; Groh et al., 2013; Lu and Lin, 1993; Ohno et al., 2012). The function of the VPM relay cells is to relay sensory information to the cortex (Petersen, 2007). POm can relay sensory information to the cortex via the paralemniscal pathway (Pierret et al., 2000;

Yu et al., 2006), or can relay cortical information to other areas of the cortex, by L5B-POm synapses (Groh et al., 2008; Groh et al., 2013; Hoogland et al., 1991; Liao et al., 2010). Probably specific properties of the nucleus (Ramcharan et al., 2005), cells properties (Landisman and Connors, 2007; Li et al., 2003), the number and type of information carried by driver synapses (Groh et al., 2013; Sherman and Guillery, 2009; Van Horn and Sherman, 2007), or the response to modulatory signals (Van Horn and Sherman, 2007; Varela and Sherman, 2007; Varela and Sherman, 2009), help to achieve the specific functions of each nucleus.

Differences also can appear in the nuclei of different rodents. EPSC response of rat L5B-POm synapses (Groh et al., 2008) is larger than in mice (Figure 3.25), even though rat response was recorded at 33-35°C and at - 70 mV, and the mice response was recorded at - 60 mV and at room temperature. The postsynaptic spike generation also can be different. Stimulation of L5B-POm synapses in acute brain slices of 3 week-old rats generates a spike response (Groh et al., 2008), while only 4 or 5 week-old mice showed the same behavior (Figure 3.28).

Even though driver synapses from first and higher order relay cells showed differences at the level of EPSC, both can generate spike responses in the postsynaptic cell that can convey the information they receive from subthalamic or cortical centers.

4.7 Information Relayed to the Cortex

Whisker information is relayed to the cortex via the thalamus. *In vivo* recordings of VPM or POm in anesthetized animals show spikes that depend on the type and frequency of stimulation (Ahissar et al., 2000; Deschênes et al., 2003; Diamond et al., 1992; Sosnik et al., 2001).

A whisker can be stimulated phasically by the cyclic movement of a piezoelectric stimulator connected to a whisker (Deschênes et al., 2003), or by a continuous or tonic stimulation by an air puff to the whisker (Sosnik et al., 2001), and the response to those stimuli can be recorded *in vivo*

in the different relay centers of the whisker system (Ahissar et al., 2000; Deschênes et al., 2003). Subthalamic relay nuclei, such as Pr5 and SP5 in the brainstem, can faithfully follow the whisker stimulation (Deschênes et al., 2003; Minnery and Simons, 2003; Sosnik et al., 2001; Veinante and Deschênes, 1999). For example, Pr5 nucleus can fire tonically during a tonic whisker stimulation (Sosnik et al., 2001), but cells from Pr5 fire a cyclic train of burst spikes during cyclic whisker stimulation (Deschênes et al., 2003). Thalamic nuclei receive this train of stimulation coming from subthalamic nuclei, but the spike response changes.

VPM and POm nuclei fire in phase with cyclic whisker stimuli (Sosnik et al., 2001), but they can not follow a tonic whisker stimulation (Ahissar et al., 2000; Deschênes et al., 2003; Sosnik et al., 2001), showing depression at 50 ms stimuli at 8 Hz (Ahissar et al., 2000), and also a decrease of response to an increase on frequency of stimulation (Ahissar et al., 2000). The depression showed by L5B-POm EPSCs (Figure 3.27) or Pr5-VPM EPSCs and postsynaptic spike responses (Figure 3.3 and Figure 3.7d) can be involved in the frequency-dependent response in VPM (Ahissar et al., 2000; Deschênes et al., 2003) and POm (Ahissar et al., 2000) nuclei to whisker stimulation. This frequency-dependent firing response can be related to modulation of the sensory information in the thalamus related to the type of stimulation (Sosnik et al., 2001).

VPM and POm show differences in the response to whisker stimulation. *In vivo* recordings show a faster response in the VPM nucleus (Diamond et al., 1992), and a frequency-dependent latency in POm (Ahissar et al., 2000). POm response to whisker stimulation probably is due to paralemniscal subthalamic inputs, and the cortical input is involved in the change in latency of response (Ahissar et al., 2000). The firing differences are probably due to different modulatory signals, or to computational properties of the relay cell (Barthó et al., 2002; Bokor et al., 2005).

The difference in spike response can be related to the function of VPM and POm. VPM relays sensory information to the cortex, while POm could be involved in "temporal processing related to sensory-motor control of whisker movement" (Yu et al., 2006). POm probably fires after comparing

sensory events with the ongoing cortical activity (Ahissar and Oram, 2013; Groh et al., 2013) coming from motor descending pathways (Urbain and Deschênes, 2007) or sensory areas. Inputs from POm to motor stations (Ahissar and Oram, 2013; Deschênes et al., 1995; Hooks et al., 2013; Smith et al., 2012) could, in turn, help to correct motor commands if they are not in phase with the sensory input (Ahissar and Oram, 2013). Higher order nuclei receive information from the cortex, which probably already passed by the cortico-thalamo-cortical loop one or more times (Sherman and Guillery, 2009), making it difficult to develop a behavioral test to determine the specific function of POm (Sherman and Guillery, 2009).

4.7.1 Spike Timing

Rodents use the whisker system to describe the texture and the shape of objects (Kleinfeld et al., 2006; O'connor et al., 2013). Spike timing is important to discriminate between stimuli (Foffani et al., 2009; Montemurro et al., 2007; Petersen et al., 2009). Differences in spike timing in only 4 spikes in VPM cells could be enough to differentiate around 10^6 textures sensed by the whiskers (Montemurro et al., 2007). At the level of single synapses in VPM, one mechanism that can be used to regulate the firing rate is the spike response dependent of the membrane potential at the time of stimulation (Figure 3.6).

4.8 Outlook

The scope of the project was to describe the synaptic properties of single large terminals. This work describes properties of a higher order driver synapse, L5B-POm synapse, and a first order driver synapse, Pr5-VPM synapse. In both cases the synapse shows strong depression (Figure 3.3 and Figure 3.27) and spike generation (Figure 3.5 and Figure 3.28).

Pr5-VPM synapses convey sensory information. This thesis shows that a single synapse is enough to generate a spike response (Figure 3.5). We also start to address the question of the relay cell response considering all

the driver inputs labeled (Figure 3.20), but we need to explore in detail the number, location and connectivity between large terminals. This information is important to put the information of single terminals in the context of all the driver inputs to the relay cells and how it generates the spike response.

L5B-POm synapses show spike generation only in mice older than three weeks (Figure 3.28). In this work we did not explore why during maturation single synaptic stimulation do not generate spikes in relay cells. One possibility is differences in the composition of sodium channels subunits during maturation (Boiko et al., 2001; Rush et al., 2005; Lai and Jan, 2006). We can determine the channel distribution using immunohistochemistry with antibodies against specific subunits (Boiko et al., 2001) or determine the possible subunit composition using activation and inactivation curves of fast sodium currents (Rush et al., 2005). Another explanation is changes in morphology and passive properties (Turner et al., 1997) of relay cells that change the responsiveness of the cell to the synaptic inputs. Especially the dendritic membrane area, branching density or mean path length can affect the membrane responsiveness (Vetter et al., 2001; Weaver and Wearne, 2008; Zomorrodi et al., 2010).

There are several *in silico* models of relay cells (Antal et al., 1996; Destexhe and Sejnowski, 2003; Meuth et al., 2005; Mccormick and Huguenard, 1992; Rhodes and Llinás, 2005; Tscherter et al., 2011; Wang et al., 1991; Williams et al., 1997). We added the location of driver synapses to the model. The model needs more improvement. The model can be used to address questions related to how the thalamus relays sensory information, considering information of synaptic inputs. Some examples are what properties and how the relay cells generate spikes in response to a train of stimuli, how the back-propagation of a spike affects the next driver input (Williams and Stuart, 2000), the effect of specific currents in the generation of a spike response by synaptic inputs (Sherman and Guillery, 2009), the integration of driver and modulatory inputs in the relay cell dendritic tree or the integration of subthalamic and cortical driver inputs in dendrites of relay cells (Ahissar and Oram, 2013; Groh et al., 2013).

Acknowledgements

I would like to thanks Thomas for having accepted me in his lab, allowed me to work on this topic, and allow me to explore some ideas for which I do not have any expertise and that I wasn't supposed to do anyway, like the *in silico* modeling. I also want to thank Bob for introducing me to the thalamus and the VPM nucleus. My gratitude also goes to Mihaela and Claudia, and their amazing work in keeping everything running smoothly in the lab. I want to thank members of the Kuner lab, especially Sid and Min, for their tennis games and life/science discussion.

I want to thank also some people from the R. Kuner lab. Thanks to Deepsy, Vijayan, Simon, Lucas, Linette, Jianning. I apologise if I forgot someone's name. Thanks for being my travel and sport partners. I also want to apologise for using them as guinea pigs in order to improve my cooking and photography skills.

My eternal gratitude goes also to Maria Angela, for holding my hand in the darkest hour.

Finally, I want to thank my family and friends in Chile and around the world. Their support allows me to keep going, and they made me feel as if I were home, even though we just communicate by e-mail or skype, or saw each other just a few days per year.

Appendices

APPENDIX A

Neuron hoc Files

Files in Hoc format to be used in the Neuron Environment (Hines and Carnevale, 1997).

A.1 Morphology Segmentation

```
// HOC file created by Francisco Urra, 2013
// Get a hoc file with a cell morphology and segmented it in soma, basal and
// apical dendrites
// add currents to the segments of the cell


load_file("nrngui.hoc")

/////// neuron modeling ////////////////////


// load neuron
n = xopen("2013_05_02_neuron_WL_3Df_NT.hoc")

// generate nseg with d_lambda rule
forall {nseg = int(((L/(0.1*lambda_f(100))+0.9)/2)*2+1)}

// make odd values for nseg
```

```
forall {if (nseg/2 == int(nseg/2)) nseg+= 1}


//create objects to save soma, basal dendrites, and apical dendrites
objref somatic, basal, apical
soma somatic = new SectionRef()

// add dendrites connected to the soma to object basal
basal = new SectionList()
for i=0, somatic.nchild-1 somatic.child[i] {n = basal.append() }

// create apical dendrites section list
apical = new SectionList()
n = apical.wholetree()
n = apical.remove(basal)
access soma
n = apical.remove()


// add current mechanism and passive mechanisms
forall insert pas
forall g_pas = 0.0002
forall e_pas = -60

// Ih current
soma insert HCN
soma gmax_HCN = 0.01
forsec basal insert HCN
forsec basal gmax_HCN = 0.01

// INa current
soma insert NaT
soma gnabar_NaT = 1
forsec basal insert NaT
forsec basal gnabar_NaT = 0.01

// Ikdr current
soma insert Ikdr
soma gkdrbar_Ikdr = 1.3925
forsec basal insert Ikdr
forsec basal gkdrbar_Ikdr = 0.36

// It current
soma insert CaT
soma gcatbar_CaT = 15
forsec basal insert CaT
forsec basal gcatbar_CaT = 0.005

// Ia current
soma insert Ia
```

```
soma gmax_Ia = 2
forsec basal insert Ia
forsec basal gmax_Ia = 0.01

// procedures to block specific currents
proc block_sodium() {
        print gnabar_NaT
        print dend[0].gnabar_NaT
        soma gnabar_NaT = 0
        forsec basal gnabar_NaT = 0
}

proc block_potassium() {
        soma gkdrbar_Ikdr = 0
        forsec basal gkdrbar_Ikdr = 0
}

proc block_calcium() {
        soma gcatbar_CaT = 0
        forsec basal gcatbar_CaT = 0
}

proc block_Ia() {
        soma gmax_Ia = 0
        forsec basal gmax_Ia = 0
}
```

A.2 Current Step

A.2.1 Firing Properties

```
// HOC file created by Francisco Urra, 2013
// voltage step to relay cell model

// location of the current injection in the soma, between 0 and 1
nstim = 0.5

// initial values
tstop = 850             // for how long is the simulation
plotsms = 40            // Number of points plotted per milisecond
v_row_size = tstop*plotsms + 1

// initialize values
n = finitialize(-100)
n = frecord_init()
n = fcurrent()

celsius = 25
```

```
// current values
v_start = -0.2
v_step = 0.05

// number of elements in the matrix
v_column = 15           // number of steps
v_row = v_row_size      // number of elements in each columns

// create point process IClamp and add it to the soma
objectvar stim
soma stim = new IClamp(nstim)

// parameter of the current injection
stim.del = 50           // delay before start stim, in ms
stim.dur = 400          // duration of the stim, in ms
stim.amp = 0.4          // amplitude of the current stim, in nA

// create matrix to save the data
objref tempmatrix
tempmatrix = new Matrix(v_row, v_column)

// create vector to store the current values
objref stim_vec
stim_vec = new Vector()
stim_vec.record(&soma.v(0.5))

// loop of current injection
for(i = 0; i < v_column; i += 1) {
        // Set step current
        stim.amp = v_start + v_step*i

        //Update panel display
        n = doNotify()

        //Run simulation
        run()

        // Store step voltage in vector
        n = stim_vec.record(&soma.v(0.5))

        // Store step voltage in matrix
        tempmatrix.setcol(i, stim_vec)
}

// create file to save the data
objref savdata
savdata = new File()
n = savdata.wopen("step_current.dat")
n = tempmatrix.fprint(savdata, "␣%g")
```

```
n = savdata.close()
```

A.2.2 I_T Decrease

```
// HOC file created by Francisco Urra, 2013
// Response to current stimulation in model with diminished It

// location of the current injection in the soma, between 0 and 1
nstim = 0.5

// initial values
tstop = 300             // for how long is the simulation
plotsms = 40            // Number of points plotted per milisecond
v_row_size = tstop*plotsms + 1

// initialize values
n = finitialize(-60)
n = frecord_init()
n = fcurrent()

celsius = 25

// current values
v_start = -0.2
v_step = 0.05


// number of elements in the matrix
v_column = 11           // number of steps
v_row = v_row_size      // number of elements in each columns

// add point process IClamp in soma
objectvar stim
soma stim = new IClamp(nstim)

// starting parameters of the current step
stim.del = 50           // delay before start stim, in ms
stim.dur = 250          // duration of the stim, in ms
stim.amp = 0.2          // amplitude of the current stim, in nA

// create matrix to save the data
objref tempmatrix
tempmatrix = new Matrix(v_row, v_column)

// create vector to store the current values
objref stim_vec
stim_vec = new Vector()
stim_vec.record(&soma.v(0.5))
```

```
// starting values of It gmax in soma and basal dendrites
gmax_soma = 15
gmax_basal = 0.005

for(i = 0; i < v_column; i += 1) {
        // Set It gmax
        soma.gcatbar_CaT = gmax_soma*(i/v_column)
        forsec basal gcatbar_CaT = gmax_basal*(i/v_column)

        //Update panel display
        n = doNotify()

        //Run simulation
        run()

        // Store step voltage in vector
        n = stim_vec.record(&soma.v(0.5))

        // Store step voltage in matrix
        tempmatrix.setcol(i, stim_vec)
}

// create file to save the data
objref savdata
savdata = new File()
n = savdata.wopen("step_current_Cat.dat")
n = tempmatrix.fprint(savdata, "␣%g")
n = savdata.close()
```

A.2.3 I_A Decrease

```
// HOC file created by Francisco Urra, 2013
// current step, response with diminished Ia current

// location of the current injection in the soma, between 0 and 1
nstim = 0.5

// initial values
tstop = 300             // for how long is the simulation
plotsms = 40            // Number of points plotted per milisecond
v_row_size = tstop*plotsms + 1

// initialize values
n = finitialize(-60)
n = frecord_init()
n = fcurrent()

celsius = 25
```

```
// current values
v_start = -0.2
v_step = 0.05


// number of elements in the matrix
v_column = 11            // number of steps
v_row = v_row_size       // number of elements in each columns

// add point proccess IClamp
objectvar stim
soma stim = new IClamp(nstim)

// IClamp parameters
stim.del = 50            // delay before start stim, in ms
stim.dur = 250           // duration of the stim, in ms
stim.amp = 0.2           // amplitude of the current stim, in nA

// create matrix to save the data
objref tempmatrix
tempmatrix = new Matrix(v_row, v_column)

// create vector to store the current values
objref stim_vec
stim_vec = new Vector()
stim_vec.record(&soma.v(0.5))

// starting values of Ia gmax in soma and basal dendrites
gmax_soma = 2
gmax_basal = 0.01

for(i = 0; i < v_column; i += 1) {
        // Set Ia gmax
        soma.gmax_Ia = gmax_soma*(i/v_column)
        forsec basal gmax_Ia = gmax_basal*(i/v_column)

        //Update panel display
        n = doNotify()

        //Run simulation
        run()

        // Store step voltage in vector
        n = stim_vec.record(&soma.v(0.5))

        // Store step voltage in matrix
        tempmatrix.setcol(i, stim_vec)
}

// create file to save the data
```

```
objref savdata
savdata = new File()
n = savdata.wopen("step_current_Ia.dat")
n = tempmatrix.fprint(savdata, "_%g")
n = savdata.close()
```

A.3 Location of Single Synapses

```
// HOC file created by Francisco Urra, 2013
// Add synaptic location obtained by visual inspection of 3D reconstruction
// Calculate the distance from synapse to soma using the dendrites as path

celsius = 25

// number of elements in the matrix
v_row = v_row_size       // number of elements in each columns

// create vector to save dendrites that have synapses
objref dend_vec, dend_synap
// store dendrites that have synapses
dend_vec = new Vector()
dend_vec.append(17,22,14)
// Store location of each synapse in the dendrite
dend_synap = new Vector ()
dend_synap.append(0.16666, 0.5, 0.8333333)

// get number of synapses
n_synapses = dend_vec.size()

v_column = n_synapses            // number of columns

// create matrix to save the data
objref tempmatrix, tempmatrix_loc
tempmatrix = new Matrix(v_row, v_column)
tempmatrix_loc = new Matrix(3, 2)

// Create object to call synapses
objectvar synapse[n_synapses]

// create vector to save locations
objref loc_vec
loc_vec = new Vector()

// add parameters to all the synapses
for(i=0; i < n_synapses; i += 1) {
        // put soma as 0 distance
        access soma
        n = distance()
```

```
        // add synapse to specific dendrite
        n_dend = dend_vec.x[i]                  // dendrite having the synapse
        n_loc = dend_synap.x[i]                 // location in the dendrite

        // put synapse in dendrite
        dend[n_dend] synapse[i] = new AlphaSynapse(n_loc)

        // calculate distance from synapse to soma
        access dend[i]
        loc_vec.append(distance(n_loc))

}


// save data in matrix
objref savdata, savdata1
tempmatrix_loc.setcol(0, dend_vec)              // dendrite having the synapse
tempmatrix_loc.setcol(1, loc_vec)               // Distance to soma

savdata1 = new File()
savdata1.wopen("synapses_location.dat")
tempmatrix_loc.fprint(savdata1, "\t%g")
savdata1.close()

// create file to save the data
savdata = new File()
n = savdata.wopen("synapses_location_vol_seq.dat")
n = tempmatrix.fprint(savdata, "\t%g")
n = savdata.close()
```

A.4 Synaptic Stimulation

```
//HOC file created by Francisco Urra, 2013
// response of model to single synapse, at different voltages
// need the model cell with a object "synapse" already in

// Synapse stimulation
// note:.. values in uS
// S = I/V
// S = 1 nA / -60 mV
// S = 1*10^-9 A/-60*10^3 V
// S = 0.0166666 uS

// location of the current injection in the soma, between 0 and 1
nsynapse = 0.5

// initial values
```

```
tstop = 100             // for how long is the simulation
plotsms = 40            // Number of points plotted per milisecond
v_row_size = tstop*plotsms + 1

// initialize values
n = finitialize(-75)
n = frecord_init()
n = fcurrent()

celsius = 25

// number of elements in the matrix
v_column = 6            // number of steps
v_row = v_row_size      // number of elements in each columns

synapse.onset = 10              // delay before start synapse, in ms
synapse.gmax = 0.01666666       // max conductance in uS
synapse.e = 50                  // reversal potential, asuming Na
synapse.tau = 1.5               // taken from EPSC

// create matrix to save the data
objref tempmatrix
tempmatrix = new Matrix(v_row, v_column)

// create vector to store the current values
objref synapse_vec, synapse_current
synapse_vec = new Vector()
synapse_current = new Vector()

for(i = 0; i < v_column; i += 1) {

        //Update panel display
        n = doNotify()

        v_init = -75 + i*5

        //Run simulation
        run()

        // Store step voltage in vector
        n = synapse_vec.record(&soma.v(0.5))

        // store synapse current
        n = synapse_current.record(&synapse.i)

        // Store step voltage in matrix
        tempmatrix.setcol(i, stim_vec)
}

// create file to save the data
```

```
objref savdata
savdata = new File()
n = savdata.wopen("single_synapse.dat")
n = tempmatrix.fprint(savdata, "␣%g")
n = savdata.close()
```

Bibliography

Ahissar E, Sosnik R, Haidarliu S (2000) Transformation from temporal to rate coding in a somatosensory thalamocortical pathway. *Nature* 406:302–306.

Ahissar E, Oram T (2013) Thalamic Relay or Cortico-Thalamic Processing? Old Question, New Answers. *Cerebral Cortex* Advance online publication:doi:10.1093/cercor/bht296.

Andersen P, Eccles JC, Sears TA (1964) THE VENTRO-BASAL COMPLEX OF THE THALAMUS: TYPES OF CELLS, THEIR RESPONSES AND THEIR FUNCTIONAL ORGANIZATION. *The Journal of Physiology* 174:370–399.

Antal K, Emri Z, Tóth TI, Crunelli V (1996) Model of a thalamocortical neurone with dendritic voltage-gated ion channels. *Neuroreport* 7:2655–2658.

Arsenault D, Zhang Zw (2006) Developmental remodelling of the lemniscal synapse in the ventral basal thalamus of the mouse. *J Physiol (Lond)* 573:121–132.

Auladell C, Pérez-Sust P, Supèr H, Soriano E (2000) The early development of thalamocortical and corticothalamic projections in the mouse. *Anatomy and Embryology* 201:169–179.

Avermann MM, Tomm CC, Mateo CC, Gerstner WW, Petersen CCHC (2012) Microcircuits of excitatory and inhibitory neurons in layer 2/3 of mouse barrel cortex. *Journal of Neurophysiology* 107:3116–3134.

Bal T, von Krosigk M, Mccormick DA (1995a) Role of the ferret perigeniculate nucleus in the generation of synchronized oscillations in vitro. *The Journal of Physiology* 483 (Pt 3):665–685.

Bal T, von Krosigk M, Mccormick DA (1995b) Synaptic and membrane mechanisms underlying synchronized oscillations in the ferret lateral geniculate nucleus in vitro. *The Journal of Physiology* 483 (Pt 3):641–663.

Barthó PP, Freund TFT, Acsády LL (2002) Selective GABAergic innervation of thalamic nuclei from zona incerta. *The European journal of neuroscience* 16:999–1014.

Beak SK, Hong EY, Lee HS (2010) Collateral projection from the forebrain and mesopontine cholinergic neurons to whisker-related, sensory and motor regions of the rat. *Brain research* 1336:30–45.

Bellingham MC, Walmsley B (1999) A novel presynaptic inhibitory mechanism underlies paired pulse depression at a fast central synapse. *NEURON* 23:159–170.

Birnbaum SG, Varga AW, Yuan LL, Anderson AE, Sweatt JD, Schrader LA (2004) Structure and function of Kv4-family transient potassium channels. *Physiological Reviews* 84:803–833.

Bodor AL, Giber K, Rovó Z, Ulbert I, Acsády L (2008) Structural correlates of efficient GABAergic transmission in the basal ganglia-thalamus pathway. *The Journal of neuroscience : the official journal of the Society for Neuroscience* 28:3090–3102.

Boiko T, Rasband MN, Levinson SR, Caldwell JH, Mandel G, Trimmer JS, Matthews G (2001) Compact myelin dictates the differential targeting of two sodium channel isoforms in the same axon. *NEURON* 30:91–104.

Bokor H, Acsády L, Deschênes M (2008) Vibrissal responses of thalamic cells that project to the septal columns of the barrel cortex and to the second somatosensory area. *Journal of Neuroscience* 28:5169–5177.

Bokor H, Frère SG, Eyre MD, Slézia A, Ulbert I, Lüthi A, Acsády L (2005) Selective GABAergic Control of Higher-Order Thalamic Relays. *NEURON* 45:929–940.

Bosman LWJ, Houweling AR, Owens CB, Tanke N, Shevchouk OT, Rahmati N, Teunissen WHT, Ju C, Gong W, Koekkoek SKE, De Zeeuw CI (2011) Anatomical pathways involved in generating and sensing rhythmic whisker movements. *Frontiers in integrative neuroscience* 5:53.

Bourassa J, Pinault D, Deschênes M (1995) Corticothalamic projections from the cortical barrel field to the somatosensory thalamus in rats: a single-fibre study using biocytin as an anterograde tracer. *The European journal of neuroscience* 7:19–30.

Branco T, Staras K (2009) The probability of neurotransmitter release: variability and feedback control at single synapses. *Nature Reviews Neuroscience* 10:373–383.

Brecht M, Sakmann B (2003) Dynamic representation of whisker deflection by synaptic potentials in spiny stellate and pyramidal cells in the barrels and septa of layer 4 rat somatosensory cortex. *The Journal of Physiology* 543:49–70.

Bruno RM, Sakmann B (2006) Cortex is driven by weak but synchronously active thalamocortical synapses. *Science (New York, NY)* 312:1622–1627.

Burkhalter A, Gonchar Y, Mellor RL, Nerbonne JM (2006) Differential expression of IA channel subunits Kv4. 2 and Kv4. 3 in mouse visual cortical neurons and synapses. *The Journal of neuroscience : the official journal of the Society for Neuroscience* 26:12274–12282.

Cai X, Liang CW, Muralidharan S, Muralidharan S, Kao JPY, Tang CM, Thompson SM (2004) Unique roles of SK and Kv4.2 potassium channels in dendritic integration. *NEURON* 44:351–364.

Carnevale NT, Hines ML (2006) *The NEURON book* Cambridge Univ Pr.

Carvell GE, Simons DJ (1996) Abnormal tactile experience early in life disrupts active touch. *The Journal of neuroscience : the official journal of the Society for Neuroscience* 16:2750–2757.

Castro-Alamancos MAM (2002) Properties of primary sensory (lemniscal) synapses in the ventrobasal thalamus and the relay of high-frequency sensory inputs. *Journal of Neurophysiology* 87:946–953.

Çavdar S, Hacioğlu H, Şirvanci S, Keskinöz E, Onat F (2011) Synaptic organization of the rat thalamus: a quantitative study. *Neurological Sciences* 32:1047–1056.

Chen JL, Carta S, Soldado-Magraner J, Schneider BL, Helmchen F (2013) Behaviour-dependent recruitment of long-range projection neurons in somatosensory cortex. *Nature* 499:336–340.

Chersi F, Mirolli M, Pezzulo G, Baldassarre G (2013) A spiking neuron model of the cortico-basal ganglia circuits for goal-directed and habitual action learning. *Neural networks : the official journal of the International Neural Network Society* 41:212–224.

Cholvin T, Loureiro M, Cassel R, Cosquer B, Geiger K, De Sa Nogueira D, Raingard H, Robelin L, Kelche C, Pereira de Vasconcelos A, Cassel JC (2013) The ventral midline thalamus contributes to strategy shifting in a memory task requiring both prefrontal cortical and hippocampal functions. *Journal of Neuroscience* 33:8772–8783.

Connor JA, Stevens CF (1971) Prediction of repetitive firing behaviour from voltage clamp data on an isolated neurone soma. *The Journal of Physiology* 213:31–53.

Coulter DA, Huguenard JR, Prince DA (1989) Calcium currents in rat thalamocortical relay neurones: kinetic properties of the transient, low-threshold current. *The Journal of Physiology* 414:587–604.

Cruikshank SJ, Urabe H, Nurmikko AV, Connors BW (2010) Pathway-Specific Feedforward Circuits between Thalamus and Neocortex Revealed by Selective Optical Stimulation of Axons. *NEURON* 65:16–16.

Dayan P, Abbott LF (2005) *Theoretical Neuroscience: Computational and Mathematical Modeling of Neural Systems (Computational Neuroscience)* The MIT Press, 1 edition.

de Schutter E (2010) *Computational Modeling Methods for Neuroscientists* MIT Press (MA).

Delvendahl I, Weyhersmuller A, Ritzau-Jost A, Hallermann S (2013) Hippocampal and cerebellar mossy fibre boutons - same name, different function. *The Journal of Physiology* 591:3179–3188.

Deschênes M, Bourassa J, Parent A (1995) Two different types of thalamic fibers innervate the rat striatum. *Brain research* 701:288–292.

Deschênes M, Paradis M, Roy JP, Steriade M (1984) Electrophysiology of neurons of lateral thalamic nuclei in cat: resting properties and burst discharges. *Journal of Neurophysiology* 51:1196–1219.

Deschênes M, Veinante P, Zhang ZW (1998) The organization of corticothalamic projections: reciprocity versus parity. *Brain research Brain research reviews* 28:286–308.

Deschênes M, Timofeeva E, Lavallée P (2003) The relay of high-frequency sensory signals in the Whisker-to-barreloid pathway. *The Journal of neuroscience : the official journal of the Society for Neuroscience* 23:6778–6787.

Deschênes M, Timofeeva E, Lavallée P, Dufresne C (2005) The vibrissal system as a model of thalamic operations. *Progress in brain research* 149:31–40.

Destexhe A, Neubig M, Ulrich D, Huguenard J (1998) Dendritic low-threshold calcium currents in thalamic relay cells. *The Journal of neuroscience : the official journal of the Society for Neuroscience* 18:3574–3588.

Destexhe A, Sejnowski TJ (2003) Interactions between membrane conductances underlying thalamocortical slow-wave oscillations. *Physiological Reviews* 83:1401–1453.

Destexhe A, Sejnowski TJ (1997) Synchronized oscillations in thalamic networks: insights from modeling studies. *Thalamus* 2:331–372.

Diamond JS, Jahr CE (1995) Asynchronous release of synaptic vesicles determines the time course of the AMPA receptor-mediated EPSC. *NEURON* 15:11–11.

Diamond JS, Jahr CE (1997) Transporters buffer synaptically released glutamate on a submillisecond time scale. *The Journal of neuroscience : the official journal of the Society for Neuroscience* 17:4672–4687.

Diamond ME, Armstrong-James M, Budway MJ, Ebner FF (1992) Somatic sensory responses in the rostral sector of the posterior group (POm) and in the ventral posterior medial nucleus (VPM) of the rat thalamus: dependence on the barrel field cortex. *The Journal of Comparative Neurology* 319:66–84.

Diamond MEM (2000) Neurobiology. Parallel sensing. *Nature* 406:245–247.

Diamond ME, Arabzadeh E (2013) Whisker sensory system - from receptor to decision. *Progress in neurobiology* 103:28–40.

Diamond ME, Armstrong-James M, Ebner FF (1992) Somatic sensory responses in the rostral sector of the posterior group (POm) and in the ventral posterior medial nucleus (VPM) of the rat thalamus. *The Journal of Comparative Neurology* 318:462–476.

Diamond ME, von Heimendahl M, Knutsen PM, Kleinfeld D, Ahissar E (2008) 'Where' and 'what' in the whisker sensorimotor system. *Nature Reviews Neuroscience* 9:601–612.

Diochot S, Drici MD, Moinier D, Fink M, Lazdunski M (1999) Effects of phrixotoxins on the Kv4 family of potassium channels and implications for the role of Ito1 in cardiac electrogenesis. *British Journal of Pharmacology* 126:251–263.

Dörfl J (1985) The innervation of the mystacial region of the white mouse: A topographical study. *Journal of anatomy* 142:173–184.

Drion G, Franci A, Seutin V, Sepulchre R (2012) A novel phase portrait for neuronal excitability. *PLoS ONE* 7:e41806.

Ehrengruber MU, Hennou S, Büeler H, Naim HY, Déglon N, Lundstrom K (2001) Gene transfer into neurons from hippocampal slices: comparison of recombinant Semliki Forest Virus, adenovirus, adeno-associated virus, lentivirus, and measles virus. *Molecular and cellular neurosciences* 17:855–871.

Eliasmith C, Stewart TC, Choo X, Bekolay T, DeWolf T, Tang Y, Tang C, Rasmussen D (2012) A large-scale model of the functioning brain. *Science (New York, NY)* 338:1202–1205.

Erisir A, Harris JL (2003) Decline of the critical period of visual plasticity is concurrent with the reduction of NR2B subunit of the synaptic NMDA receptor in layer 4. *Journal of Neuroscience* 23:5208–5218.

Errington AC, Renger JJ, Uebele VN, Crunelli V (2010) State-dependent firing determines intrinsic dendritic Ca2+ signaling in thalamocortical neurons. *The Journal of neuroscience : the official journal of the Society for Neuroscience* 30:14843–14853.

Erzurumlu RSR, Gaspar PP (2012) Development and critical period plasticity of the barrel cortex. *The European journal of neuroscience* 35:1540–1553.

Fanselow EEE, Nicolelis MAM (1999) Behavioral modulation of tactile responses in the rat somatosensory system. *The Journal of neuroscience : the official journal of the Society for Neuroscience* 19:7603–7616.

Fanselow EEE, Sameshima KK, Baccala LAL, Nicolelis MAM (2001) Thalamic bursting in rats during different awake behavioral states. *Proceedings of the National Academy of Sciences of the United States of America* 98:15330–15335.

Feldmeyer D (2012) Excitatory neuronal connectivity in the barrel cortex. *Frontiers in Neuroanatomy* 6:24.

Feng GG, Mellor RHR, Bernstein MM, Keller-Peck CC, Nguyen QTQ, Wallace MM, Nerbonne JMJ, Lichtman JWJ, Sanes JRJ (2000) Imaging Neuronal Subsets in Transgenic Mice Expressing Multiple Spectral Variants of GFP. *NEURON* 28:11–11.

Fioravante DD, Regehr WGW (2011) Short-term forms of presynaptic plasticity. *Current Opinion in Neurobiology* 21:269–274.

Foffani G, Morales-Botello ML, Aguilar J (2009) Spike timing, spike count, and temporal information for the discrimination of tactile stimuli in the rat ventrobasal complex. *Journal of Neuroscience* 29:5964–5973.

Fox K (2008) *Barrel Cortex* Cambridge University Press.

Garg S, Oran AE, Hon H, Jacob J (2004) The hybrid cytomegalovirus enhancer/chicken beta-actin promoter along with woodchuck hepatitis virus posttranscriptional regulatory element enhances the protective efficacy of DNA vaccines. *Journal of immunology (Baltimore, Md : 1950)* 173:550–558.

Gavériaux-Ruff C, Kieffer BL (2007) Conditional gene targeting in the mouse nervous system: Insights into brain function and diseases. *Pharmacology & therapeutics* 113:619–634.

Gentet LJ, Stuart GJ, Clements JD (2000) Direct measurement of specific membrane capacitance in neurons. *Biophysical Journal* 79:314–320.

Gerstner W, Kistler WM (2002) *Spiking neuron models* single neurons, populations, plasticity. Cambridge Univ Pr.

Geurts AM, Cost GJ, Freyvert Y, Zeitler B, Miller JC, Choi VM, Jenkins SS, Wood A, Cui X, Meng X, Vincent A, Lam S, Michalkiewicz M, Schilling R, Foeckler J, Kalloway S, Weiler H, Ménoret S, Anegon I, Davis GD, Zhang L, Rebar EJ, Gregory PD, Urnov FD, Jacob HJ, Buelow R (2009) Knockout rats via embryo microinjection of zinc-finger nucleases. *Science (New York, NY)* 325:433.

Giber K, Bokor H, Nusser Z, Acsády L (2008) Synaptic input specific A-type potassium-channels in the thalamus. *SFN meeting. Abstract* pp. 1–1.

Godwin DW, Vaughan JW, Sherman SM (1996) Metabotropic glutamate receptors switch visual response mode of lateral geniculate nucleus cells from burst to tonic. *Journal of Neurophysiology* 76:1800–1816.

Gold JI, Bear MF (1994) A model of dendritic spine Ca2+ concentration exploring possible bases for a sliding synaptic modification threshold. *Proceedings of the National Academy of Sciences of the United States of America* 91:3941–3945.

Golding NL, Mickus TJ, Katz Y, Kath WL, Spruston N (2005) Factors mediating powerful voltage attenuation along CA1 pyramidal neuron dendrites. *J Physiol (Lond)* 568:69–82.

Golomb D, Ahissar E, Kleinfeld D (2006) Coding of stimulus frequency by latency in thalamic networks through the interplay of GABAB-mediated feedback and stimulus shape. *Journal of Neurophysiology* 95:1735–1750.

Groh A (2007) A giant driver synaptic connection in the cortico-thalamic pathway of the rodent whisker system Ph.D. diss., Ruperto-Carola University of Heidelberg.

Groh A, Bokor H, Mease RA, Plattner VM, Hangya B, Stroh A, Deschênes M, Acsády L (2013) Convergence of Cortical and Sensory Driver Inputs on Single Thalamocortical Cells. *Cerebral Cortex* Advance online publication:doi:10.1093/cercor/bht173.

Groh A, de Kock CPJ, Wimmer VC, Sakmann B, Kuner T (2008) Driver or coincidence detector: modal switch of a corticothalamic giant synapse controlled by spontaneous activity and short-term depression. *Journal of Neuroscience* 28:9652–9663.

Guillery RW (2005) Is postnatal neocortical maturation hierarchical? *Trends in Neurosciences* 28:512–517.

Haidarliu S, Yu C, Rubin N, Ahissar E (2008) Lemniscal and Extralemniscal Compartments in the VPM of the Rat. *Frontiers in Neuroanatomy* 2:4.

Hallanger AE, Levey AI, Lee HJ, Rye DB, Wainer BH (1987) The origins of cholinergic and other subcortical afferents to the thalamus in the rat. *The Journal of Comparative Neurology* 262:105–124.

Hallermann S, Fejtova A, Schmidt H, Weyhersmüller A, Silver RA, Gundelfinger ED, Eilers J (2010) Bassoon speeds vesicle reloading at a central excitatory synapse. *NEURON* 68:710–723.

Hao J, Wang Xd, Dan Y, Poo Mm, Zhang Xh (2009) An arithmetic rule for spatial summation of excitatory and inhibitory inputs in pyramidal neurons. *Proceedings of the National Academy of Sciences* 106:21906–21911.

Helmstaedter M, de Kock CPJ, Feldmeyer D, Bruno RM, Sakmann B (2007) Reconstruction of an average cortical column in silico. *Brain research reviews* 55:193–203.

Henson MA, Larsen RS, Lawson SN, Pérez-Otaño I, Nakanishi N, Lipton SA, Philpot BD (2012) Genetic deletion of NR3A accelerates glutamatergic synapse maturation. *PLoS ONE* 7:e42327.

Hines ML, Carnevale NT (1997) The NEURON simulation environment. *Neural computation* 9:1179–1209.

Hines ML, Carnevale NT (2001) NEURON: a tool for neuroscientists. *The Neuroscientist* 7:123–135.

Hines MLM, Carnevale NTN (2000) Expanding NEURON's repertoire of mechanisms with NMODL. *Neural computation* 12:995–1007.

Hodgkin AL, Huxley AF (1952) A quantitative description of membrane current and its application to conduction and excitation in nerve. *The Journal of Physiology* 117:500–544.

Hoffman DA, Magee JC, Colbert CM, Johnston D (1997) K+ channel regulation of signal propagation in dendrites of hippocampal pyramidal neurons. *Nature* 387:869–875.

Holmes WR, Woody CD (1989) Effects of uniform and non-uniform synaptic 'activation-distributions' on the cable properties of modeled cortical pyramidal neurons. *Brain research* 505:12–22.

Homberg JR, Olivier JDA, Smits BMG, Mul JD, Mudde J, Verheul M, Nieuwenhuizen OFM, Cools AR, Ronken E, Cremers T, Schoffelmeer ANM, Ellenbroek BA, Cuppen E (2007) Characterization of the serotonin transporter knockout rat: a selective change in the functioning of the serotonergic system. *NSC* 146:1662–1676.

Honoré T, Davies SN, Drejer J, Fletcher EJ, Jacobsen P, Lodge D, Nielsen FE (1988) Quinoxalinediones: potent competitive non-NMDA glutamate receptor antagonists. *Science (New York, NY)* 241:701–703.

Hoogland PV, Wouterlood FG, Welker E, Van der Loos H (1991) Ultrastructure of giant and small thalamic terminals of cortical origin: a study of the projections from the barrel cortex in mice using Phaseolus vulgaris leuco-agglutinin (PHA-L). *Experimental brain research Experimentelle Hirnforschung Expérimentation cérébrale* 87:159–172.

Hooks BM, Mao T, Gutnisky DA, Yamawaki N, Svoboda K, Shepherd GMG (2013) Organization of cortical and thalamic input to pyramidal neurons in mouse motor cortex. *Journal of Neuroscience* 33:748–760.

Hosoi N, Holt M, Sakaba T (2009) Calcium dependence of exo- and endocytotic coupling at a glutamatergic synapse. *NEURON* 63:216–229.

Howard DB, Powers K, Wang Y, Harvey BK (2008) Tropism and toxicity of adeno-associated viral vector serotypes 1, 2, 5, 6, 7, 8, and 9 in rat neurons and glia in vitro. *Virology* 372:24–34.

Hsu CLC, Yang HWH, Yen CTC, Min MYM (2010) Comparison of synaptic transmission and plasticity between sensory and cortical synapses on relay neurons in the ventrobasal nucleus of the rat thalamus. *The Journal of Physiology* 588:4347–4363.

Huguenard JR, Coulter DA, Prince DA (1991) A fast transient potassium current in thalamic relay neurons: kinetics of activation and inactivation. *Journal of Neurophysiology* 66:1304–1315.

Huguenard JR, Mccormick DA (1992) Simulation of the currents involved in rhythmic oscillations in thalamic relay neurons. *Journal of Neurophysiology* 68:1373–1383.

Huguenard JR, Prince DA (1994) Intrathalamic rhythmicity studied in vitro: nominal T-current modulation causes robust antioscillatory effects. *The Journal of neuroscience : the official journal of the Society for Neuroscience* 14:5485–5502.

Hutson KA, Masterton RB (1986) The sensory contribution of a single vibrissa's cortical barrel. *Journal of Neurophysiology* 56:1196–1223.

Jerng HH, Pfaffinger PJ, Covarrubias M (2004) Molecular physiology and modulation of somatodendritic A-type potassium channels. *Molecular and cellular neurosciences* 27:343–369.

Jinno S, Jeromin A, Kosaka T (2005) Postsynaptic and extrasynaptic localization of Kv4.2 channels in the mouse hippocampal region, with special reference to targeted clustering at gabaergic synapses. *NSC* 134:483–494.

Jones EG (2007) *The Thalamus 2 Volume Set* Cambridge University Press.

Joshi I, Wang LY (2002) Developmental profiles of glutamate receptors and synaptic transmission at a single synapse in the mouse auditory brainstem. *The Journal of Physiology* 540:861–873.

Jouvet-Mounier D, Astic L, Lacote D (1970) Ontogenesis of the states of sleep in rat, cat, and guinea pig during the first postnatal month. *Developmental psychobiology* 2:216–239.

Kandel E, Schwartz J, Jessell T, Siegelbaum S, Hudspeth AJ (2013) *Principles of Neural Science, Fifth Edition* McGraw Hill Professional.

Kaplan MR, Cho MH, Ullian EM, Isom LL, Levinson SR, Barres BA (2001) Differential control of clustering of the sodium channels Na(v)1.2 and Na(v)1.6 at developing CNS nodes of Ranvier. *NEURON* 30:105–119.

Katz Y, Menon V, Nicholson DA, Geinisman Y, Kath WL, Spruston N (2009) Synapse distribution suggests a two-stage model of dendritic integration in CA1 pyramidal neurons. *NEURON* 63:171–177.

Khodakhah K, Melishchuk A, Armstrong CM (1997) Killing K channels with TEA+. *Proceedings of the National Academy of Sciences of the United States of America* 94:13335–13338.

Kim J (2005) Kv4 potassium channel subunits control action potential repolarization and frequency-dependent broadening in rat hippocampal CA1 pyramidal neurones. *The Journal of Physiology* 569:41–57.

Kim J, Jung SC, Clemens AM, Petralia RS, Hoffman DA (2007) Regulation of dendritic excitability by activity-dependent trafficking of the A-type K+ channel subunit Kv4.2 in hippocampal neurons. *NEURON* 54:933–947.

Kleinfeld D, Ahissar E, Diamond ME (2006) Active sensation: insights from the rodent vibrissa sensorimotor system. *Current Opinion in Neurobiology* 16:435–444.

Kollo M, Holderith NB, Nusser Z (2006) Novel subcellular distribution pattern of A-type K+ channels on neuronal surface. *Journal of Neuroscience* 26:2684–2691.

Koralek KA, Jensen KF, Killackey HP (1988) Evidence for two complementary patterns of thalamic input to the rat somatosensory cortex. *Brain research* 463:346–351.

Körber C (2011) Functional characterization of the vertebrate-specific presynaptic protein Mover in the calyx of Held. Ph.D. diss., Ruperto-Carola University of Heidelberg.

Lai HC, Jan LY (2006) The distribution and targeting of neuronal voltage-gated ion channels. *Nature Reviews Neuroscience* 7:548–562.

Lam YW, Cox CL, Varela C, Sherman SM (2005) Morphological correlates of triadic circuitry in the lateral geniculate nucleus of cats and rats. *Journal of Neurophysiology* 93:748–757.

Landisman CE, Connors BW (2007) VPM and PoM nuclei of the rat somatosensory thalamus: intrinsic neuronal properties and corticothalamic feedback. *Cerebral Cortex* 17:2853–2865.

Lavallée P, Urbain N, Dufresne C, Bokor H, Acsády L, Deschênes M (2005) Feedforward inhibitory control of sensory information in higher-order thalamic nuclei. *Journal of Neuroscience* 25:7489–7498.

Lavrova AI, Zaks MA, Schimansky-Geier L (2012) Modeling rhythmic patterns in the hippocampus. *Physical review. E, Statistical, nonlinear, and soft matter physics* 85:041922.

Lee CH, Ruben PC (2008) Interaction between voltage-gated sodium channels and the neurotoxin, tetrodotoxin. *Channels* 2:407–412.

Lee SM, Friedberg MH, Ebner FF (1994) The role of GABA-mediated inhibition in the rat ventral posterior medial thalamus. I. Assessment of receptive field changes following thalamic reticular nucleus lesions. *Journal of Neurophysiology* 71:1702–1715.

Lee S, Ahmed T, Lee S, Kim H, Choi S, Kim DS, Kim SJ, Cho J, Shin HS (2012) Bidirectional modulation of fear extinction by mediodorsal thalamic firing in mice. *Nature Neuroscience* 15:308–314.

Li H, Fertuzinhos S, Mohns E, Hnasko TS, Verhage M, Edwards R, Sestan N, Crair MC (2013) Laminar and Columnar Development of Barrel Cortex Relies on Thalamocortical Neurotransmission. *NEURON* 79:970–986.

Li J, Bickford ME, Guido W (2003) Distinct firing properties of higher order thalamic relay neurons. *Journal of Neurophysiology* 90:291–299.

Liao CC, Chen RF, Lai WS, Lin RCS, Yen CT (2010) Distribution of large terminal inputs from the primary and secondary somatosensory cortices to the dorsal thalamus in the rodent. *The Journal of Comparative Neurology* 518:2592–2611.

Linkert M, Rueden CT, Allan C, Burel JM, Moore W, Patterson A, Loranger B, Moore J, Neves C, Macdonald D, Tarkowska A, Sticco C, Hill E, Rossner M, Eliceiri KW, Swedlow JR (2010) Metadata matters: access to image data in the real world. *The Journal of Cell Biology* 189:777–782.

Liu XB, Honda CN, Jones EG (1995) Distribution of four types of synapse on physiologically identified relay neurons in the ventral posterior thalamic nucleus of the cat. *The Journal of Comparative Neurology* 352:69–91.

Liu XB, Murray KD, Jones EG (2004) Switching of NMDA receptor 2A and 2B subunits at thalamic and cortical synapses during early postnatal development. *Journal of Neuroscience* 24:8885–8895.

Llinas R, Jahnsen H (1982) Electrophysiology of mammalian thalamic neurones in vitro. *Nature* 297:406–408.

London M, Larkum ME, Häusser M (2008) Predicting the synaptic information efficacy in cortical layer 5 pyramidal neurons using a minimal integrate-and-fire model. *Biological Cybernetics* 99:393–401.

Longair MH, Baker DA, Armstrong JD (2011) Simple Neurite Tracer: open source software for reconstruction, visualization and analysis of neuronal processes. *Bioinformatics* 27:2453–2454.

Low LK, Cheng HJ (2006) Axon pruning: an essential step underlying the developmental plasticity of neuronal connections. *Philosophical Transactions of the Royal Society B: Biological Sciences* 361:1531–1544.

Lu SM, Lin RC (1993) Thalamic afferents of the rat barrel cortex: a light- and electron-microscopic study using Phaseolus vulgaris leucoagglutinin as an anterograde tracer. *Somatosensory & Motor Research* 10:1–16.

Luján R (2010) Organisation of potassium channels on the neuronal surface. *Journal of chemical neuroanatomy* 40:1–20.

Lupa MT, Krzemien DM, Schaller KL, Caldwell JH (1993) Aggregation of sodium channels during development and maturation of the neuromuscular junction. *The Journal of neuroscience : the official journal of the Society for Neuroscience* 13:1326–1336.

Markram H (2006) The blue brain project. *Nature Reviews Neuroscience* 7:153–160.

Mateo C, Avermann M, Gentet LJ, Zhang F, Deisseroth K, Petersen CCH (2011) In vivo optogenetic stimulation of neocortical excitatory neurons drives brain-state-dependent inhibition. *Current Biology* 21:1593–1602.

Mccormick DA, Huguenard JR (1992) A model of the electrophysiological properties of thalamocortical relay neurons. *Journal of Neurophysiology* 68:1384–1400.

Mccormick DA, Pape HC (1990) Properties of a hyperpolarization-activated cation current and its role in rhythmic oscillation in thalamic relay neurones. *The Journal of Physiology* 431:291–318.

McCormick DA (1992) Neurotransmitter actions in the thalamus and cerebral cortex and their role in neuromodulation of thalamocortical activity. *Progress in neurobiology* 39:337–388.

McKay BE, McRory JE, Molineux ML, Hamid J, Snutch TP, Zamponi GW, Turner RW (2006) Ca(V)3 T-type calcium channel isoforms differentially distribute to somatic and dendritic compartments in rat central neurons. *The European journal of neuroscience* 24:2581–2594.

Meuth P, Meuth SG, Jacobi D, Broicher T, Pape HC, Budde T (2005) Get the rhythm: modeling neuronal activity. *Journal of undergraduate neuroscience education : JUNE : a publication of FUN, Faculty for Undergraduate Neuroscience* 4:A1–A11.

Meyer AC, Neher E, Schneggenburger R (2001) Estimation of quantal size and number of functional active zones at the calyx of held synapse by nonstationary EPSC variance analysis. *Journal of Neuroscience* 21:7889–7900.

Meyer HS, Wimmer VC, Hemberger M, Bruno RM, de Kock CPJ, Frick A, Sakmann B, Helmstaedter M (2010) Cell type-specific thalamic innervation in a column of rat vibrissal cortex. *Cerebral cortex (New York, NY : 1991)* 20:2287–2303.

Minnery BS, Simons DJ (2003) Response properties of whisker-associated trigeminothalamic neurons in rat nucleus principalis. *Journal of Neurophysiology* 89:40–56.

Miyata M, Imoto K (2006) Different composition of glutamate receptors in corticothalamic and lemniscal synaptic responses and their roles in the firing responses of ventrobasal thalamic neurons in juvenile mice. *The Journal of Physiology* 575:161–174.

Montemurro MA, Panzeri S, Maravall M, Alenda A, Bale MR, Brambilla M, Petersen RS (2007) Role of precise spike timing in coding of dynamic vibrissa stimuli in somatosensory thalamus. *Journal of Neurophysiology* 98:1871–1882.

Morris RG (1989) Synaptic plasticity and learning: selective impairment of learning rats and blockade of long-term potentiation in vivo by the N-methyl-D-aspartate receptor antagonist AP5. *The Journal of neuroscience : the official journal of the Society for Neuroscience* 9:3040–3057.

Mosconi TT, Woolsey TAT, Jacquin MFM (2010) Passive vs. active touch-induced activity in the developing whisker pathway. *The European journal of neuroscience* 32:1354–1363.

Neher EE, Sakaba TT (2008) Multiple Roles of Calcium Ions in the Regulation of Neurotransmitter Release. *NEURON* 59:12–12.

Nicholls JG, Martin AR, Fuchs PA, Brown DA, Diamond ME (2012) *From Neuron to Brain* A Cellular and Molecular Approach to the Function of the Nervous System. Sinauer Associates Incorporated.

Nicolelis MALM, Fanselow EEE (2002) Thalamocortical [correction of Thalamcortical] optimization of tactile processing according to behavioral state. *Nature Neuroscience* 5:517–523.

Norris AJ, Nerbonne JM (2010) Molecular dissection of IA in cortical pyramidal neurons reveals three distinct components encoded by Kv4.2, Kv4.3, and Kv1.4 alpha-subunits. *The Journal of neuroscience : the official journal of the Society for Neuroscience* 30:5092–5101.

O'connor DH, Hires SA, Guo ZV, Li N, Yu J, Sun QQ, Huber D, Svoboda K (2013) Neural coding during active somatosensation revealed using illusory touch. *Nature Neuroscience* 16:958–965.

Ohara PT, Havton LA (1994) Dendritic architecture of rat somatosensory thalamocortical projection neurons. *The Journal of Comparative Neurology* 341:159–171.

Ohara PT, Ralston HJ, Havton LA (1995) Architecture of individual dendrites from intracellularly labeled thalamocortical projection neurons in the ventral posterolateral and ventral posteromedial nuclei of cat. *The Journal of Comparative Neurology* 358:563–572.

Ohno S, Kuramoto E, Furuta T, Hioki H, Tanaka YR, Fujiyama F, Sonomura T, Uemura M, Sugiyama K, Kaneko T (2012) A morphological analysis of thalamocortical axon fibers of rat posterior thalamic nuclei: a single neuron tracing study with viral vectors. *Cerebral Cortex* 22:2840–2857.

Ollion J, Cochennec J, Loll F, Escudé C, Boudier T (2013) TANGO: a generic tool for high-throughput 3D image analysis for studying nuclear organization. *Bioinformatics* 29:1840–1841.

Papaioannou S, Brigham L, Krieger P (2013) Sensory deprivation during early development causes an increased exploratory behavior in a whisker-dependent decision task. *Brain and behavior* 3:24–34.

Pape HC, Budde T, Mager R, Kisvárday ZF (1994) Prevention of Ca(2+)-mediated action potentials in GABAergic local circuit neurones of rat thalamus by a transient K+ current. *The Journal of Physiology* 478 Pt 3:403–422.

Parnaudeau S, O'Neill PK, Bolkan SS, Ward RD, Abbas AI, Roth BL, Balsam PD, Gordon JA, Kellendonk C (2013) Inhibition of mediodorsal thalamus disrupts thalamofrontal connectivity and cognition. *NEURON* 77:1151–1162.

Paxinos G (2004) *The rat nervous system* Academic Press.

Paxinos G, Franklin KBJ (1997) *The Mouse Brain* In Stereotaxic Coordinates. San Diego : Academic Press.

Paxinos G, Watson C (1986) *The Rat Brain in Stereotaxic Coordinates* Hard Cover Edition. Academic Press, second edition edition.

Peng H, Ruan Z, Long F, Simpson JH, Myers EW (2010) V3D enables real-time 3D visualization and quantitative analysis of large-scale biological image data sets. *Nature biotechnology* 28:348–353.

Perez-Reyes E (2003) Molecular physiology of low-voltage-activated t-type calcium channels. *Physiological Reviews* 83:117–161.

Peschanski M, Roudier F, Ralston HJ, Besson JM (1985) Ultrastructural analysis of the terminals of various somatosensory pathways in the ventrobasal complex of the rat thalamus: an electron-microscopic study using wheatgerm agglutinin conjugated to horseradish peroxidase as an axonal tracer. *Somatosensory research* 3:75–87.

Peters F, Gennerich A, Czesnik D, Schild D (2000) Low frequency voltage clamp: recording of voltage transients at constant average command voltage. *Journal of Neuroscience Methods* 99:129–136.

Petersen CCH (2007) The functional organization of the barrel cortex. *NEURON* 56:339–355.

Petersen RS, Panzeri S, Maravall M (2009) Neural coding and contextual influences in the whisker system. *Biological Cybernetics* 100:427–446.

Petreanu L, Huber D, Sobczyk A, Svoboda K (2007) Channelrhodopsin-2-assisted circuit mapping of long-range callosal projections. *Nature Neuroscience* 10:663–668.

Pierret T, Lavallee P, Deschênes M (2000) Parallel streams for the relay of vibrissal information through thalamic barreloids. *The Journal of neuroscience : the official journal of the Society for Neuroscience* 20:7455–7462.

Piskorowski RA, Chevaleyre V (2012) Synaptic integration by different dendritic compartments of hippocampal CA1 and CA2 pyramidal neurons. *Cellular and molecular life sciences : CMLS* 69:75–88.

Poulet JFA, Fernandez LMJ, Crochet S, Petersen CCH (2012) Thalamic control of cortical states. *Nature Neuroscience* 15:370–372.

Purves D (2004) *Neuroscience* Sinauer Associates Inc.

Quairiaux C, Mégevand P, Kiss JZ, Michel CM (2011) Functional development of large-scale sensorimotor cortical networks in the brain. *Journal of Neuroscience* 31:9574–9584.

Quinlan EM, Olstein DH, Bear MF (1999) Bidirectional, experience-dependent regulation of N-methyl-D-aspartate receptor subunit composition in the rat visual cortex during postnatal development. *Proceedings of the National Academy of Sciences of the United States of America* 96:12876–12880.

Rall W (1967) Distinguishing theoretical synaptic potentials computed for different soma-dendritic distributions of synaptic input. *Journal of Neurophysiology* 30:1138–1168.

Ramcharan EJ, Gnadt JW, Sherman SM (2005) Higher-order thalamic relays burst more than first-order relays. *Proceedings of the National Academy of Sciences of the United States of America* 102:12236–12241.

Reichova I, Sherman SM (2004) Somatosensory corticothalamic projections: distinguishing drivers from modulators. *Journal of Neurophysiology* 92:2185–2197.

Rhodes PA, Llinás R (2005) A model of thalamocortical relay cells. *The Journal of Physiology* 565:765–781.

Rios JC, Rubin M, St Martin M, Downey RT, Einheber S, Rosenbluth J, Levinson SR, Bhat M, Salzer JL (2003) Paranodal interactions regulate expression of sodium channel subtypes and provide a diffusion barrier for the node of Ranvier. *Journal of Neuroscience* 23:7001–7011.

Rizzoli SO, Betz WJ (2005) Synaptic vesicle pools. *Nature Reviews Neuroscience* 6:57–69.

Robert W Gereau IV, Swanson GT (2008) *The Glutamate Receptors* Springer.

Rush AM, Dib-Hajj SD, Waxman SG (2005) Electrophysiological properties of two axonal sodium channels, Nav1.2 and Nav1.6, expressed in mouse spinal sensory neurones. *The Journal of Physiology* 564:803–815.

Safaai H, von Heimendahl M, Sorando JM, Diamond ME, Maravall M (2013) Coordinated population activity underlying texture discrimination in rat barrel cortex. *Journal of Neuroscience* 33:5843–5855.

Sakaba T, Schneggenburger R, Neher E (2002) Estimation of quantal parameters at the calyx of Held synapse. *Neuroscience research* 44:343–356.

Sätzler K, Söhl LF, Bollmann JH, Borst JGG, Frotscher M, Sakmann B, Lübke JHR (2002) Three-dimensional reconstruction of a calyx of Held and its postsynaptic principal neuron in the medial nucleus of the trapezoid body. *The Journal of neuroscience : the official journal of the Society for Neuroscience* 22:10567–10579.

Scheuss V, Schneggenburger R, Neher E (2002) Separation of presynaptic and postsynaptic contributions to depression by covariance analysis of successive EPSCs at the calyx of held synapse. *Journal of Neuroscience* 22:728–739.

Schindelin J, Arganda-Carreras I, Frise E, Kaynig V, Longair M, Pietzsch T, Preibisch S, Rueden C, Saalfeld S, Schmid B (2012) Fiji: an open-source platform for biological-image analysis. *Nature Methods* 9:676–682.

Schneggenburger R, Meyer AC, Neher E (1999) Released fraction and total size of a pool of immediately available transmitter quanta at a calyx synapse. *NEURON* 23:399–409.

Schwarz SKW, Puil E (2002) Effects of QX-314 on membrane properties of neurons in the ventrobasal thalamus. *Proceedings of the Western Pharmacology Society* 45:29–31.

Serôdio P, Rudy B (1998) Differential Expression of Kv4 K+ Channel Subunits Mediating Subthreshold Transient K+ (A-Type) Currents in Rat Brain. *Journal of Neurophysiology* .

Sheng M, Tsaur ML, Jan YN, Jan LY (1992) Subcellular segregation of two A-type K+ channel proteins in rat central neurons. *NEURON* 9:271–284.

Sherman SM (2001) Tonic and burst firing: dual modes of thalamocortical relay. *Trends in Neurosciences* 24:122–126.

Sherman SM, Guillery RW (2009) *Exploring the Thalamus and Its Role in Cortical Function* MIT Press (MA).

Sherman SM, Guillery RW (2013) *Functional Connections of Cortical Areas* A New View from the Thalamus. MIT Press.

Shibata R, Nakahira K, Shibasaki K, Wakazono Y, Imoto K, Ikenaka K (2000) A-type K+ current mediated by the Kv4 channel regulates the generation of action potential in developing cerebellar granule cells. *Journal of Neuroscience* 20:4145–4155.

Shoykhet M, Land PW, Simons DJ (2005) Whisker trimming begun at birth or on postnatal day 12 affects excitatory and inhibitory receptive fields of layer IV barrel neurons. *Journal of Neurophysiology* 94:3987–3995.

Shoykhet M, Simons DJ (2008) Development of thalamocortical response transformations in the rat whisker-barrel system. *Journal of Neurophysiology* 99:356–366.

Simons DJ, Land PW (1987) Early experience of tactile stimulation influences organization of somatic sensory cortex. *Nature* 326:694–697.

Smith JBJ, Mowery TMT, Alloway KDK (2012) Thalamic POm projections to the dorsolateral striatum of rats: potential pathway for mediating stimulus-response associations for sensorimotor habits. *Journal of Neurophysiology* 108:160–174.

Sosnik R, Haidarliu S, Ahissar E (2001) Temporal frequency of whisker movement. I. Representations in brain stem and thalamus. *Journal of Neurophysiology* 86:339–353.

Spacek J, Lieberman AR (1974) Ultrastructure and three-dimensional organization of synaptic glomeruli in rat somatosensory thalamus. *Journal of anatomy* 117:487–516.

Spruston N (2008) Pyramidal neurons: dendritic structure and synaptic integration. *Nature Reviews Neuroscience* 9:206–221.

Stern EA, Maravall M, Svoboda K (2001) Rapid Development and Plasticity of Layer 2/3 Maps in Rat Barrel Cortex In Vivo. *NEURON* 31:11–11.

Sterratt D, Graham B, Gillies A, Willshaw D (2011) *Principles of Computational Modelling in Neuroscience* Cambridge University Press, 1 edition.

Strichartz GR (1973) The inhibition of sodium currents in myelinated nerve by quaternary derivatives of lidocaine. *Journal of General Physiology* 62:37–57.

Stritt C, Knöll B (2010) Serum response factor regulates hippocampal lamination and dendrite development and is connected with reelin signaling. *Molecular and cellular biology* 30:1828–1837.

Stuart G, Spruston N, Häusser M (2008) *Dendrites* Oxford University Press.

Sugitani M, Yano J, Sugai T, Ooyama H (1990) Somatotopic organization and columnar structure of vibrissae representation in the rat ventrobasal complex. *Experimental brain research Experimentelle Hirnforschung Expérimentation cérébrale* 81:346–352.

Sun JY, Wu LG (2001) Fast kinetics of exocytosis revealed by simultaneous measurements of presynaptic capacitance and postsynaptic currents at a central synapse. *NEURON* 30:171–182.

Sun J, Kouranova E, Cui X, Mach RH, Xu J (2013) Regulation of dopamine presynaptic markers and receptors in the striatum of DJ-1 and Pink1 knockout rats. *Neuroscience Letters* .

Taschenberger H, Leão RM, Rowland KC, Spirou GA, Von Gersdorff H (2002) Optimizing synaptic architecture and efficiency for high-frequency transmission. *NEURON* 36:1127–1143.

Theyel BB, Llano DA, Sherman SM (2010) The corticothalamocortical circuit drives higher-order cortex in the mouse. *Nature Neuroscience* 13:84–88.

Thompson S (1982) Aminopyridine block of transient potassium current. *The Journal of General Physiology* 80:1–18.

Tóth TI, Hughes SW, Crunelli V (1998) Analysis and biophysical interpretation of bistable behaviour in thalamocortical neurons. *NSC* 87:519–523.

Traub RD, Contreras D, Cunningham MO, Murray H, LeBeau FEN, Roopun A, Bibbig A, Wilent WB, Higley MJ, Whittington MA (2005) Single-column thalamocortical network model exhibiting gamma oscillations, sleep spindles, and epileptogenic bursts. *Journal of Neurophysiology* 93:2194–2232.

Trussell LO, Zhang S, Raman IM (1993) Desensitization of AMPA receptors upon multiquantal neurotransmitter release. *NEURON* 10:1185–1196.

Tscherter A, David F, Ivanova T, Deleuze C, Renger JJ, Uebele VN, Shin HS, Bal T, Leresche N, Lambert RC (2011) Minimal alterations in T-type calcium channel gating markedly modify physiological firing dynamics. *The Journal of Physiology* 589:1707–1724.

Turner JP, Anderson CM, Williams SR, Crunelli V (1997) Morphology and membrane properties of neurones in the cat ventrobasal thalamus in vitro. *The Journal of Physiology* 505 (Pt 3):707–726.

Urbain N, Deschênes M (2007) Motor cortex gates vibrissal responses in a thalamocortical projection pathway. *NEURON* 56:714–725.

Van der Loos H (1976) Barreloids in mouse somatosensory thalamus. *Neuroscience Letters* 2:1–6.

Van Horn SC, Sherman SM (2007) Fewer driver synapses in higher order than in first order thalamic relays. *NSC* 146:463–470.

Van Horn SC, Erisir A, Sherman SM (2000) Relative distribution of synapses in the Alaminae of the lateral geniculate nucleus of the cat. *The Journal of Comparative Neurology* 416:509–520.

Varela C, Sherman SM (2007) Differences in response to muscarinic activation between first and higher order thalamic relays. *Journal of Neurophysiology* 98:3538–3547.

Varela C, Sherman SM (2009) Differences in response to serotonergic activation between first and higher order thalamic nuclei. *Cerebral Cortex* 19:1776–1786.

Varela JA, Sen K, Gibson J, Fost J, Abbott LF, Nelson SB (1997) A quantitative description of short-term plasticity at excitatory synapses in layer 2/3 of rat primary visual cortex. *The Journal of neuroscience : the official journal of the Society for Neuroscience* 17:7926–7940.

Veinante P, Deschênes M (1999) Single- and multi-whisker channels in the ascending projections from the principal trigeminal nucleus in the rat. *Journal of Neuroscience* 19:5085–5095.

Veinante P, Jacquin MF, Deschênes M (2000) Thalamic projections from the whisker-sensitive regions of the spinal trigeminal complex in the rat. *The Journal of Comparative Neurology* 420:233–243.

Vetter P, Roth A, Häusser M (2001) Propagation of action potentials in dendrites depends on dendritic morphology. *Journal of Neurophysiology* 85:926–937.

Viaene ANA, Petrof II, Sherman SMS (2011) Properties of the thalamic projection from the posterior medial nucleus to primary and secondary somatosensory cortices in the mouse. *Proceedings of the National Academy of Sciences of the United States of America* 108:18156–18161.

Von Gersdorff H, Borst JGG (2002) Short-term plasticity at the calyx of held. *Nature Reviews Neuroscience* 3:53–64.

von Krosigk M, Bal T, Mccormick DA (1993) Cellular mechanisms of a synchronized oscillation in the thalamus. *Science (New York, NY)* 261:361–364.

Wang D, Schreurs BG (2006) Characteristics of IA currents in adult rabbit cerebellar Purkinje cells. *Brain research* 1096:85–96.

Wang H, Liu H, Zhang Zw (2011) Elimination of redundant synaptic inputs in the absence of synaptic strengthening. *Journal of Neuroscience* 31:16675–16684.

Wang H, Zhang Zw (2008) A critical window for experience-dependent plasticity at whisker sensory relay synapse in the thalamus. *The Journal of neuroscience : the official journal of the Society for Neuroscience* 28:13621–13628.

Wang XJX, Rinzel JJ, Rogawski MAM (1991) A model of the T-type calcium current and the low-threshold spike in thalamic neurons. *Journal of Neurophysiology* 66:839–850.

Warren RA, Jones EG (1997) Maturation of neuronal form and function in a mouse thalamo-cortical circuit. *The Journal of neuroscience : the official journal of the Society for Neuroscience* 17:277–295.

Watson C, Paxinos G, Puelles L (2011) *The Mouse Nervous System* Academic Press.

Wearne SL, Rodriguez A, Ehlenberger DB, Rocher AB, Henderson SC, Hof PR (2005) New techniques for imaging, digitization and analysis of three-dimensional neural morphology on multiple scales. *NSC* 136:661–680.

Weaver CM, Wearne SL (2008) Neuronal firing sensitivity to morphologic and active membrane parameters. *PLoS computational biology* 4:e11.

Williams K (1993) Ifenprodil discriminates subtypes of the N-methyl-D-aspartate receptor: selectivity and mechanisms at recombinant heteromeric receptors. *Molecular pharmacology* 44:851–859.

Williams MNM, Zahm DSD, Jacquin MFM (1994) Differential foci and synaptic organization of the principal and spinal trigeminal projections to the thalamus in the rat. *The European journal of neuroscience* 6:429–453.

Williams SRS, Stuart GJG (2000) Action potential backpropagation and somato-dendritic distribution of ion channels in thalamocortical neurons. *The Journal of neuroscience : the official journal of the Society for Neuroscience* 20:1307–1317.

Williams SRS, Tóth TIT, Turner JPJ, Hughes SWS, Crunelli VV (1997) The 'window' component of the low threshold Ca2+ current produces input signal amplification and bistability in cat and rat thalamocortical neurones. *The Journal of Physiology* 505 (Pt 3):689–705.

Wimmer VC, Bruno RM, de Kock CPJ, Kuner T, Sakmann B (2010) Dimensions of a projection column and architecture of VPM and POm axons in rat vibrissal cortex. *Cerebral cortex (New York, NY : 1991)* 20:2265–2276.

Wimmer VC, Nevian T, Kuner T (2004) Targeted in vivo expression of proteins in the calyx of Held. *Pflügers Archiv - European Journal of Physiology* 449:319–333.

Woolsey TA, Van der Loos H (1970) The structural organization of layer IV in the somatosensory region (SI) of mouse cerebral cortex. The description of a cortical field composed of discrete cytoarchitectonic units. *Brain research* 17:205–242.

Wu ZZ, Li DP, Chen SR, Pan HL (2009) Aminopyridines potentiate synaptic and neuromuscular transmission by targeting the voltage-activated calcium channel beta subunit. *Journal of Biological Chemistry* 284:36453–36461.

Xu WW, Südhof TCT (2013) A neural circuit for memory specificity and generalization. *Science (New York, NY)* 339:1290–1295.

Xu-Friedman MAM, Regehr WGW (2003) Ultrastructural contributions to desensitization at cerebellar mossy fiber to granule cell synapses. *The Journal of neuroscience : the official journal of the Society for Neuroscience* 23:2182–2192.

Yamada KA, Tang CM (1993) Benzothiadiazides inhibit rapid glutamate receptor desensitization and enhance glutamatergic synaptic currents. *The Journal of neuroscience : the official journal of the Society for Neuroscience* 13:3904–3915.

Yu CC, Derdikman DD, Haidarliu SS, Ahissar EE (2006) Parallel thalamic pathways for whisking and touch signals in the rat. *PLoS Biology* 4:e124–e124.

Yuan W, Burkhalter A, Nerbonne JM (2005) Functional role of the fast transient outward K+ current IA in pyramidal neurons in (rat) primary visual cortex. *The Journal of neuroscience : the official journal of the Society for Neuroscience* 25:9185–9194.

Zembrzycki A, Chou SJ, Ashery-Padan R, Stoykova A, O'Leary DDM (2013) Sensory cortex limits cortical maps and drives top-down plasticity in thalamocortical circuits. *Nature Neuroscience* 16:1060–1067.

Zhou Q, Godwin DW, O'Malley DM, Adams PR (1997) Visualization of calcium influx through channels that shape the burst and tonic firing modes of thalamic relay cells. *Journal of Neurophysiology* 77:2816–2825.

Zomorrodi R, Ferecskó AS, Kovács K, Kröger H, Timofeev I (2010) Analysis of morphological features of thalamocortical neurons from the ventroposterolateral nucleus of the cat. *The Journal of Comparative Neurology* 518:3541–3556.

Zufferey R, Donello JE, Trono D, Hope TJ (1999) Woodchuck hepatitis virus posttranscriptional regulatory element enhances expression of transgenes delivered by retroviral vectors. *Journal of virology* 73:2886–2892.

Zuo Y, Perkon I, Diamond ME (2011) Whisking and whisker kinematics during a texture classification task. *Philosophical Transactions of the Royal Society B: Biological Sciences* 366:3058–3069.

List of Figures

List of Tables